Ministry of
Northern Development
and Mines
Ontario

ONTARIO GEOLOGICAL SURVEY

Open File Report 5806

Geology and Mineral Potential of Banting Township and the Western Part of Best Township, District of Nipissing

By

M.C. Smyk, P. Born and L. Owsiacki

1991

CANADA ONTARIO
Mineral Development Agreement / Entente sur le développement minéral

This project is part of the five-year Canada-Ontario 1985 Mineral Development Agreement (COMDA), a subsidiary agreement to the Economic and Regional Development Agreement (ERDA) signed by the governments of Canada and Ontario.

Ontario Geological Survey

OPEN FILE REPORT

Open File Reports are made available to the public subject to the following conditions:

This report is unedited. Discrepancies may occur for which the Ontario Geological Survey does not assume liability. Recommendations and statements of opinions expressed are those of the author or authors and are not to be construed as statements of government policy.

This Open File Report is available for viewing at the following locations:

(1) Mines Library
Ministry of Northern Development and Mines
8th floor, 77 Grenville Street
Toronto, Ontario M7A 1W4

(2) The office of the Regional or Resident Geologist in whose district the area covered by this report is located.

Copies of this report may be obtained at the user's expense from a commercial printing house. For the address and instructions to order, contact the appropriate Regional or Resident Geologist's office(s) or the Mines Library. Microfiche copies (42x reduction) of this report are available for $2.00 each plus provincial sales tax at the Mines Library or the Public Information Centre, Ministry of Natural Resources, W-1640, 99 Wellesley Street West, Toronto.

Handwritten notes and sketches may be made from this report. Check with the Mines Library or Regional/Resident Geologist's office whether there is a copy of this report that may be borrowed. A copy of this report is available for Inter-Library loan.

This report is available for viewing at the following Regional or Resident Geologist's offices:

Cobalt-Box 230,Presley St., Cobalt POJ 1C0
Porcupine-60 Wilson Ave.,Timmins P4N 2S7
Sudbury-2nd Floor,159 Cedar St.,Sudbury P3E 6A5

V.G. Milne, Director
Ontario Geological Survey

FOREWORD

Until 1989 the geological map coverage of Banting Township and the Western Part of Best Township was at a reconnaissance level. The present detailed mapping project was designed to encourage mineral exploration interests and to provide a mineral and land use evaluation.

The work reported here was funded under the Canada-Ontario Mineral Development Agreement (COMDA) a subsidiary agreement to the Economic and Regional Development Agreement (ERDA) signed by the government of Canada and Ontario.

The Precambrian bedrock of Banting Township and the Western Part of Best Township hosts some small poly-metallic mineral occurrences that contain copper, silver, and trace gold mineralization. Currently, there are no producing mines within the map area.

V.G.Milne
Director
Ontario Geological Survey

CONTENTS

LIST OF FIGURES

List of Photos

LIST OF TABLES

ABSTRACT

This report describes the geology and economic mineral potential of Banting Township and the western part of Best Township, District of Nipissing. The study area is bounded by Latitudes 47°08'45" N and 47°14'05" N, and Longitudes 75°51'00" W and 80°01'06" W, and covers approximately 124 km^2 (48 square miles).

All lithologic units in the map area are of Precambrian age. Archean metavolcanics consist of steeply dipping, mafic to intermediate tholeiitic flows and calc-alkalic pyroclastic rocks which occur in a narrow, branching belt. These rocks have undergone at least two and possibly three phases of folding and regional, lower greenschist metamorphism. Both brittle and ductile deformation occurred contemperanous with folding. It produced several major deformation zones with the most prominent being the ENE-trending Anima-Nipissing River Deformation Zone (ANRDZ). The metavolcanic rocks have been intruded by gabbroic, dioritic and later granitic rocks. Rocks in the contact aureoles of the granite batholiths are of albite-epidote - and hornblende - hornfels facies. Late Archean mafic to intermediate intrusive rocks, including lamprophyre, intrude the granites and older Archean gabbro.

Archean rocks are unconformably overlain by Early Proterozoic glaciogenic sedimentary rocks of the Coleman Member of the Gowganda Formation of the Huronian Supergroup. An undulating sill of Early Proterozoic Nipissing diabase intrudes Archean basement and Huronian sedimentary rocks and is exposed as

several eroded diabase arches and diabase basins. A northwest-trending, olivine diabase dike (Sudbury Swarm) and several swarms of narrower, later diabase dikes postdate the Nipissing diabase and are the youngest rocks in the study area.

Prospecting and exploration activity has been sporatic in the area. Small test pits and trenches were located and are presumably 50 to 80 years old. No significant mineral occurrences were discovered, largely owing to the absence of Cobalt-type, silver-arsenide vein deposits, despite lithologic and stratigraphic relationships present that are similar to those in Cobalt. Quartz +/- calcite veins in the upper, varied-texture portions of the Nipissing diabase sill contain minor gold, silver and copper values. Quartz veins in Archean basement rocks are typically barren of sulphides but have returned gold values of up to 0.05 ounces Au per ton. These anomalous gold and copper values are mainly associated with the main ENE-trending Anima-Nipissing River Deformation Zone (ANRDZ). Other gold mineralization may be related to the lamprophyric suite of rocks located near the main deformation zone. The Archean hornblende gabbro may have potential for base metal and platinum group element mineralization.

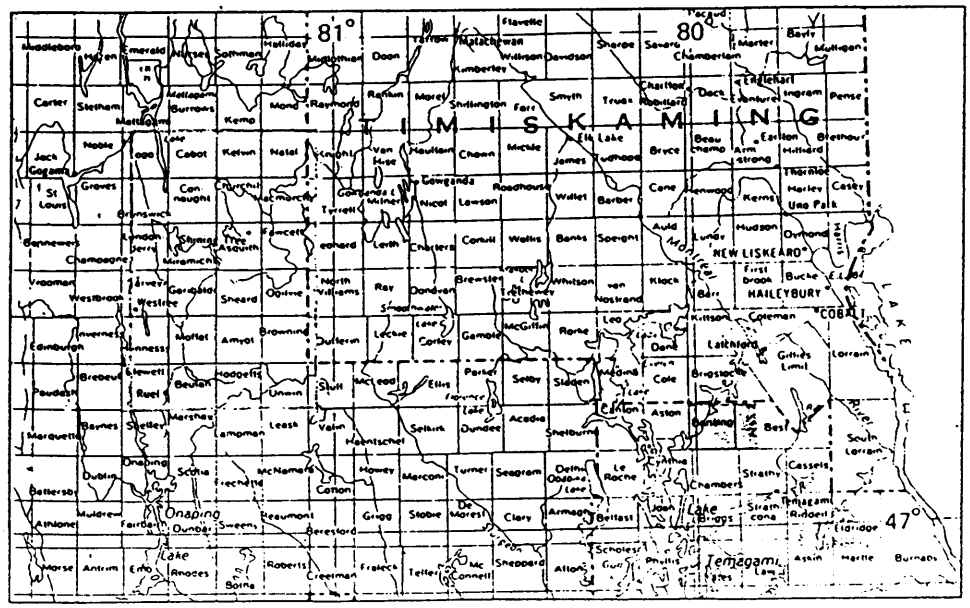

LOCATION MAP Scale : 1:1 584 000 or 1 inch to 25 miles

1: Key map showing location of Banting Township and the Western Part of Best Township.

Geology and Mineral Potential of Banting Township and the Western Part of Best Township, District of Nipissing

M.C. Smyk[1]

Peter Born[2]

Leo Owsiacki[3]

INTRODUCTION

Detailed geological mapping of Banting Township and the western part of Best Township was carried out between 1983 and 1989 at a scale of 1:7920 (1 inch to 660 feet),and represents an extension of an earlier investigation of a narrow volcanic inlier situated in the MacLean Lake-Lundy Lake area (Owsiacki, 1983, 1984, and Symk and Owsiacki 1986). Initially the funding was provided by the Ministry of Northern Development and Mines under the Special Projects to Assist Resources Communities (SPARC) Program and finally completed through the Canada Ontario Mineral

[1]Staff Geologist, Ontario Ministry of Northern Development and Mines, Northwest Region, Thunder Bay

[2]Geologist,Ontario Ministry of Northern Development and Mines, Northeast Region, Cobalt

[3]Resident Geologist, Ontario Ministry of Northern Development and Mines, Northeast Region, Cobalt

Critical reader: B. Dressler
Manuscript approved for publication by B. Dressler, supervising geologist, Detailed and Synoptic Mapping.
This report is published with the permission of V.G. Milne, Director, Ontario Geological Survey, Toronto.

Development Agreement (COMDA) a subsidiary agreement to the Economic and Regional Development Agreement (ERDA) signed by the governments of Canada and Ontario.

The boundaries of the orignial study area have been enlarged to include all of Banting Township and the adjacent western part of Best Township, bounded by Latitudes 47°08'45" N and 47°14'05" N, and Longitudes 75°51'00" W and 80°01'06" W. This represents a total area of approximately 124 km^2 (48 square miles). The earliest geolgical mapping in the area was done by A.E. Barlow (1899) of the Geological Survey of Canada in 1899. Revised editions of his map were published in 1908 at a scale of 4 inches to the mile. Later reconnaissance investigations were carried out by DeLury (1907) in the vicinity of Anima-Nipissing and Whitewater lakes. The first comprehensive, more detailed geological survey however, was completed by Todd (1926). His work covered a large area including Banting and Best Townships on a scale of one inch to one mile (1: 63,360). More recent mapping in the areas to the west was completed by Card et al (1973) in the Maple Mountain Area. Chambers and Strathy Townships to the south have been mapped by Bennett (1978) and more recently by Fyon et al (1987, 1988, 1989). Detailed geological mapping in areas to the north and northeast of Banting and Best Townships were most recently completed by Born and Burbidge (1990) and Born and Hitch (1990), respectively. Areas immediately to the east of the present map area are not covered by detailed geological mapping.

Quaternary geology of the area is outlined on Ontario Geological Survey Map 5024 (Haileybury) (Roed 1979). The regional geology map is 2362, Sudbury-Cobalt sheet (Card and Lumbers, 1977) and the regional aeromagnetic maps are GSC Aeromagnetic Series Maps 1491G (Timagami) and 1503G (Obabika Lake).

Acknowledgements

The authors gratefully acknowledge field assistance from the following persons: Doug Irwin, Randy Clarke, Dave Bailey, Andrew Marvin, Elaine Dodd. Logistical and administrative support was provided by Karen Larabie and much of the drafting was done by Larry Francis. The authors also wish to thank Mr. Conrad Hamilton of the Ministry of Natural Resources in Temagami for the use of Whitney Lake Camp during the 1989 field season.

Topography and Drainage

Average relief in the map area is approximately 50 m with the lowest part located along the shores of Red Squirrel Lake and the highest point to the southwest of Lenore Lake. Rock Lithologies tend to influence local topographic variations. Generally Early Proterozoic Nipissing Diabase forms several north-trending ridges that transects the map area. Elsewhere the relief is of a more gently rolling nature with the lower areas occupied by many creeks and swamps.

Because much of the area has been lumbered and clear cut the bedrock exposures are generally good and the area is

characterized by an average of 25% outcrop. Structure patterns control the local drainage with several creeks following prominant northwest - and west trending lineaments. These creeks are commonly bounded by long linear outcrops parallel to faults and linements.

Water covers approximately 15% of the map area with Anima-Nipissing, Whitewater, Red Squirrel, Lundy and Lenore lakes as major bodies of water. Other smaller lakes are Tyndall, Contact, Gilbert, Snare, Mannajigama, and Breeches lakes. All of the lakes and streams drain into Red Squirrel Lake and eventually into Lake Temagami to the south of the map sheet.

GENERAL GEOLOGY

The geology of Banting Township and the western part of Best Township comprises a variety of Archean and Proterozoic rocks of the eastern part of the Cobalt Plain (Stockwell et al, 1970). Lithologic relationships attest to a complex structural, intrusive and depositional history (Figures 1, 2, and 3).

Archean mafic to intermediate metavolcanics, consisting of flows and pyroclastic rocks, are the oldest rocks in the study area. Hypabyssal feldspar porphyry dikes intrude the succession. Metavolcanics lie within a narrow, branching belt whose structure has been modified by the intrusion of ultramafic, intermediate and felsic rocks.

Hornblende gabbro and diorite occupy the southern contact of the metavolcanics and granitoid rocks. The Archean rocks were

subject to predominantly regional greenschist metamorphism except in contact aureoles of the granitoid bodies where they are characterized by hornblende - hornfels facies assemblages. Late Archean mafic stocks and dikes, associated with faults and diatremes, intrude these rocks.

The Archean basement is unconformably overlain by Early Proterozoic glaciogenic sediments of the Gowganda Formation of the Huronian Supergroup, consisting of basal breccia, diamictite, sandstone and mudstone. An undulating sheet of Early Proterozoic Nipissing diabase intrudes basement and Huronian rocks, forming several eroded diabase arches and basins (Figure 3). A northwest-trending Sudbury-type olivine diabase dike and several swarms of smaller, later dikes postdate the Nipissing diabase and represent the youngest lithologic units in the study area.

Unconsolidated glaciogenic till, sand and gravel deposits of Pleistocene age overlie bedrock.

A generalized summary of the rock types occuring within Banting Township and the western part of Best Township is given in Table 1.

ARCHEAN

Metavolcanic Rocks

Mafic to Intermediate Metavolcanics

Metavolcanic rocks occur for the most part in an east-trending belt, 500 m to 2 km wide, that extends through the centre of the study area. These rocks likely comprise the western part of a volcanic inlier within an area underlain by

Huronian rocks and extend southwestward from Mountain Lake, parallel to the main Temagami metavolcanic - metasedimentary belt to the south (Bennett, 1978; Fyon et al, 1987,1988,1989). They are displaced and in part assimilated by intrusive rocks. In places they are overlain by Huronian metasediments or intruded by Nipissing diabase. The main belt branches into three distinct arms that extend to the northest, east and southeast. The southesterly trending arm merges with a splay of the Temagami greenstone belt which is exposed in northern Chambers and Strathy Townships. Structural and stratigraphic relationships appear to be consistent with the Teamagmi greenstone belt in Chambers Township (Fyon and Cole, 1989).

For the most part the belt in Banting Township consists of steeply-dipping, altered and deformed Archean metavolcanic flows in which a lower and upper unit can be distinguished. The basal unit consists of commonly pillowed, mega-feldspar phyric mafic flows (map unit 1a). This unit is distinctive (Photo 1) and mappable across and along strike for a long distance. It is similar to rocks described by Fyon et al. (1987, 1988 and 1989) in Chamber and Strathy townships.

Mega-feldspar phyric flows contain numerous round to sub-round, 1-3 cm size feldspar aggregates in a dark green, chloritic matrix. Ocassionally the aggregates consist of a collection of smaller, subhedral to rhombic crystals and occur either in the selvages or the cores of the pillows. In areas of high strain the aggregates are elongated and lineated (Photo 1) and pillows are stretched. The core of deformed pillows contain 1-2 mm long,

streched white amygdules. All top indicators point north and indicate a south to north younging direction.

Based on similar textural features, the feldspar mega-phyric flows may be correlative with Archean gabbro-anorthosite bodies (Phinney, 1988) and the nearest such body described by Fyon et al. (1987, 1988 and 1989) is the Net Lake Intrusion and possibly the Kanichee Intrusion in Strathy Township or the younger Archean Hornblende Gabbro intrusion (map unit 4) that cuts the metavolcanic rocks in Banting Township

The upper unit consists of mafic pillowed and massive flows (map unit 1b) but without the distinctive feldspar aggregates or knots. Numerous thin and laterally discontinuous tuffaceous interbeds occur in the eastern portion of this unit. A series of well-formed pillowed and amygdaloidal flows define the top of the volcanic sequence and occur primarily in the central map area. Pillows are commonly less than 1m in size. They may contain 1-4mm size amygdules of quartz, calcite, sericite and chlorite, usually concentrated near pillow cores. Selvages are typically siliceous and leucocratic. Hyaloclastite occurs discontinuously in interpillow spaces. Subhedral to euhedral plagioclase and quartz filled amygdules up to 2.5 cm in size are present within pillows and selvages. Weakly to strongly foliated units with thin felsic bands defining elliptical shapes are widespread and probably represent deformed pillowed flows. The distinction between these units and intercalated tuffs within highly strained rocks is difficult.

All of the metavolcanic rocks are within the contact aureole of the Chambers-Strathy batholith and may be described as albite-epidote-chlorite or plagioclase-hornblende hornfels and schists. The hornfelses are most common adjacent to the intrusive contacts of the granitic rocks. They commonly consist of chlorite, tremolite-actinolite, hornblende, epidote, quartz and variably altered plagioclase. Grain size ranges from <0.01 mm to 2 mm and averages 0.5 mm. Chlorite-amphibole and quartz-plagioclase commonly exhibit lepidoblastic textures. Most original volcanic textures have been obscured or destroyed by metamorphism and deformation. Rare compositional banding occurs locally and may represent relict primary bedding features within tuffaceous rocks. In few places ash-sized plagioclase crystals have been observed in these rocks.

Smaller lenticular to sinuous metavolcanic bodies, usually less than 100 m wide, are enclosed by granitoid rocks. The bodies on the flanks of the main belt probably represent large xenoliths which have been passively block stoped by granitoid intrusions (cf. Card et al. 1973). Isolated xenoliths of metavolcanics within the granitic rocks and further away from the main belt of metavolcanics also occur, for example in the southwest, southeast and northeast corner of of the map area. Their relationship to the main belt in not readily apparent. The relative isolation and thinness of the metavolcanic units has increased their susceptibility to pervasive contact metamorphism during emplacement of the granitoid rocks. Consequently, the original mineralogic, geochemical and structural characteristics

of the metavolcanics have been obscured. It is therefore, difficult to determine the original volcanic protolith. Some metavolcanic xenoliths are relatively rich in quartz which may be attributed to silicification. These silicified rocks are generally fine- to coarse-grained amphibolites and minor schists which exhibit varying degrees of migmatization (Mehnert, 1971) and illustrate some agmatic (breccia), phlebitic (vein) and ptygmatic types of migmatite structures. Similar rocks have been described in Brigstocke Townships to the north of Banting Township by Born and Burbidge (1987). Here the volcanic rocks form a narrow greenstone belt which extends to the northeast from Mountain Lake across the southwestern corner of Brigstocke Township. Elsewhere in Brigstocke Township the metavolcanic rocks occur as narrow slivers or rafts within the felsic plutonic rocks similar to areas in Banting Township that border the granitic batholiths.

In some outcrops migmatitic metavolcanics exhibit nebulitic and agmatite structures, and parallel banding with ptygmatic sweats and feldspar porphyroblasts. The paleosome consists of quartz, feldspar and biotite and is typically dark, siliceous with common epidote veining prominent along some of the joint faces.

At other localities the amphibolites are cut by granitic veinlets. Some other outcrops of metavolcanic rocks exhibit plagioclase phenocrysts and light brown weathered and medium green fresh surfaces. These metavolcanics consist of medium- to

coarse-grained and recrystallized amphibolites with chlorite and plagioclase and amphiboles. They are also cut by granite.

Evidence of alteration is pervasive in thin sections. The alteration is characterized by granoblastic carbonate, and lesser epidote, quartz, sericite and magnetite. Plagioclase is mostly altered to epidote and sericite. A range of textural variations exists.

Fine-grained amphibolites are less common and are usually totally enclosed by granite or gabbro as remnant xenoliths caught up in intrusive rocks or migmatites. Some migmatized meta-volcanics of andesite composition exhibit pillows with the intrapillow hyaloclastite material being selectively replaced by the moblizate.

In thin section these fine-grained amphibolites are granoblastic and exhibit disseminated carbonate and chlorite growth in a retrograde metamorphic assemblage..

Other fine-grained mafic metavolcanic rocks are located adjacent to some veinlets and pods of granite which is either of igneous intrusive or migmatitic origin. They consist of granoblastic and equant hornblende and altered plagioclase represented by retrograded muscovite and epidote with a grain size of 0.2-0.4 mm. In handspecimen these rocks have the appearance of a medium-grained and dark green, plagioclase-phyric flow.

Intermediate to Felsic Pyroclastic Rocks

Intermediate to felsic pyroclastic rocks also occur in the main belt and overlie the mafic volcanics. Contacts between units are sharp to gradational. Intercalation of mafic and intermediate metavolcanics is common on all scales (Photo 2).

Heterolithic tuff-breccia generally occupies the northern flank of the main belt of metavolcanics rocks and is distinguished by the presence of lapilli- to bomb-sized lithic fragments of various lithologic composition (Photo 2). There is apparently a transition within this unit from more felsic, locally fragment-supported tuff-breccia in the western and eastern portions of the belt into a central, more mafic, matrix-supported unit chacterized by large, epidotized bombs. This transition reflects gross distribution patterns of coarse to fine intercalation of coarse and fine material is common on a small scale.

Heterolithic lapilli-tuff and tuff-breccia are best exposed southeast of Carrying Lake (Photo 2). Lapilli-sized fragments predominate and locally may comprise up to 75% of the rock. They are ellipsoidal to subangular and elongate. Their shape and orientation are a result of deformation. Fragments are aligned parallel to a sub-vertical foliation in the ash matrix. Within discrete tuffaceous beds there is no discernable bedding features, however, well defined bedding features are exhibited by sharp contacts between individual tuffaceous beds. Alternating very- to extremely- thick-bedded units reflect changes in matrix and fragment composition, size and a relative proportions of lapilli clasts to matrix ratio. Essential fragments of crystal

and tuff predominate, with lesser pumiceous and rhyolite lapilli lithic fragments. The matrix ranges in composition from a dark green mafic tuff to a light grey-green coarse tuff with conspicuous plagioclase and quartz crystals. Variations in matrix composition and grain size may be the result of alteration and/or metamorphic recrystallization. Siliceous alteration haloes surrounding fragments have been noted and indicate in-situ silicification.

The central portion of the heterolithic tuff-breccia unit is characterized by epidotized felsic lapilli and bombs up to 3 m in length. The mafic to intermediate matrix is schistose and contains 10 to 30% fragments which may coalesce during deformation.

Generally there is little fine-grained matrix in the rocks of this unit in the central part of the volcanic belt. Therefore, this rock unit possibly represents a proximal vent facies. To the east and west from the central part of the volcanic belt distribuiton of fine to coarse clasts defines a possible proximal to distal transition.

Petrochemistry of the Metavolcanic Rocks

Samples of 15 Archean metavolcanic rocks were collected for whole rocks analyses (Table 2) by X-Ray Laboratories, Toronto, Ontario. Sample locations are given in Figure 4. The main purpose of the analyses is to determine the geochemial affinities of the metavolcanics. The analyses are illustrated on several

plots commonly applied to volcanic rocks namely a cation plot (Jensen, 1976, Figure 5) and a standard AFM weight percent diagram (Figure 6, Irvine and Baragar, 1971). In these figures approximately half of the samples plot in the tholeiitic field and half in the calc-alkalic fields. Within the tholeiitic field, two samples plot as iron-rich varieties whereas the seven others are magnesium-rich tholeiites. It should be noted that sample #2 is from a feldspar knot and thus does not constitute the bulk composition of the mafic volcanic in which it is hosted. Most of the tuffaceous rocks plot in the calc-alkalic field in both diagrams as dacite, andesite and basalt. All amphibolites from the Breeches Lake area are enclosed in granites and also plot as calc-alkalic basalts and andesites. Significant alteration and silicification from the granite host rocks probably caused these samples to become more silica-rich than their original mafic metavolcanic protolith. Thus it could be concluded from the uncontaminated and unsilicified samples that the mafic volcanic sequence is generally a tholeiite with an iron-enrichment trend overlain by intermediate to felsic pyroclastic volcanic package of calc-alkalic affinity. These results agree with similar studies in Brigstocke Township (Born and Burbidge,1990), and in the Temagami area by Fyon et al (1987,1988 and 1989). Thus, there is a good geochemical correlation which confirms the lithological and structural similarities between the volcanics in Banting Township and squence "A" of Fyon and Cole (1989). These rocks probably

represent the oldest volcanics in the Temagami belt (Fyon and Cole, 1989).

Plotting of metavolcanic whole rock geochemistry on a total alkali versus silca diagram (modified after Cox et al. 1979) reveal a range in chemical compositions (Figure 7). The rocks range in compostion from tholeiitic or sub-alkalic basalt, through basaltic andesite to andesite. A felsic pyroclast from the tuff-breccia is a rhyolite.

Several binary plots illustrate elemental differences between the mafic metavolcanics and the more siliceous amphibolites and pyroclastic rocks. The weight percent plot of SiO_2 vs Na_2O+K_2O (Figure 8) indicates that all of the samples are sub-alkalic and thus can be plotted on diagrams such as Figures 4 and 5. The K_2O/Na_2O vs Si_2O plot (Figure 9) indicates that the more siliceous pyroclastic and contaminated amphibolites exhibit lower K_2O/Na_2O values and define a separate trend than the more mafic igneous flows. Similar trends are also reflected in the Mg/Mg+Fe vs Cr plot (Figure 10) with most mafic flows having higher Cr values for any given Mg number of .12 to .40. The Al_2O_3 vs MgO/(MgO+FeO) plot (Figure 11) indicates a range of Mg values for all rock types but the Al_2O_3 values are consistently higher in the pyroclastic and contaminated amphibolites (15.6-24% Al_2O_3) than in mafic metavolcanics (12-15.5% Al_2O_3). In the MgO vs Ti_2O plot (Figure 12) mafic metavolcanics generally have higher MgO (4-9%)and Ti_2O values (0.8-2%)than the pyroclastic or contaminated amphibolites which have 3.5-5% MgO amd 0.4-0.82% TiO_2. The range of TiO_2 and Mg values shown in the mafic

volcanics is typical of tholeiitic volcanics and one of the more reliable and discriminatory characteristics.

Hypabyssal Intrusive Rocks

Hypabyssal intrusive rocks (map unit 3), namely feldspar porphyry dikes represent a relatively rare lithology exposed only in a series of outcrops to the east of Lundy Lake.

Small feldspar porphyry dikes intrude the metavolcanics. They are characterized by 2 to 5 mm subhedral to euhedral feldspar phenocrysts in an aphanitic groundmass. Small (< 2 cm) rounded mafic xenoliths are locally present and usually are less resistant to weathering than the host metavolcanic rocks. Similarities exist between the porphyry dikes and intrusive gabbro (map unit 4) which intrudes the metavolcanic belt along its southern margin. Rocks of map unit 4 occur along the southern contact of the metavolcanic belt and are rich in magnetite. The porphyry dikes are fine grained and intrude pyroclastic rocks rather than mafic tholeiitic volcanics. The gabbro is more coarse-grained and tholeiitic in nature. The dikes occur along the northern edge of the volcanic belt, the gabbro along the southern edge of the metavolcanic belt.

Intermediate to Ultramafic Intrusive Rocks

A large, arcuate body of intermediate to ultramafic intrusive rocks, 100 to 750 m wide, is situated along the southern margin of the main metavolcanic belt. The gabbric rocks may represent a subvolcanic intrusion, are considered to be

intrusive and postdate the metavolcanics. This interpretation is based largely on crosscutting relationships, the presence of metavolcanic xenoliths and the similarity of these rocks to similar rocks of the Net Lake Intrusion and possiblly the Kanichee Intrusion to the south in Strathy Township (Bennett 1978, Fyon et al 1987,1988 and 1989).

Hornblende gabbro is distinguished by its coarse-grained, mottled dark green to black and white appearance. It is weakly to strongly foliated, commonly parallel to contacts with granitoid intrusions. The rock is fine grained in some areas and superficially resembles an ultramafic fine-grained rock. Disseminated to semi-massive magnetite with minor pyrite and chalcopyrite locally comprise up to 25% of the rock but commonly makes up less than 10 % of the rocks. Quartz in the hornblende gabbro is notably absent but occurs in an associated quartz diorite.

Plagioclase and hornblende together comprise approximately 90 to 95% of the rock. Subhedral to euhedral, 2 to 8 mm crystals of pleochroic brown to green hornblende form a granular, foliated to decussate texture. There are minute (<0.01 mm) inclusions of magnetite along hornblende cleavage traces. Poikilitic inclusions of plagioclase and minor quartz in crystal cores are common. Accessory minerals such as chlorite, calcite, quartz and sulphides and oxides are found interstitial to the hornblende and plagioclase. Plagioclase occurs as variably saussuritized laths up to 4 mm in length.

Dioritic rocks constitute the border phase of the hornblende gabbro and occupy the western part of the intrusion. Their relationship to the gabbroic rocks is unclear. Isolated xenoliths of hornblende gabbro in diorite have been observed and suggest separate intrusive events. Gabbroic and dioritic rocks may represent the lower and upper levels of a composite intrusion, respectively. Diorite and quartz diorite are distinguished from granite by their characteristic mottled "salt-and-pepper" texture, and from the hornblende gabbro by their greater proportion of felsic minerals and the presence of macroscopic quartz. They are medium -grained, massive to foliated, equigranular rocks. Hornblende and plagioclase occur in roughly equal amounts; quartz may comprise up to 20% of the rock. All minerals occur as anhedral to subhedral grains 1 to 2 mm in size and in places form larger, crystal aggregates (Photo 3). The composition of plagioclase is indeterminate because of its pervasive saussuritization. Chlorite, apatite, calcite and zircon are accessory minerals. Biotite is notably absent.

In the gabbro, as in the adjacent volcanics, there is evidence of ductile and brittle deformation such as fractures. These fractures in places, are occupied by grantic dikes. Some local partial melting or migmatization also occurred.

Rocks similar to the gabbros of the map area also occur to the north in Brigstocke Township (Born and Burbidge,1990). These corresponding rocks types have been generally mapped as mafic diorite and as part of the larger and more diverse granite basement complex, not as a separate intrusive unit. Other rocks

which may also be correlative are some of the coarse-grained amphibolites common to the metavolcanic belt near Mountain Lake in the northeastern part of the map.

Petrochemistry of the Intermediate to Ultramafic Intrusive Rocks

Geochemical analyses of four representative gabbro and four diorite samples are presented in Table 3. Sample locations are shown in Figure 4. These rocks basically reflect a tholeiitic geochemical affinity similar to the mafic metavolcanic rocks which they intrude and plot into the respective gabbro and diorite fields on the binary weight percent plot of SiO_2 vs Na_2O+K_2O (Figure 7).

Intermediate to Felsic Intrusive Rocks

Approximately 80% of the Archean basement rocks in the study area are granitic plutonic rocks. Card et al. (1973) have noted that granitic bodies elsewhere in the area occur as discrete plutons, 6 to 13 km in diameter, whose margins are marked by narrow metavolcanic belts and/or migmatitic zones. In the present area it is difficult to define batholithic boundaries because the rocks are not homogenous throughout and because the granitic rocks are in places overlain by younger rocks. Granitoids in the southern part of the map area comprise the northern part of the Chambers - Strathy Batholith (Bennett 1978; Fyon et al 1987,1988 and 1989; Fyon and Wheatley, 1988). Similar rocks in the northern part of Banting Township lie within

spatially, but not necessarily petrologically, distinct bodies termed the Whitewater, Snare and McLean granites (Card 1979).

Crosscutting relationships and lithologic variety are indicative of a complex intrusive history. The most predominant rock type is a homogeneous, foliated granite which appears to be the earliest phase of the felsic intrusive sequence. The later phases are dikes of non-foliated granite, aplite, and pegmatite and quartz veins. Mylonitic and migmatitic phases have resulted from deformational and assimilation processes.

Most felsic intrusive rocks of the area are coarse- to medium-grained, massive to foliated, equigranular granites. Other felsic intrusive rocks such as alkali-feldspar granite and granodiorite and late aplite and pegmatite, comprise a subordinate portion of the granitoids.

Local granites are phaneritic, medium- to coarse-grained, light grey to pink rocks. Alkali feldspar granites are commonly brick-red in colour, presumably due to the presence of microscopic hematite in the feldspar. Hematite - rich zones are distinct within the outcrop and are spatially associated with fractures and joints. This suggests that hematization in the granite is related to deuteric alteration.

In thin section the granites consists of quartz (20 to 40%), albitic plagioclase (5 to 15%) and microcline, and/or perthite (30 to 50%). Quartz occurs interstitially to the feldspars as anhedral aggregates. It typically develops subgrains with sutured, lobate grain boundaries and displays undulose extinction, even in weakly foliated rocks. Feldspars

are subhedral and variably altered to sericite and/or epidote. Banded to flame-like perthites predominate in many rocks. Epidote, calcite, magnetite and chlorite, pseudomorphic after biotite, are the common accessory minerals.

Porphyritic granites are characterized by subhedral to euhedral phenocrysts of feldspar and quartz up to 15 mm long. Glomerocrysts of quartz, plagioclase and alkali feldspar may occur in a fine-grained, equigranular matrix.

Porphyritic rocks are present but are not common. They have been noted on the northern shore of Guppy Lake and east of Gilbert Lake.

Modal anaylses of the granitoid rocks indicate a granite composition (Streckeisen, 1976) for rocks which comprise the northern part of the Chambers-Strathy batholith (Bennett, 1978). These rocks in adjacent Strathy Township were previously refered to as quartz monzonites by Bennett (1978) under a different classification scheme.

Migmatites

Along the southern margin of the volcanic belt metavolcanics are migmatized. Rafting or roof pendant development near the top of the intrusion has been observed. Sharp, slightly irregular contacts of the granitic leucosome with the metavolcanics occur. Narrow, sub-parallel, intercalations of volcanic rocks and granitic material is common. Zones of extensive migmatization also extend along the northern boundary of Banting Township, close to Anima-Nipissing and Mannajiugama Lakes.

The degree of granite veining and diking in the volcanics increases towards the main intrusive body. Passive block-stoping of volcanic material during emplacement of the granitic rocks has resulted in development of agmatitic structures similar to those described both in the nearby Maple Mountain Area, and Brigstocke Township by Card et al (1973) and Born and Burbidge (1987), respectively.

Migmatites, megascopically composite rocks consisting of distinct granitic neosome and paleosome components (Menhert, 1968), are developed along batholith margins in contact with older intrusive and metavolcanic rocks. Although in the narrow definition of the term, migmatite commonly infers partial or complete melting of the paleosome component, most local migmatite-like rocks display relatively little assimilation, alteration and/or melting of the paleosome. They may be more aptly described as a type of igneous intrusive breccia in some cases. These rocks are spatially associated with metatectic migmatites in which definite partial melting and deformation has occurred. Intercalation of these two broad varieties of "migmatitic" rocks with country rocks and each other precludes their distinction at map scale. Migmatitic zones straddling granite-country rock contacts attain widths of several metres to 1.6 km (1 mile) in the south-central map area (Photo 4).

Agmatic (breccia), schollen (raft) and phlebitic (vein) structures are typical in weakly deformed or altered migmatitic rocks. Aplite, pegmatite and granite comprise the leucosome or matrix and are commonly manifested as anastomosing or reticulate

dike networks (Photo 5). The degree of brecciation and xenolith assimilation increases from the country rock toward the granitic body. The orientation of tabular, stoped xenoliths is commonly parallel to contacts and to local, highly variable foliation in the country rocks. Later granitoid dikes and quartz veins are usually oblique to thes fabrics and structures.

Metatectic migmatites are characterized by stromatic (layered), schlieric, and ptygmatic structures. Partial melting is usually manifested in the segregation of the melanocratic and leucocratic components of the migmatitic into distinct haloes or envelopes around xenoliths. This is commonly accompanied by the destruction of primary textures, structures and mineral assemblages. Metavolcanic xenoliths may superficially resemble hornblende schist or quartz - feldspar - hornblende gneiss in outcrop, due to partial melting, mineral segregation and/or addition of felsic minerals.

Brecciation and migmatization are believed to have been repeated processes in the formation of these rocks. Crosscutting relationships are developed in metatectic migmatites as well as in igneous breccias and dikes. Isolated occurrences of heterolithic igneous breccia containing xenoliths of metavolcanics, hornblende gabbro, quartz diorite and granite in a granite matrix, are illustrative of the extensive degree of brecciation, scavenging and mixing that has occurred. The coincidence of metatectic migmatites, igneous breccias, dikes and deformation zones with granitic contacts suggests that their respective development was essentially coeval and related to

batholith emplacement. The abundance and extensive areal distribution of large metavolcanic xenoliths in the granite may reflect their passive block stoping during intrusion and their preservation as roof pendants in the upper levels of the intrusion.

Mylonitic Rocks

Mylonitic rocks have been identified in several faults and deformation zones in the vicinity of Jamieson Lake and the Anima-Nipissing River.

Mylonitic rocks have only been recognized within the granites and are recognized in the field by the presence of highly strained, foliated, fine-grained zones within medium- to coarse-grained, somewhat foliated rock. Such zones may be sharply bounded and range in width from less than 1 cm to 2-3 m (Photos 6 and 7). Despite textural and mineralogic variations in local quartzo-feldspathic mylonitic rocks, common characteristics exist that attest to the high degree of deformation (Photo 7). Quartz subgrains, 0.1 to 0.2 mm (0.004 to 0.008 inches) in diameter, are ubiquitous and have sutured, lobate grain boundaries. Highly strained quartz may develop into rod-shaped aggregates 2 to 3 mm (0.08 to 0.12 inches) wide and several centimetres long.

Foliations are weakly to strongly developed and curve around larger feldspar grains, which commonly have micaceous strain shadows. Mechanical twinning produces "chessboard" albite, which resembles microcline. Bent, broken and displaced polysynthetic twins are common in plagioclase. Conjugate sets of narrow zones

of intense sub-grain growth in plagioclase have been observed. Annealed textures result from post-deformational recrystallization. The majority of mylonitic rocks are protomylonites. Mylonites, which consist mainly of fine recrystallized plagioclase sub-grains, are present but rare. Even weakly foliated granites far removed from high strain fault zones show significant quartz sub-grain growth.

Peterochemistry of the Granitoid Rocks

Whole rocks geochemical analyses of 11 representative samples of the granitic rocks are presented in Table 4 and their location in Figure 4. These samples plot in the granite field on the binary weight percent plot of SiO_2 vs Na_2O+K_2O (Figure 7). Normative plots of these analyses and corresponding modal estimations show that they basically represent a granite composition according to the Streckeisen (1976) classification (Figure 13). This is entirely in agreement with estimates of alkali feldspar, plagioclase feldspar and quartz obtained from petrographic examinations. Figure 14 is another normative plot that illustrates the respective normative feldspar compositons. According to a classification scheme using these proportions (Barker 1979), the rock types fall approximately half into the trondjhemite field and half into the granite field. Generally all of the trondjhemitic rocks are from strongly foliated samples and the more massive and porphyritic varieties are classified as granites. This type of distribution of granitoid rock types is identical to similar findings by Fyon and Cole (1989) in an area

directly to the south of Banting Township. They conclude that a chloritic trondhjemite occurs principally in Chambers Township whereas the granitic phase occurs in northern Strathy Township.

Major element and Rare earth patterns indicates that the chloritic trondhjemites are characterized by Al_2O_3 values in excess of 14.5 weight %, and fractionated REE patterns with La_N/Yb_N= 10 to 22, and have negative europium anomoly (Eu/Eu^*=-0.6 to -1.0). Granitic rocks generally have less than 14.5 weight % Al_2O_3 with less fractionated La_N/Yb_N= 4 to 6 but display a marked, negative europium anomoly (Eu/Eu^*=-5.2 to -13.7).

Fyon and Cole (1989) tentatively conclude that the trondhjemitic phases of the Chambers-Strathy batholith were comagmatic with the cal-alkalic, metavolcanic rocks in northern Chambers (sequence "A"). Intermediate to felsic pyroclastic rocks that occur in central Banting Township are probably correlative with the sequence A rocks decribed and characterized by Fyon and Cole (1989). The granites however have less fractionated "tholeiitic-like" REE patterns with significant europium anonalies. These patterns are similar to dacitic and rhyolitic metavolcanic rocks east of the Net-Vermillon Lake fault (sequence B).

Studies by Fyon and Wheatley (1988) on the Strathy-Chambers batholith indicates that the batholith represents a hypersolvus intrusion with water presssures of less than 5 Kb and temperatures ranging from 660-900° C. There is also some possible magmatic epidote that indicates the presence of a mixed water-CO_2 fluid phase.

Fyon and Cole (1989) concluded that the composite and or separate batholith was intruded proior the earliest north-south compressional event and prior to development of the Net-Vermillion lakes deformation zone.

Comparison of the granitic rocks in Banting Township with similar rocks to the north indicates that a larger variety of felsic plutonic rocks occur in Brigstocke Township (Born and Burbidge, 1990). Much of the granitic terrain in Brigstocke Township commonly contains agmatitic and migmatitic textures and consist of rocks probably more correlative with the roof pendenant zone in Banting Township. The bulk of the granitoid rocks in Brigstocke Township are either granodiorites or granites with lesser amounts of quartz diorite, tonalite, trondhjmetite and mafic diorite. The latter is probably equivilent to the gabbro-diorite (map unit 4) in Banting Township. Large volumes of homogenous, foliated granite are common in Banting Township whereas a more heterogenous grantoid assemblage occurs in Brigstocke Township.

Mafic Intrusive Rocks

Post-granite, presumably Late Archean intrusive rocks are :

(1) lamprophyre and other mafic dikes

(2) pyroxene-phyric mafic to intermediate dikes, stocks

(3) diatreme and igneous breccias.

Lamprophyre and other mafic dikes

Lamprophyre and other mafic dikes are straight to irregular bodies 1 to 15 m wide. Usually they are small and discontinuous. Some dikes can be traced for distances of greater than 2.5 km. These long dikes are dominantly north-trending and occupy major lineaments or faults.

Lamprophyres are typically dark green to black on weathered and fresh surfaces. They tend to weather more easily than the intruded rocks, which for the most part are granites. Steeply dipping joints are developed in some of the wider dikes. Chilled margins are narrow (1 to 5 cm) and indistinct. Some lamprophyres, especially those with irregular shapes, contain xenoliths which comprise up to 20% of the dike. Xenoliths of granite and other lamprophyres range in size from 2 cm to several metres, averaging 10 to 20 cm. The xenoliths are sub-angular to rounded, indicating various degrees of in-situ milling and assimilation. Alteration of the xenoliths is minimal.

Locally, the lamprophyres are porphyritic with fine-grained matrices. They have been subdivided on the basis of their phenocrysts into phlogopite-(augite-) and hornblende-lamprophyres. The original mineralogy has been altered by deuteric and/or later processes.

Phlogopite-(augite-) lamprophyre occurs in the southern part of Banting Township. In thin section (Photo 8), conspicuous phlogopite phenocrysts, less than 2 mm long, occur in a fine-grained (< 0.5 mm) matrix of subhedral, calcic plagioclase and tremolite-actinolite. Augite has been uralitized. Primary calcite ocelli or infilled gas cavities are 0.5 mm in diameter,

and are overgrown by later growth of phlogopite. Secondary scapolite is closely associated with the ocelli. Fine-grained chlorite and disseminated magnetite grains are ubiquitous.

Hornblende-lamprophyre occurs as north-trending dikes in the northeast corner of the study area. Corroded hornblende phenocrysts are small (<0.5 mm) lathlike to subhedral crystals. Colourless, inclusion-rich hornblende phenocrysts are in places mantled by brown hornblende. Opaque inclusions are concentrated in the cores of phenocrysts and along cleavage traces and may comprise up to 50% of the host crystal. The aphanitic matrix consists largely of chlorite and tremolite-actinolite which have grown at the expense of feldspars. Some euhedral, skeletal ilmeno-magnetite grains are also present.

Similar, fine-grained, non-porphyritic mafic dike rocks also occur. They are narrow and contain a higher proportion of felsic minerals than the porphyritic lamprophyres described above. They have a fine-grained, granular matrix consisting of anhedral plagioclase, variably altered to saussurite and chlorite, and acicular to lathlike tremolite-actinolite crystals <1 mm long. Chlorite and epidote are also common, occurring as sheaf-like aggregates and stubby, anhedral grains, respectively. The most significant feature perhaps, is the presence of rare, pod-like patches of optically continuous calcite, up to 1 cm long. Calcite pods are rimmed by a fine-grained, translucent mineral resembling leucoxene. Calcite also occurs as small (<0.02 mm) isolated rhombs. The carbonate pods are either primary magmatic or are related to deuteric or near-surface alteration processes.

Anima-Nipissing River and Snare Creek Intrusions

A group of mafic to intermediate intrusive rocks occur as several small stocks, dikes and igneous breccias. They are exposed in two main bodies along the Red Squirrel Road. The western one lies between the Anima-Nipissing River and Tyndall Lake, while the eastern body is situated a few hundred metres west of Snare Creek. The restricted areal extent of these rocks and their morphologic and petrologic similarities suggest a common origin.

The intrusive bodies consist of medium- to coarse-grained equigranular to porphyritic mafic to intermediate rocks. An arcuate breccia zone envelopes the intrusions of the western body. This breccia consists entirely of large, angular, unaltered blocks of host metavolcanics up to several metres in size. The absence of an igneous matrix and the interlocking nature of the fragments indicates in-situ brecciation, perhaps by gaseous explosion. This "explosion" or diatreme breccia occupies the contact zone between country rocks (metavolcanics and granite) and the intrusive bodies.

Small pyroxene-phyric mafic dikes, up to 2 m (6.6 feet) in width, intrude the diatreme breccia. They resemble fine- to medium-grained diabase and contain subhedral pyrite grains 3 mm in size as well as larger pods of pyrite up to 1 cm long. Pyroxene phenocrysts (1 to 3 mm) occur and are uralitized. Tabular to lathlike plagioclase grains less than 2 mm long are

altered to chlorite and epidote. The fine-grained matrix consists of altered feldspar and acicular tremolite-actinolite.

Medium- to coarse-grained pyroxene-phyric mafic rocks comprise the bulk of the intrusive rocks. They have a circular to arcuate surface expression, 100 to 500 m in diameter. Uralitized pyroxene phenocrysts up to 1 cm across occur in a fine- to medium-grained matrix of altered plagioclase and tremolite-actinolite. Phenocrysts may comprise up to 50% of the rock.

Igneous breccias that surround the intrusive bodies are composed of angular xenoliths of the spatially associated and surrounding rocks, namely fragments of pyroxene phyric gabbro, in addition to fragments of metavolcanic and granitic rocks and quartz veins up to 60 cm in size. Near their margins, the igneous breccia is manifest by the formation of reticulate dikes which illustrates incipient in-situ brecciation and stoping. In the central portion of the breccia, however, the proportion of matrix to xenoliths is roughly equal (Photo 9). The presence of exotic xenoliths possibly indicates scavenging and transport from depth. The angularity of in-situ volcanic fragments and the lack of matrix suggests that it may represent an explosive (gas escape ?) diatreme breccia which is spatially related to the fault systems.

The matrix of the breccia is varied-texture, fine, medium to coarse grained and noticeably more felsic than the other intrusive rocks of the map area. Phenocrysts of uralitized pyroxene, plagioclase, phlogopite and quartz up to 3 mm are conspicuous on weathered surfaces. Crosscutting relationships

indicate that the small, discontinuous felsic dikes apparently postdate breccia development.

Large zones of hydrothermal alteration, characterized by fracture and joint fillings of epidote and hematite occur around the Snare Creek intrusion and extend up to 500 metres into the surrounding granitic host rocks. Paramorphic mineral assemblages and whole rock geochemistry (Table 5) suggest that these rocks are pyroxene-phyric melagabbro, gabbro and diorite.

The distinctive epidote-hematite alteration halo around the easternmost intrusions is indicative of local hydrothermal activity during or after the intrusion of the stock.

Comparison of the mafic to ultramafic intrusive suite described in this section with similar rocks in adjacent areas indicates that several similar intrusions occur in both Chambers and Strathy townships and in Brigstocke Township. In Chambers Township lamprophyre dikes cut the Chambers-Strathy batholith and occur near the margins of regional deformation zones. These have been described by Bennett (1978) and by Fyon et al. (1987, 1988 and 1989) as biotite lamprophyre dikes that are preferentially localized within or adjacent to zones of high strain (deformation zones). The dikes have two main orientations directions of north and N60^{o}W, parallel to some deformation zones and Proterozoic diabase dikes. Biotite lamprophyres cut the outer margin of the Iceland Lake and the Spawning Lake stocks (Fyon and Cole, 1989).

Rocks similar to the lamprophyres and diatremes of Banting Township also occur to the north in Brigstocke and Kittson townships (Born and Burbidge,1990). Here, lamprophyre dikes

generally trend in a northerly direction and consist of biotite- and phlogopite-rich ultramafic dikes that range in width from 1-30 metres. The intrusive relationships suggest a Late Proterozoic age because in one outcrop the dikes cut Early Proterozoic sediments of the Coleman Member of the Gowganda Formation. Diatreme breccias also occur and cross-cut all Early Proterozoic sedimentary rocks of the Coleman Member and the Firstbrook Member of the Gowganda Formation and also the Lorrain Formation. Other related lithologies also include "Lake Temagami-type breccias" within arkoses of the Lorrain Formation that are related to north-trending structural lineaments and show evidence of in-situ milling similar to the lamprophyres.

In Banting Township the undeformed nature of the lamprophyre intrusions suggests emplacement after the last Archean deformational event (D3). This data does not then conflict with a younger age post-dating the deposition of the Coleman Member as indicated by field evidence elsewhere, namely Brigstocke Township. Also the general undeformed nature and unaltered mineralogy is most similar to Late Proterozoic olivine dikes of the Sudbury Swarm which were also emplaced along major pre-existing structural lineaments. Thus there are several reasons as mentioned above to question a Late-Archean age for this rock suite. The observation made here would suggest a Late-Proterozoic age for this suite of rocks.

Petrochemistry of the Lamprophyric Suite of Rocks

Representative geochemical analyses from 8 samples of the lamprophyric suite of rocks are presented in Table 5. Locations are given in Figure 4. Although most common geochemistry plots are usually reserved for volcanic rocks, they can also be used to compare and contrast composition of magmatic liquids from which these intrusive rocks crystallized. It is also known that in the case of most dike rocks the whole rock bulk composition is a close approximation of the intial liquid composition.

On the binary weight percent plot of SiO_2 vs Na_2O+K_2O (Figure 7), these samples plot in various fields: Mafic dikes plot as diorite, lamprophyres as gabbros, and the pyroxene-phyric gabbro in a range from gabbro to diorite to monzonite. However, a more discriminating plot such as a standard geochemical cation plots (Figure 15) illustrate the predominant ultramafic nature of most samples. This data is also plotted in a standard AFM diagram (Figure 16).

The most striking feature of lamprophyre geochemistry is the marked lack of Na_2O and K_2O (Table 5) as compared to other lamprophyres (Cox et al., 1979). This could reflect a major primary difference or alternativley represents near surface alteration and alkali leaching which may coincide with the syn- to post-intrusive hydrothermal activity that produce the surrounding epidote-hematite alteration zone.

There is an observed progressive increase in the amounts of Na_2O + K_2O and SiO_2, and a progressive decrease in Cr (Table 5) from presumably early gabbroic dikes, through the main intrusive phases to late igneous breccia. This trend may represent either

igneous fractionation of a parental magma and/or hydrothermal alteration involving selective silicification and alkali metasomatism or leaching. Further sampling and petrography is required to throughly test theses hypotheses.

The morphology and field relationships of the intrusive rocks may be interpreted on the basis of a diatreme or breccia pipe model, similar to that described by McCallum (1976). Upward migration of mafic to ultramafic magma was perhaps facilitated by regional faulting such as along the Anima-Nipissing River Fault. The initial phase of emplacement involved explosive, in-situ brecciation of the country rocks. This was followed by intrusive and igneous brecciation events and subsequent hydrothermal alteration of the intrusive body and the surrounding host rocks..

Rare Earth Element Geochemistry

Three samples of mafic to intermediate intrusive rocks from the Anima-Nipissing River Intrusion and one sample of a mafic dike exposed near the Anima-Nipissing River Fault were analyzed for La, Ce, Nd, Sm, Eu, Tb, Yb, and Lu (Table 6). Rare earth element (REE) contents were chondrite normalized and plotted (Figure 17).

REE distribution trends are similar for all four samples. All samples are characterized by moderate light REE enrichment ($(La/Lu)_{cn}$ = 4.29 to 9.29) and small, negative Eu anomalies. Eu/Sm ratios lie in a very narrow range from 0.235 to 0.245. These data, although limited, suggest similar geochemical characteristics and perhaps a common petrogenesis for these rocks

but the REE geochemistry of these local rocks is not diagnostic in their classification (cf. Cullers and Graf 1984 a,b).

Generally the REE patterns for lamprophyric rocks from other lamprophyric suites documented in the literature are fairly distinctive (Henderson,1984). Normally, the REE abundances an LREE/HREE ratios are large $(La/Lu)_{cn}$= 20-55 and similar to the REE content of kimberlites; there are no Eu anomalies (Eu/Sm=0.22-0.29). There may be a correlation of increased LREE content in lamprophyres with increased alkalinity. Petrogenesis of lamprophyres includes only 5% melting of an upper mantle peridotite followed by fractional crystallization or volitile transport (Henderson, 1984) from deep crustal sources.
REE analyses of Figure 17 illustrate a lower abundances of REE and much less fractionated LREE pattern than those described by Henderson (1984) and only slightly HREE enriched with no Eu anomaly. The slope is fairly flat and more typical of komatiitic rocks. This feature reflects the fact that most of the analysed REE samples of the "lamprophyre suite" are in fact pyroxene-phyric gabbro or ultramafic intrusives and not micaeous lamprophyres in sensu stricto. This is also in agreement with the cation plot which indicates the majority of the rocks have a komatiitic geochemical affinity. Thus, it is believed that the REE patterns for "lamprophyric" rocks from Banting Township are not that similar to common lamprophyres but more typical of ultramafic rocks.

A alternative petrogenitic hypothesis for this suite of rocks might invoke a carbonatite origin. However, typical

carbonatite REE patterns are very different to the Banting suite of mafic to ultramafic rocks. Carbonatites contain the largest REE contents (REE=72-15 515 ppm) and LREE/HREE ratios $(La/Lu)_{cn}$= 7.1-1240) of any rock types (Henderson, 1984) as indicated by the typical strongly fractionated patterns. Both of these features are incompatable with the Banting REE data.

Correlation with similar REE data from "lamprophyre" dikes located in Chambers and Strathy Township (Fyon et al 1987,1988 and 1989) is fairly good. It shows that both the relative abundances and HREE fractionation trends are similar and not typical to most lamprophyres documented in the literature.

Considering the geochemical and field relations of the ultramafic ("lamprophyric") suite of rocks in Banting Township, it is possible to correlate them with similar rocks in Brigstocke Township in the vicinity of Mountain Lake (Born and Burbidge, 1990). These rocks are correlative with ultramafic intrusive and possible extrusive rocks. As in Banting Township, their general undeformed nature indicates a relative age which post-dates the last Archean deformation, and the crosscutting relationships also suggests that the dikes post-date emplacement of the granitic plutons.

EARLY PROTEROZOIC

Huronian Supergroup

Cobalt Group

<u>Gowganda Formation</u>

The Coleman Member of the lower Gowganda Formation unconformably overlies the Archean basement and represents the only Proterozoic sedimentary rocks in the study area. These rocks are gently dipping and occupy a narrow trough that extends northeastward from Red Squirrel Lake, and bifurcates northward and northeastward through Anima-Nipissing and Gilbert lakes, respectively. A small outlier is also exposed along the southern and southwestern shores of Whitewater Lake. The unconformity is exposed in several locations and reflects a smooth to very irregular paleotopography of low to moderate relief.

Sediments of the Coleman Member have been most recently described by Born and Burbidge(1990), Mustard and Donaldson (1987) and Burbidge (Ph. D. thesis, University of Ottawa, in progress) in the Lake Anima Nipissing, Cobalt and Lake Temagami areas, respectively. The nomenclature of Mustard and Donaldson (1987) has been adopted in classifying local rocks.

The predominant local Coleman Member lithofacies are basal breccia, diamictite, sandstone and mudstone. Units typically have limited lateral continuity and are complexly interbedded.

A basal breccia is preserved in several locations and consists of angular fragments of subjacent Archean granitic and metavolcanic rocks. Local exposures are believed to be the most extensive and well-preserved examples of the basal breccia of the Gowganda Formation documented anywhere. Outcrops east of Snare Lake cover an area of approximately 2000 m^2. The breccia attains a maximum thickness of 1.5 m. The matrix to the fragments is massive to thickly laminated mudstone or siltstone which appears

to drape over fragments and infill spaces between them (Photo 10).

Diamictite, a poorly sorted admixture of mud, sand and gravel, invariably comprises the basal portion of the sedimentary sequence execpt where the basal breccia is present. It also occurs as interbeds at higher stratigraphic levels. The lithology is polymictic and contains sub-rounded to rounded, pebbles to boulders of Archean rocks, including rare massive sulphide and quartz clasts. An increase in the degree of sorting during deposition is reflected in the local development of internal stratification, graded beds and interbedded orthoconglomerate in stratigraphically higher diamictite units.

Thin- to medium-bedded and interbedded sandstone and mudstone are the most abundant lithofacies. Sandstone is commonly pebbly (>5% gravel) and massive, but it also occurs as lenses in thinly bedded mudstone (Photo 11). Load casts, pseudonodules, ball-and-pillow structures and planar crossbedding are evident in interbedded sandstone and mudstone. Crossbedding defines paleocurrent flow from the north or northeast.

Mudstone is generally thickly laminated or very thinly bedded, commonly with thinly interbedded siltstone. It generally lacks primary sedimentary structures. However, slump folds have been observed in thick sequences (Photo 11).

The Coleman Member has been ascribed a glaciogenic origin (Schenk, 1965; Lindsey, 1969), most recently by Mustard and Donaldson (1987). Basal breccia and basal diamictite represent periglacial regolith and primary till, respectively. Interbedded

sandstone - siltstone - conglomerate/diamictite results from subaqueous outwash fan and interfan deposition. A relatively thick, monotonous section of mudstone, exposed on the southwest shore of Whitewater Lake may be attributed to deposition in a relatively distal, glaciomarine environment. Dropstones occur in all units and are deposited during the melt-out of ice-rafted debris. The degree of rucking or disturbance of host beds is related to dropstone size and the cohesion of the pierced sediments (Thomas and Connell 1985). Dropstones are commonly pebbles, but boulders have also been observed.

An unusual sedimentary dike intrudes thinly bedded mudstone and siltstone on the north shore of a pond, south of Snare Lake. It is 10 to 15 cm wide and has been traced for approximately 15 metres along its length. It is steeply dipping and truncates sub-horizontal beds. Dike contacts are sharp and straight to corrugated. The dike is clast-supported and consists of angular to sub-rounded siltstone fragments 0.25 to 10 cm in a very fine-grained silt matrix. Its emplacement probably resulted from fluid overpressures during syn-depositional de-watering. Small dish-shaped structures, 0.75 cm in diameter, occur near dike contacts and may be small fluid escape structures (cf. Lowe 1975).

Mafic Intrusive Rocks

Nipissing-Intrusive Rocks

A Nipissing diabase sill approximately 200-250 m thick, intrudes Archean basement and Huronian sedimentary rocks in

Banting Township. No apparrent contact metamorphism or chlorite-spotting of either the Archean or Proterozoic lithologies has been observed in the map area. In contrast, chlorite contact metamorphism is common adjacent to a Nipissing diabase sill of approximately the same thickness (250 m) in the Cobalt Silver Mining Camp. In Banting Township, the gently undulating sill of Nipissing diabase forms two diabase arches and two diabase basins. Figure 3 is a northwest-southeast cross-section of the map area which illustates these features. Both limbs of the main north-south trending arch extend through the study area in a rather arcuate fashion. The western limb of the main north-south trending Lundy Lake Diabase arch extends from Whitewater Lake south to Lenore Lake. Its contacts dip westerly at 10 to 15°. The eastern limb extends southward from Breeches Lake to the southeastern corner of the study area. The other unnamed diabase arch is located along the eastern boundary of the map area. That means that all the rocks to the west of the main arch are underlain by a 250 m thick west limb and all rocks to the east are likewise underlain by the east limb of the same 250 m thick sill. The main diabase basin is located in the northeast area and has been named by the authors as the Mountain Lake Diabase Basin. All of the rocks between the west and east limbs of the basin are underlain by the same 250 m thick diabase sill which curves and faces inwards like a bowl or basin. In this case the sill intrudes the Archean granites. The diabase sill is exposed irregularly in this southeast corner due to topographic effects and steeper contacts and undulations in the sill; the dips of

contacts may locally reach 45°. Field evidence also indicates the presence of a second sill which cuts Archean metavolcanics in the southeast part of the map area. This second, minor sill is sub-parallel to the main sill, is less than 20 m thick, and intrudes Archean mafic metavolcanics above the main sill. Nipissing diabase is also exposed near the Banting Township boundary south of Red Squirrel Lake. It is probably part of a sill that extends northward from Cynthia Township (cf. Simony 1964).

Differentiation of the diabase sill and contact effects produce characteristic mineralogic and textural zonation, first described by Hriskevich (1952) in the Cobalt area. The upper and lower contacts of the sill are characterized by a massive, fine-grained quartz diabase chilled zone. The lower half of the sill usually consists of massive, medium-grained orthopyroxene (hypersthene) diabase, while the upper half typically exhibits a clotty or varied texture gabbro or diabase. Miarolitic cavities and pegmatitic patches also occur in this upper part of the sill hosted in varied-texture diabase. Granophyre, previously referred to as "red rock", occurs in many nearby locations such as Brigstocke and Kittson Townships (Born and Burbidge,1990) but was not recognized in the Banting-Best study area.

Dark green to grey-weathering, massive, fine- to medium-grained quartz diabase occurs along the upper and lower contacts of the sill. While chilled margins may be only 1 to 2 m thick, the quartz diabase may extend up to 50 m from the contact. Thin section petrography reveals a fine-grained, relict subophitic to

intergranular texture of labradorite and uralitized clinopyroxene. Quartz comprises approximately 5% of the diabase and is present as anhedral, intergranular aggregates. Epidote, biotite, ilmenite-magnetite and leucoxene are accessory minerals.

The varied-textured portion of the sill is characterized by coarse-grained to pegmatitic patches and zones within medium-grained, equigranular diabase. Clots of mafic minerals, miarolitic cavities and pegmatite and felsite dikes are common. Thin compositional layering, developed in pyroxene and plagioclase cumulates, is sub-parallel to the upper contact of the sill. Microscopy provides evidence of pervasive deuteric alteration of the varied-texture diabase. Plagioclase and pyroxenes are completely saussuritized and uralitized, respectively. Pseudomorphs, atoll structures, skeletal grains and zonal and cleavage-related replacement are common. Quartz, myrmekite, biotite, epidote, stilpnomelane, leucoxene and ilmenite-magnetite - amphibole symplectites are characteristic. Zircon has been observed in some sections.

The majority of the sill consists of medium-grained, subophitic enstatite to hypersthene gabbro (Photo 12). Orthopyroxene is partially altered to vermicular antigorite and may contain Ca-rich clinopyroxene exsolution lamellae. Labradorite is relatively pristine and displays oscillatory, discontinuous compositional zonation. Rare crystals may have up to 25 distinct concentric zones. Large, subhedral orthopyroxene oikocrysts, up to 5 mm in size, are discernable in hand specimen and weather to a distinctive reddish-brown. Olivine occurs

sparingly as small, anhedral crystals, partially altered to antigorite and magnetite. Tremolite-actinolite, biotite and titano-magnetite are common accessory minerals.

Regional correlation of the main diabase sill indicates that it extends both to the north into Brigstocke Township (Born and Burbidge,1990) and to the south into Chambers and Strathy Township (Fyon et al 1987,1988 and 1989, and Bennett, 1978). The nature of the sill in both areas is typical of the zonation previously discussed with a lower hypersthene gabbro overlain by an upper varied-textured gabbro locally overlain by a granophyre phase. Also, chilled contact zones commonly consist of fine-grained quartz gabbro (diabase).

Petrochemistry of the Nipissing Diabase Rocks

Representative analyses of the various Nipissing diabase rock types from Banting Township are presented in Table 7. Sample locations are shown in Figure 4. Rock types include 3 samples of the varied textured diabase from the upper part of the sill, 2 samples of hypersthene gabbro from the lower part of the sill and a chilled quartz diabase sample from the lower sill contact. The latter is probably most representative of the orignial Nipissing liquid composition. Standard geochemical plots of these analyses indicate that on the binary weight percent plot of SiO2 vs Na2O+K2O (Figure 7), these samples plot in various fields: the more mafic gabbros plot as gabbros, whereas the varied textured rocks are more silicous and plot as basaltic andesite. In a standard geochemical cation plot (Figure

18) and an AFM diagram (Figure 19) all samples are tholeiites. The intial liquid is a Mg-rich tholeiite but intermediate in composition between the more Al- and Fe-rich varied textured samples and the more Al-poor and Mg-rich hypersthene gabbro from the lower part of the sill. This is to be expected in a fractionated tholeiitic sill like the Nipissing with Fe-enrichment in the most fractionated upper rocks represented by the varied textured diabase.

Similar trends are reflected in the normative feldspar compositions plotted in Figure 20. The intial feldspar composition is fairly calcic but less An-rich than those found in the lower part of the sill in the hypersthene gabbro. Feldspars from the varied textured diabase of the upper part of the sill are, however, more Na-rich. This interpretation is consistent with the predicted tholeiitic fractionation trends previously illustrated by Figures 18 and 19.

Whole rock geochemistry of the Nipissing diabase sill in Banting Township (Table 7) is largely consistent with results obtained by Card et al. (1973). Significant changes in major element distribution are observed between massive hypersthene diabase, quartz diabase and varied-texture diabase. The geochemistry of the upper, varied-texture to pegmatitic portion of the sill reflects decreases in CaO, MgO and Ni and Cr and increases in Na2O, K2O, Fe2O3, MnO, TiO2, P2O5 and in Sr, Rb, Y, Zr, Ni and Zn. The decrease in CaO and MgO is probably due to a normal differentiation process involving gravity settling of early orthopyroxene. Ca, Mg and perhaps Ni and Cr would be

depleted as a result. The geochemistry of quartz diabase from the sill contacts reflects oxide proportions intermediate between those of the hypersthene diabase and varied-texture diabase.

Although the major element geochemical results from this study area indicate a parent tholeiitic liquid, other results from the Bay Lake area (Born and Hitch, 1990) indicate a more felsic or calc-alkalic liquid composition for similar Nipissing Diabse rocks. Conrod (1989) also proposes a calc-alkalic composition for the Nipissing liquids throughout much of the Southern Structural Province. It is also suggested by Conrod (1989) that the Nipissing suite of rocks is not similar to rift-related continental flood basalts such as the Keenawan basalts. Rather, it is possibly more similar to calc-alkalic collision-type magmas commonly found at destructive plate margins such as the Andes.

If Nipissing intrusive rocks are tholeiitic in origin then they are probably related to a rift environment. If they are clac-alkalic they may represent a subduction zone at a destructive plate margin (Conrod, 1989). Conrod (1989) classified the Nipissing liquids as calc-alkalic on the basis of several trace element discriminant diagrams and not just major element geochemical analyses.

Detailed geochemical work is beyond the scope of this report, it has not been done on data from Banting Township. The authors of the present report, however, believe that the Nipissing Diabase are tholeiitic rocks. This is based on the data published in the literature in general and those from

Banting, Best, Brigstocke, Kittson, Cassels and Riddell townships (Born and Burbidge, 1990 and Born, 1989).

Data presented by Conrod (1989) and Born and Hitch (1990) in the adjacent Bay Lake area, however, suggest a calc-alkalic origin. A destructive plate margin setting for the Nipissing intrusives is unlikely as it does not take into account obvious tectonic constraints such as the relatively undeformed state of the Cobalt Plate. A rift tectonic setting for the Nipissing intrusives has been proposed by Kissin (1988, 1989) and numerous other workers and would explain the large-scale geological and tectonic setting of the Nipissing intrusive rocks.

Late Precambrian

Mafic Intrusive Rocks

Late Precambrain diabase dike swarms of regional extent (Card and Lumbers 1977) are well exposed in the study area. These intrusions are subdivided into "Sudbury-type" olivine diabase and later diabase dikes. Although crosscutting relationships between these two groups of dikes are not evident in the study area, Card et al. (1973) have determined these relative ages. A Middle Proterozoic age has been assigned to these dike swarms by Fahrig and West (1986).

Sudbury-type Olivine Diabase

A northwest-trending, Sudbury-type olivine diabase dike, 125 to 175 m wide, can be traced across the entire study area. It is characterized by a strong linear aeromagnetic signature (GSC Map

1491G, 1965). The rock is highly susceptible to weathering and typically forms knobbly, gossany outcrops. Chilled margins are narrow. The dike has a coarse-grained, intergranular to sub-ophitic texture.

Plagioclase laths, 2 to 10 mm are intergrown with subhedral titanaugite (Photo 13). Olivine occurs as interstitial, anhedral to subhedral crystals less than 1 mm (0.04 inches) in size, and totally enclosed by pyroxene. Titano-magnetite and biotite are intergranular to plagioclase. Euhedral apatite also occur as discrete crystals totally enclosed within pyroxene.

Late diabase dikes

Late diabase dikes are narrow (1 to 40 m) intrusions occurring in subparallel swarms with north-northeasterly, northeasterly and northwesterly trends. Dikes are commonly parallel to lineaments and faults and are readily distinguishable in granitic and Huronian rocks, but are difficult to identify in medium-grained Nipissing diabase, with which they bear marked textural and mineralogic similarity. Their distinction then relies mainly on the detection of narrow (< 0.5 m) chilled margins and joint sets parallel and perpendicular to dike margins.

These rocks typically weather to a light grey-brown and are locally porphyritic. Subhedral to euhedral plagioclase phenocrysts with a diameter of up to 2.5 cm occur in a medium-grained, subophitic matrix (Photo 14). Within narrow, less than 2 m wide, fine-grained dikes that cut the Nipissing diabase the

phenocrysts are only 2 to 3 mm in size. In thin section, some larger phenocrysts display discontinuous, oscillatory zonation. Plagioclase and pyroxene have been altered to saussurite and sericite, and uralite and chlorite, respectively. Large (5 mm) skeletal leucoxene crystals with titano-magnetite lamellae are common. Quartz occurs as anhedral, interstitial crystals and in myrmekite, comprising up to 5% of the rock.

These dikes are petrologically similar but less altered than Archean "Matatchewan-type" diabase (Card et al. 1973; Bennett 1978). Age relationships are also different since they intrude Huronian rocks. Lithological similarities, however, make it difficult to distinguish between the two types in areas where only Archean rocks are exposed.

Petrochemistry of the Middle Proterozoic dikes

Several representative samples of both lithologies have analysed and the results are listed in Table 7 along with Nipissing Diabase samples. Locations for all samples are plotted in Figure 4.

Standard geochemical plots of these analyses indicate that on the binary weight percent plot of SiO_2 vs Na_2O+K_2O (Figure 7), the olivine diabase samples plot in the alkali olivine basalt field, whereras the more siliceous, late diabase dikes plot in the basalt (gabbro) and basaltic andesite fields. However, in a standard geochemical cation plot (Fgure 18) and an AFM diagram (Figure 19), all samples are tholeiitic.

The normative feldspar data (Figure 20) indicates that the feldspar compositions are more fractionated in the olivine diabase sample than in the late diabase dikes. Also, feldspars compositions in the olivine diabase dikes are similar to the upper and more fractionated portion of the Nipissing diabase sill. By contrast, compositions of feldspars in the late diabase dikes are similar to the lower and less fractionated parts of the sill.

Pleistocene and Recent

The study area is predominantly free of extensive glaciogenic deposits. Bedock exposures are abundant and may exceed 20 % in areas of recent logging activity. Thin, discontinuous ground moraine covers most of the area and consists of bouldery till which generally reflects bedrock composition (Roed, 1979). Boulder fields and glacial pavements are commonly found on lakeshores and in stream and river beds.

Glaciofluvial landforms consist of isolated eskers and outwash plains. Esker segments up to 1 km in length occur in the northern part of the study area near Breeches and Mannajigama lakes. They are single, sinuous ridges up to 20 m high, with steeply sloping sides and narrow crests, trending north-south (cf. Boissoneau 1968). Outwash plain deposits are best exposed along timber roads and in small gravel pits. They consist of thinly bedded sand and silt with isolated gravel lenses, commonly overlying coarse, massive sandy gravel. Current structures such

as crossbedding and asymmetric ripples are present but not common.

Glacial striae are best observed on wave-washed, shoreline outcrops on larger lakes. Striae indicate ice-flow directions ranging from north to N15^{o}E.

Talus piles at the bases of steep escarpments comprise colluvial deposits. Glaciolacustrine deposits are not evident.

Structural Geology

Introducution

Generally there is a lack of metasedimentary rocks with primary structural features, stratigraphic indicators and intercalated within the Archean metavolcanic succession. Pillow top directions and crudely developed beds in tuffaceous units are the only data to indicate the general younging direction of the supracrustal sequence. Primary features have largely been obscured or destroyed by regional and contact metamorphism. The structure of the Proterozoic rocks is more amenable to study because of their relative lack of metamorphism and deformation and abundance of primary sedimentary structures and top indicators.

Archean Structures

The structural geology of the Archean rocks is summarized by Figure 21. It shows the main deformational zones in dashed lines; the main fold axis directions with three arrows (D1, D2,

D3), and the foliation trajectories with curved double lines. These trajectories illustrate that the fabric generally wraps around the granite batholith in the southern parts whereas it is parallel to the main ENE-trending deformational zone elsewhere in the map area.

Regional scale folding of the metavolcanics is suggested by broad spatial associations between units in the study area and those in the main Temagami Greenstone belt (Fyon et al. (1987,1988 and 1989) and Bennett (1978)). Minor folds, kink bands and subvertical foliations are related to deformation on a large scale.

Foliations of the supracrustal rocks are parallel to contacts with the enclosing granites. Flattening of bombs and lapilli in pyroclastic units indicates north-south compression.

The metavolcanics of the present area apparently comprise the extensions of belts exposed to the east near Mountain and Rib lakes (Born and Burbidge (1990), Born and Hitch (1990))and to the south in Chambers and Strathy Townships (Fyon et al. 1987, 1988 and 1989) and Bennett (1978). Metavolcanics in the southeast corner of the study area match up with the northern limb of an east-northeast - trending synform of the main Temagami belt (cf. Bennett 1978). The gross distribution of local metavolcanic rocks is the result of regional scale folding and subsequent modification during the intrusion of granitic batholiths.

The major structural components consist of several phases of folding and the contemporaneous development of several deformation zones.

The Archean rocks have undergone a complex deformational history. The first folding phase (D1) probably represents the strongest deformational event. It created E-W oriented, steeply-dipping, isoclinal minor folds and steep lineations. These structures are accompanied by a strong axial planar schistosity (S_1) which parallels primary bedding (S_o), trends variably from 058° to 090°, and dips southerly between 67°-87°. Mineral lineations plunge steeply to the west.

The D1 deformation is followed by a similar D2 event which produced steeply dipping, WSW trending foliations and the dominant Anima-Nipissing River Deformational Zone (ANRDZ) and deflected earlier foliations in a direction parallel to the ANRDZ. Ductile deformation of granites within the ANRDZ produced some mylonitic textures.

Changes in foliations and banding orientation within the main metavolcanics belt suggests the presence of a synformal structure. Foliations dip steeply to the south and north on either side of a northeasterly trending synformal fold axis in the Lundy Lake area, parallel to the main WSW-trending deformation zone. This main deformation zone also acts as a domain boundary separating rocks to the north with steeply oriented and southerly dipping foliations from rocks to the south that exhibit steeply northerly dipping foliations. Steeply southerly dipping foliations are axial planar to minor folds (Photo 15) and perhaps major isoclinal folds, striking between 80° to 100° in the central part of the volcanic belt. Parallel bands of tuffaceous rocks are locally folded on an outcrop scale.

A weak, later fabric (D2) occurs as small scale crenulations of So and S1 and a broad warping of the volcanic belt into gentle open folds. The axial trace of these folds is approximately oriented in the 053° direction. In summary, schistosity, foliation, and banding indicate folding about a southwesterly-trending synform axis contempareous with the main WSW-trending deformation zone. However, all top indicators suggest a north-facing stratigraphy. In the eastern map area the volcanic rocks have been split into three thin divergent zones by granitic lobes. The schistosity changes direction and parallels the trend of these thin divergent zones.

Later kink bands and faults with minor offsets, striking 326° to 335°, parallel some of the major lineaments indentified in the area.

The granitoid rocks also exhibit an ENE-trending, moderate-to weakly-developed foliation. This foliation is produced by parallel orientation of feldspars, hornblende, and biotite. The fabric has a uniformly steep south dip and strikes 045° parallel to the ANRDZ. It probably coincides with a D2 deformational event that produced the crenulations elsewhere in the metavolcanic sequence.

The last minor deformation (D3) is represented by north-trending minor structures, minor crenulations and a spaced axial planar cleavage within the metavolcanic rocks. Along these cleavage planes there is a common dextral displacement of several centimetres. Effects of this last minor deformation (D3) occurs only locally within the metavolcanic rock. By contrast the

fabric within the intrusive granitoid rocks appears to only be a result of D2 deformation and has not been transposed during the later D3 deformation.

The undeformed nature of the lamprophyre intrusions suggests emplacement after the last deformational event (D3).

Proterozoic Structure

Huronian sedimentary rocks in the study area form gently dipping, homoclinal sequences which occupy a bifurcating trough. Dips seldom exceed 15°. In places they steepen to 40°. Broad, upright basin-and-dome structures with north-south - trending fold axes were proposed for Huronian rocks immediately to the west of Banting Township (Card et al. 1973). In the present area, bedding orientations and the gross distribution of local sediments suggest similar north-south - trending basins or troughs. These extend south from Whitewater, Anima-Nipissing and Snare Lakes and may coincide with predepositional basins that controlled sedimentation of the Huronian rocks.

The thickest sedimentary accumulations occur in the centres of these proposed basins. There is no evidence of multiple folds in the local sedimentary rocks of the Gowganda Formation (Coleman Member) as reported near the Grenville Front in Riddell Township by Born (1990).

The Proterozoic rocks were deposited subsequent to the last Archean deformational event (D3) and appear to be largely undeformed except for a few local kink bands within mudstones of the Coleman Member. Compressional kink bands of this type (Photo

11) and indicative of tectonic activity that followed the lithification of the sediments during the Eary to Middle Peoterozoic. Possibly this activity is either related to the intrusion of Early Proterozoic Nipissing Diabase sills or to the Penokean Orogeny (Stockwell et al., 1970). Similar kink bands in adjacent map areas have been extensively described and discussed by Born and Burbidge (1990) in nearby Brigstocke and Kittson townships and by Born and Hitch (1990) in the Bay Lake area.

Lineaments,Faults and Deformational Zones

Lineaments and faults were recognized in the examination of aerial and LANDSAT photographs. They generally occur as steep-sided valleys and ravines, scarps and narrow lakes and streams. Individual lineaments can be identified in watercourses less than 3 m wide. Proterozoic diabase dike swarms are commonly parallel to these structures. Some of the lineaments have been indentified on the ground as chloritic shear zones and faults, up to 20 cm wide.

Four groups of lineaments and presumed faults have been identified in the study area. Regional faults with similar orientations have undergone both dip-slip and strike-slip movement (Card et al. 1973).

Northwest-trending faults, including the Snare Creek and Thieving Bear - Breeches Lake faults, are parallel to the Timiskaming Fault system (Lovell and Caine 1970). Other members of this fault system, such as the Montreal River and Latchford

Faults, have apparent horizontal displacements of several kilometres (Card et al. 1973).

North- to northeast-trending faults may be parallel to fold axes in Huronian rocks. These are not as well defined as the northwest-trending faults in the study area, but have been recognized elsewhere (Card et al. 1973; Simony 1964; Bennett 1978). Local examples occur south of Whitewater, Anima-Nipissing and Snare lakes. Horizontal displacment of up to 200 m of olivine diabase dikes of the Sudbury Swarm occur at these faults. One such fault indicates a dextral sense of movement whereas another is sinistral.

West-northwest - trending faults, locally are occupied by Sudbury-type olivine diabase dikes eg. the fault which extends from Red Squirrel Lake to Jackpine Lake. Mylonitic zones have been recognized in granites near this fault in the vicinity of Jamieson Lake.

Northeast-trending faults are parallel to the Anima-Nipissing River Fault, which bisects the study area. In addition to mylonitic granites south of Carrying and McLean lakes, there is a strong spatial correlation between this fault and the late Archean Anima-Nipissing River and Snare Creek Intrusions. This fault zone presumably influenced the location of diatreme and intrusive activity.

As previouly mentioned, there are two Archean deformation zones, one trending to the southeast through Lenore Lake and the other to the ENE across the central part of the map . The main one, however, is the ENE-trending zone called the Anima Nipissing

River Deformational Zone with exhibits both brittle and ductile deformation. Foliation trajectories to the north and south of the deformational zone represent kinematic indicators that suggest the main displacement along the fault was caused by a dextral strike-slip movement. Discovery, mapping and characterization of this previously unknown Anima Nipissing River Deformational Zone was one of the most important results of the present geological study of Banting and Best townships. A discussion of mineral occurrences that are associated with this deformational zone will be given in the following section on Economic Geology. This zone may well be similar to the Net Lake-Vermillion Lake Deformation Zone which is found in adjacent Strathy Township (Fyon et al, 1987,1988 and 1989).

Discussion

The structural geology of the present area is similar to the one of Strathy and Chambers townships where research done by Fyon et al (1987,1988 and 1989) indicates that the early S1 foliation is oriented in a east-west direction, followed by a northeast-trending S2 shear foliation that produced the Net Lake-Vermilion Lake deformation zone. This zone shows a sinistral displacement of local quartz veins. A late (S3) foliation is north-trending and occurs in all metavolcanics and in the Strathy-Chambers batholith. This foliation is steeply dipping and axial planar to small open folds that have a wavelength of 10-40 cm.

The Tetapaga syncline is the main fold structure in the Temagami greenstone belt and its axis is oriented in an east-west

direction parallel to S1 foliations. It is probably related to the major regional folding event in the metavolcanic belt during S1 deformation.

In Brigstocke Township north of Banting and Best townships, Archean plutonic and metavolcanic rocks are generally weakly foliated with a near vertical east- and north-trending fabric (Born and Burbidge, 1990). This would correspond to the S1 and S3 foliation directions found in Banting and Best Townships and elsewhere in the Temagami greenstone belt. Brittle deformation and brecciation also occur along several NNW shears which transect the Archan basement. Ductile deformation occurs within an east-west trending mylonite zone which cuts the Archean plutonic rocks on the east arm of Mountain Lake. This orientation is also similar to the orientation of S2 shear fabrics found elsewhere in the Anima-Nipissing River Deformation Zone and the Net-Vermilion Deformation Zone.

Correlation of Aeromagnetic and Gravity Data with Geology

Banting and Best townships are covered by GSC Geophysical Series Maps 1490G (Timagami) and 1503G (Obabika Lake) (GSC, 1965).

The main feature outlined by the aeromagnetic survey are several northwest-trending zones with steep isomagnetic contours and high magnetic values of 2000-3000 gammas. These correspond directly to the northwest-trending olivine diabase dikes of the Sudbury Swarm (map unit 9a).

Other areas with high magnetic values correspond to Archean gabbro (map unit 4b) and are characterized by sub-circular shaped anomalies and more gently sloping magnetic gradients. In this unit the areas of greatest magnetic attraction is just to the east and north of Jakepine Lake in the southern part of Banting Township.

A similar magnetic expression is caused by the western limb of the Proterozoic Nipissing diabase arch. This limb is outlined by several circular anomalies of >2000 gammas with steep magnetic gradients. However, the diabase basin in the northeast part of the map sheet and the eastern limb of the diabase arch does not have any distinct magnetic expression. A magnetic depression occurs to the south of Breeches Lake along the top of the sill which is at the northern edge of the diabase basin.

Generally the Huronian sedimentary rocks and the Archean granites exhibit gently sloping magnetic gradients and low magnetic values of <2000 gammas. Several of the magnetic lows are underlain by sedimentary rocks of the Coleman Member (Gowganda Formation) in an area just east of Anima-Nipissing Lake.

The main feature of the regional gravity map (Gupta and Wadge, 1980) is a pronounced gravity low that occurs to the south of Mountain Lake. Elsewhere in the map area the isogravity contours trend in an east-west direction and illustrate a fairly steep gravity gradient between the gravity low and a gravity high located to the north in Kittson Township.

Underlying the area of low gravity are Archean granitoid rocks which are in part overlain by younger sedimentary rocks of the Coleman Member (Gowganda Formation) in the area around Gilbert and McLean lakes.

ECONOMIC GEOLOGY

No assessment work is on file for the map area. Prospecting was confined to silver exploration in Nipissing Diabase exposed in the central parts of Banting Township. As a result, some ground was held in this area as early as 1929. That region was restaked in the period between 1948 and 1951 by Nacso Metals, Michaud and Davis, and in 1961 by Rix Athabasca Uranium Mines Limited, and lastly in 1963 by Mid-North Engineering Limited. However, there are no records of any mineral occurrences discovered during these periods of exploration activity.

Most rock types indentified within the Cobalt silver camp including a Nipissing diabase sill are also exposed in Banting and Best Townships. Carbonate veins were not observed to cut either Nipissing diabase or Huronian sedimentary rocks. Also lacking is the extensive chlorite spotted alteration commonly found in the Cobalt Camp adjacent to the Nipissing diabase sill. However, rare quartz ± calcite veins were observed in parts of the upper, varied-textured zones of the Nipissing diabase sill. In some instances, they carried anomalous gold, silver and copper values. Two such occurrences were found west and south of Whitewater Lake (Figure 21). Both sites had been previously tested with pits but no records exist describing this activity.

The veins average 20 cm in width and are made up of quartz, calcite, epidote and small xenoliths of diabase. Pyrite, minor chalcopyrite and malachite occur interstitially to the gangue minerals or as disseminated grains within the wall rock. In other composite veins, drusy quartz extends inwards from vein margins to a central, carbonate-rich zone and the sulphides are located either at the quartz-calcite interface or associated with the quartz. Although there is little alteration of the diabase, sheared and slickensided surfaces suggest that movement and deformation accompanied vein development. Minor occurrences of malachite staining and chalcopyrite mineralizaiton were noted in Nipissing Diabase.

Quartz veins cutting granitic and volcanic rocks were systematically sampled, despite the paucity of sulphides in virtually all cases. Approximately 80 samples were taken with 32 samples indicating some metal content (Table 8). Some samples returned gold values ranging from trace to 0.05 oz/ton, suggesting that these vein structures should be further investigated.

In places minor malachite staining and chalcopyrite mineralization were noted in Archean granite, amphibolite and volcanic rocks. The best gold values came from a chalcopyrite-bearing quartz vein hosted within granites in the southeastern corner of the map area, just south of Red Squirrel Road. Chalcopyrite can also occur elsewhere as disseminated clots to 2 mm in size within a quartz-poor phase of the granite. A grab sample produced an assay of 0.1% coppper (Temiskaming Testing

Labratory, Cobalt). All copper-bearing samples were analyed for gold but nil values were obtained in all instances (Table 8).

Another rock unit of economic interest is the hornblende gabbro (map unit 4). It should be explored for platinum and base metals within its magnetite and sulphide-rich portions. In the southeastern part of the map area, the gabbro body contains a banded magnetite rock that represent stoped and rafted iron formation. About 300 m south of this showing, the gabbro locally grades into a hornblendite and contains up to 25% disseminated magnetite. Chalcopyrite was also observed along fracture surfaces.

This is not unusual since there are many know within Lamprophyric rocks may be associated with gold occurrences as reported in the literature by Rock et al (1987). Heather (1989) describes lamprophyre dikes as gold exploration targets in the Wawa area where strongly deformed lamprophyre dikes are intimately associated with mineralized quartz veins in the majority of gold occurrences within granitoid rocks. The dikes represent strong compentency contrast within the homogenous granitoids and localized both the quartz veining and gold mineralization.

In Strathy Township (Fyon et al, 1987,1988 and 1989) and the present area the northerly orientation of lamprophyre dikes coincides with the D3 structural direction that parallels the Penrose and Big Dan gold-bearing structures. Thus, any northerly-trending structures, even those that post-date the D3

or last deformational event could possibly be of economic interest.

Other possible targets for mineralization are hydrothermal alteration zones (eg. associated with the pyroxene gabbro) and the ductile deformation zones of the area. These deformation zones are the southeast-trending zone that cuts through Lenore Lake (Figure 21) as well as the main, WSW-trending Anima-Nipissing Deformation zone.

Recommendations for future exploration in Banting and Best townships

Figure 21 shows the spatial relationship of the mineral occurrences (solid triangles) with the geology and the various Archean structural elements.

One of the main results of our mapping project is the discovery of numerous new mineral occurrences and the outlining of areas with anomalous precious and base metal potential. Detailed mapping, sampling and subsequent assaying have delineated several previously unknown zones of potential economic interest within the map area. These include:

Archean Mineralization

1) Possible Gold associated with the deformational zones as described by Fyon et al (1986). Figure 21 illustrates a fairly dense concentration of mineral occurrences both to the north and south of the main WSW-trending deformational zone. Archean quartz veins are generally associated with strongly deformed

granitic rocks with amomalous gold and copper values. These are mainly associated with the WSW-trending Anima-Nipissing River Deformation Zone (ANRDZ) but also occur at several localities along some later Proterozoic mafic dikes that cut the granites (Figure 21). Assay values from grab samples range from trace to 0.05 oz Au/ton.

Although ductile deformation in the ANRDZ zone is best illustrated by the mylonitic granitic rocks it also occurs in volcanic rock along strike of the zone and further to the east. These volcanic rocks probably represent a more favourable exploration target than the granites. Deformation in the mafic volcanics has resulted in a pronounced shear foliation and extreme flattening rather than ductile flow as in the granites. Previous structural studies in Archean greenstone terrains illustrated that major gold deopsits occur in regional zone of deformation (Fyon et al., 1986; Hugon and Schwerdtner, 1985). Thus the Anima-Nipissing River Deformation Zone may be an area for potential gold mineralization. It has orientation and features similar to the Net Lake-Vermilion Lake Deformation Zone in Strathy Township as described by Fyon et al. (1987,1988 and 1989). Both of these zones represent structures produced during D2 deformation. Along the northeast trending Net Lake-Vermilion Lake Deformation Zone there is however a high frequency of gold occurrences. Thus by direct analogy the Anima-Nipissing River Deformation Zone could also have some potential. Other gold bearing structures in Strathy Township such as the Big Dan and Penrose properties represent north-trending deformation zones

that probably correpond to the D3 deformation. There appears to be no analogous stuctures of this type in Banting and Best townships. Intrusion of the late lamprophyric dikes post-dates the last deformational event (D3). These dikes have a similar north-trending orientation. They intruded into structural zones that were probably produced during east-west shortening of the D3 deformation. This factor together with a known gold and lamprophyre association documented elsewhere (Rock et al., 1987; Heather, 1989) makes them a marginal but potential gold exploration target.

2) Possible Gold associated with the lamprophyre-ultramafic lithologies (map unit 6). The diatreme breccia zones appear to have some anomolous gold values. Also worthy of investigation is an extensive hematite-epidote alteration halo within the granitoid rocks surrounding the eastern-most pyroxene-phyric gabbro intrusion. Local hydrothermal activity probably occurred both during and following the intrusion of the pyroxene gabbros (map unit 6c). Also, the spatial distribution of the main lamprophyre bodies is parallel the major structural lineament. The alteration halo is also bounded by the main Anima-Nipissing River Deformation Zone and its intersection with a secondary northwest trending lineament in the eastern part of the map area. This type of spatial relationship suggests that the fault or deformation zones represent preferential and structurally favourable sites that localized the igneous intrusions. Gold, silver and possibly base metal may have been remobilized here and

deposited in structurally favourable sites along joint surfaces and other fluid pathways.

Although mineralization within the north-trending lamprophyre dikes has not been discovered, the potential for anomolous gold values associated with them exits. This has been documented in the literature by Rock et al. (1987) and Heather, (1989). Also, the dikes probably intruded into structural zones parallel the D3 deformational axis that produced the Big Dan and Penrose gold-bearing structures in Strathy Township.

Assay values of the diatreme breccia, lamprophyre and adjacent rocks range from trace to 0.01 oz Au/ton.

3) There is some base metal and possible platinum-group element potential in the hornblende gabbro along the southern margin of the greenstone belt. This unit could be correlative with the Net Lake intrusion located in Strathy Township where there are several base metal occurrences. Areas of greatest potential within Banting and Best townships are any sulphide- or magnetite-rich portions of the intrusion and also along the northern contact zone with the metavolcanic belt.

Proterozoic Mineralization:

Despite a marked similarity between rocks in the study area and those of the Cobalt silver mining camp, little evidence of silver-cobalt-arsenide mineralization exists in Banting and Best townships. There are, however, a few quartz-calcite veins in Nipissing diabase with anomalous gold, silver and copper values. Assay values of grab samples range from trace to 0.006 oz Au/ton.

By analogy with the Cobalt Camp, the likely places to find any cobalt-silver mineralization is along the basal contact of the Nipissing diabase sill or within adjacent Archean metavolcanics or metasediments or metasediments of the Coleman Member of the Huronian Gowganda Formation that occur below the lower contact of the sill. Any areas of intense chlorite spotting in the rocks adjacent to the sill would also be worthy of further investigations.

REFERENCES

Barker, F. 1979. Trondhjemite: Definition, Environment and Hypothesis of Origin; IN Trondhjemites, Dacites and Related Rocks, edited by F. Barker, Elsivier, p. 1-12.

Barlow, A.E. 1899. Geology and Natural Resources of the Nipissing and Timiskaming Map Sheets; Annual Report of the Geological Survey of Canada; Volume 10, Report I, p.172-174.

Bennett, G. 1978. Geology of the Northeast Temagami Area, District of Nipissing; Ontario Geological Survey, Geological Report 163, 128 p.

Boissoneau, A.N. 1968. Glacial History of Northeastern Ontario II. The Timiskaming - Algoma Area; Canadian Journal of Earth Sciences, Vol. 5, p. 97-109.

Born, P. 1989. Precambrian Geology, Cassels and Riddell Townships, Ontario; Ontario Geological Survey, Report 271, 73 p.

Born, P., and Burbidge, G.H., 1987. Geology of Brigstocke and Kittson Townships, District of Timiskaming; p.198-204. IN Summary of Field Work and Other Activities 1987, Ontario Geological Survey, Miscellaneous Paper 137, 429 p.

Born, P., and Burbidge, G.H., 1990 (in press). Geology of Brigstocke and Kittson Townships, District of Timiskaming; Ontario Geological Survey, Geological Report.

Born, P., and Hitch, M.W., 1990 (in press). Geology of the Bay Lake Area, District of Timiskaming; Ontario Geological Survey, Geological Report.

Card, K.D., 1979. Regional Geological Synthesis, Central Superior Province; in Current Research, Part A, Geological Survey of Canada Paper 79-1A, p.87-90.

Card, K.D., and Lumbers, S.B. 1977. Sudbury-Cobalt, District of Algoma, Manitoulin, Nipising, Sudbury and Timiskaming; Ontario Geological Survey, Map 2361, Geological Compilation Series, Scale 1:253, 440 or 1 inch to 4 miles.

Card, K.D., McIlwaine, W.H., and Meyn, H.D. 1973. Geology of the Maple Mountain Area, Operation Maple Mountain, Districts of Timiskaming, Nipissing, and Sudbury; Ontario Division of Mines, Geological Report 106, 160p.

Conrod, D.M. 1988. Petrology and Geochemistry of the Duncan Lake, Eaton Bay, and Miller Lake Nipissing Intrusion within the Gowganda Area; Ontario Geological Survey, Open File Report 5701, 210 p.

Cox, K.G., Bell, J.D., and Pankhurst, R.J., 1979. The Interpretation of Igneous Rocks. George Allen and Unwin Ltd., 450p.

Cullers, R.L., and Graf, J.L., 1984a. Rare Earth Elements in Igneous Rocks of the Continental Crust: Predominantly Basic and Ultrabasic Rocks;p. 237-274 in Rare Earth Element Geochemistry, P. Henderson, ed., Elsevier, p.

Cullers, R.L., and Graf, J.L., 1984b. Rare Earth Elements in Igneous Rocks of the Continental Crust: Intermediate and Silicic Rocks - Ore Petrogenesis; p. 275-316, in Rare Earth Element Geochemistry, P. Henderson,ed., Elsevier,.

DeLury, J.S., 1907. Other Timiskaming Cobalt Areas, Area West of Bay Lake on Montreal River. Ontario Bureau of Mines, Vol. XVI, pt.2, p.138-146.

Fahrig, F.W. and West, T.D., 1986. Diabase Dike Swarms of the Canadian Shield; Geological Survey of Canada, Map 1627 A.

Fyon, J.A. and Crocket, J.H., 1986. Exploration Potential for Base and Precious Metals Mineralization in Parts of Strathy Township, Temagami; Ontario Geological Survey, Open File Report 5591, 46 p.

Fyon, J.A. and O'Donnell, L., 1987. Metallogenic Studies in the Temagami Greestone Belt, District of Nipissing; p.190-197. IN Summary of Field Work and Other Activities 1987, Ontario Geological Survey, Miscellaneous Paper 137, 429 p.

Fyon, J.A., Hrabi, R.B., and Maitland, W.M., 1988. Relationships Between Lithological, Alteration, and Structural Features and Precious-Metal Occurrences in the Temagami Greestone

Belt, District of Nipissing; p. 212-218. IN Summary of Field Work and Other Activities 1988, Miscellaneous Paper 141, 498 p.

Fyon, J.A and Wheatley, K.J., 1988. Peterographic Characteristics of Archean Granitoid Rocks; p. 381-383. IN Summary of Field Work and Other Activities 1988, Ontario Geological Survey, Miscellaneous Paper 141, 498 p.

Fyon, J.A and Cole, S., 1989. Geology of Part of the Temagami Greenstone Belt, District of Nipissing: Including Relationships Between Litholgical, Alteration, and Structural Features and Precious Metal Occurrences; p.108-115 IN Summary of Field Work and Other Activities 1989, Ontario Geological Survey, Miscellaneous Paper 146.

Geological Survey of Canada, 1965. Aeromagnetic Map 1491G - Timagami, Ontario, Scale one inch to one mile or 1:63, 360.

Geological Survey of Canada, 1965: Aeromagnetic Map 1503G - Obabika Lake, Ontario, Scale one inch to one mile or 1:63, 360.

Gupta, V.K., and Wadge, D.R., 1980. Bouger Gravity and Generalized Geology Map Temagami-Englehart area, District of Timiskaming, Nipissing and Sudbury, Preliminary Map P. 2296, Geophys. Ser. scale 1:100, 000.

Gupta, V.K., and Wadge, D.R., 1989. Heather K.B., The Geological and Structural Setting of Gold Mineralization in the Renabie Portion of the Missanabie-Renabie Gold District;

p.99-107 IN Summary of Field Work and Other Activities 1989, Ontario Geological Survey, Miscellaneous Paper 146.

Henderson, P., 1984. Rare Earth Element Geochemistry, Elsevier.

Hriskevich, M.E., 1952. Petrology of the Nipissing Diabase Sheet of the Cobalt Area of Ontario; unpublished Ph.D. Thesis, Princeton University, Princeton, New Jersey, 129p.

Hugon, H. and Schwerdtner, W.M., 1985. Structural Signature and Tectonic History of Deformed Gold-bearing Rocks in Northwestern Ontario; Grant 149, p.62-72 IN Geoscience Research Grant Program, Summary of Research 1984-1985, edited by V.G. Milne, Ontario Geological Survey, Miscellaneous Paper 127, 246 p.

Irvine, T.N. and Baragar,W.R.A., 1971. A guide to Chemical Classification of the Common Volcanic Rocks; Canadian Journal of Earth Sciences, vol. 8, p. 523-548.

Jensen, L.S., 1976. A New Cation Plot for Classifying Subalkaline Volcanic Rocks; Ontario Division of Mines, Miscellaneous Paper 66, 22p.

Kissin, S.A., 1988. Nickel-coblat-native silver (five element) veins: A rift related ore type. p.268-279 in G. Kisvarsanyi and S.K. Grant, eds, Proceddings volume, North American Conference on Tectonic Controls of Ore Deopsits and the Vertical and Horizontal Extent of Ore Systems. University of Misouri-Rolla.

Kissin, S.A., 1989. The Five-Element Suite: An indication of Non-Magmatic ore types related to rifting and basin Development. Explore, No. 64, pp.5-8.

Lindsey, D.A., 1969. Glacial Sedimentalogy of the Precambrian Gowganda Formation, Ontario, Canada; Geological Society of America, Bulletin 80, p. 1685-1702.

Lovell, H.L., and Caine, T.W., 1970. Lake Timiskaming Rift Valley; Ontario Department of Mines, Miscellaneous Paper 39, 16p.

Lowe, D.R., 1975. Water escape structures in coarse-grained sediments. Sedimentology, 22, p. 157-204.

McCallum, M.E., 1976. An Emplacement Model to Explain Contrasting Mineral Assemblages in Adjacent Kimberlite Pipes; Journal of Geology, vol. 84, p. 673-684.

McCrank, G.F.D., Misiura, J.D., and Brown, P.A., 1981. Plutonic Rocks in Ontario. Geological Survey of Canada, Paper 80-23. 171p.

Menhert, K.R., 1968. Migmatites and the Origin of Granitic Rocks; Elsevier, Amsterdam. 405p.

Mustard, P.S., and Donaldson, J.A., 1987. Early Proterozoic ice-proximal glaciomarine deposition: the lower Gowganda Formation at Cobalt, Ontario, Canada. Geological Society of America Bulletin, vol. 98 (in press).

Ontario Geological Survey, 1984. Best Township, District of Nipissing; Ontario Geological Survey Geological Data Inventory Folio 158.

Ontario Geological Survey, 1983. Banting Township, District of Nipissing; Ontario Geological Survey Geological Data Inventory Folio 177.

Owsiacki, L., 1983. Geology of the McLean Lake Area; p.250-252. IN Summary of Field Work. 1983 Ontario Geological Survey, edited by John Wood, Owen L. White, R.B. Barlow and A.C. Colvine, Ontario Geological Survey, Miscellaneous Paper 116, 313 p.

Owsiacki, L., 1984. Geology of the McLean Lake-Lundy Lake Area; p.237-241. IN Summary of Field Work. 1984 Ontario Geological Survey, Miscellaneous Paper 119, 309 p.

Rock, N.S.M., Duller, P., Haszeldine, S., Grovers, D.I., 1987: Lamprophyres as potential gold exploration targets: Some preliminary observations and speculations; pp 271-286. IN Recent Advances in Understanding Precambrian Gold Deposits, edited by S.E. Ho and D.I. Groves, by the Geology Department and University Extension, University of Western Australia, Publication Number 11, 268p.

Roed, M.A., 1979. Northern Ontario Engineering Geology Terrain Study, Data Base Map Haileybury, Ontario Geological Survey, Map 5024, scale 1:100 000.

Schenk, P.E., 1965. Depositional Environments of the Gowganda Formation (Precambrian) at the South End of Lake Temagami; Journal of Sedimentasry Petrology, Volume 35, Number 2, p. 309-318.

Sibson, R.H., 1977. Fault rocks and fault mechanisms; Journal of the Geological Society of London, vol. 133, p.191-213.

Simony, P.S., 1964. Geology of Northwestern Temagami Area, District of Nipissing; Ontario Department of Mines, Geological Report 28, 30p.

Smyk, M.C. and Owsiacki L., 1986. Geology of Banting Township and the Western Part of Best Township, District of Nipissing, p. 292-296. IN. Summary of Field Work and Other Activities 1986, Ontario Geological Survey, Miscellaneous Paper 132, 435 p. Accompanied by 1 Chart.

Steckeisen, A., 1976. To Each Plutonic Rock Its Proper Name; Earth-Science Review, Volume 12, p. 1-33.

Stockwell, C.H., McGlynn, J.C., Emslie, R.F., Sanford, B.V., Norris, A.W., Donalson, J.A., Fahrig, W.F., and Currie, K., 1970. Geology of the Canadian Shield; p. 44-150 IN Gology and Economic Minerals of Canada, Edited by R.J.W. Douglas, Geological Survey of Canada, Economic Geology Report Number 1, 833 p.

Thomas, G.S.P., and Connell, R.J., 1985. Iceberg Drop, Dump, and Grounding Structures From Pleistocene Glacio-Lacustrine Sediments, Scotland; Journal of Sedimentary Petrology, vol. 55, no. 2, p. 0243-0249.

Todd, E.D., 1926. The Anima-Nipissing Lake Area; Ontario Bureau of Mines Annual Report, Volume 35, part II, p.79-106.

Van Schmus, W.R., 1976. Early and Middle Proterozoic History of the Great Lake Area, North America; p. 603-628 IN Philosophical Transactions of the Royal Society of Londan, Volume A, 280, Number 1298, p. 367-667.

Winkler, H.G.F., 1971. Petrogenesis of Metamorphic Rocks; 4th Edition, Springer-Verlag, New York, 334 p.

FIGURES

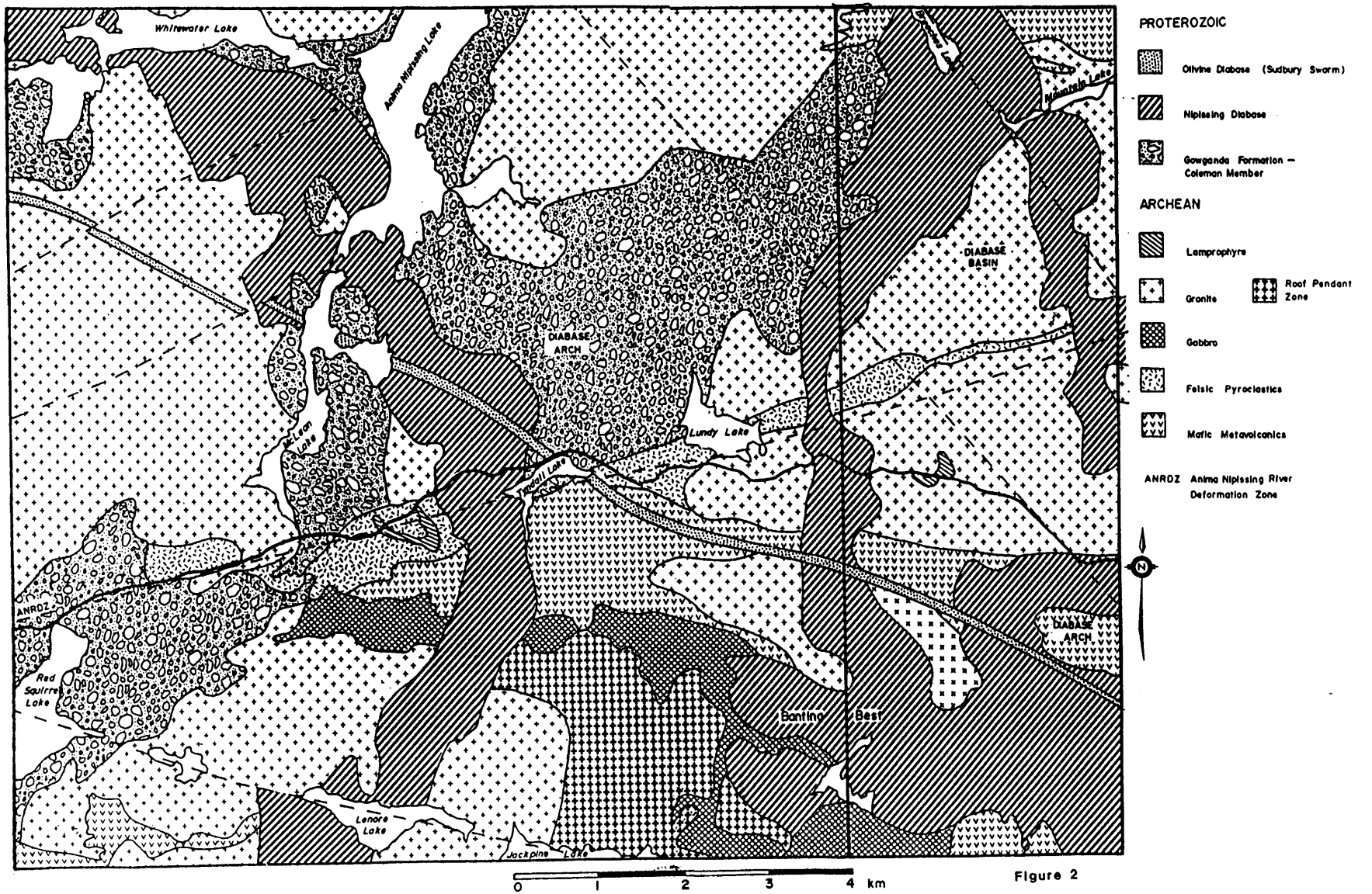

Figure 2

2: General Geology of Banting Township and the Western Part of Best Township, District of Nipissing.

Banting & Best Townships
Figure 3

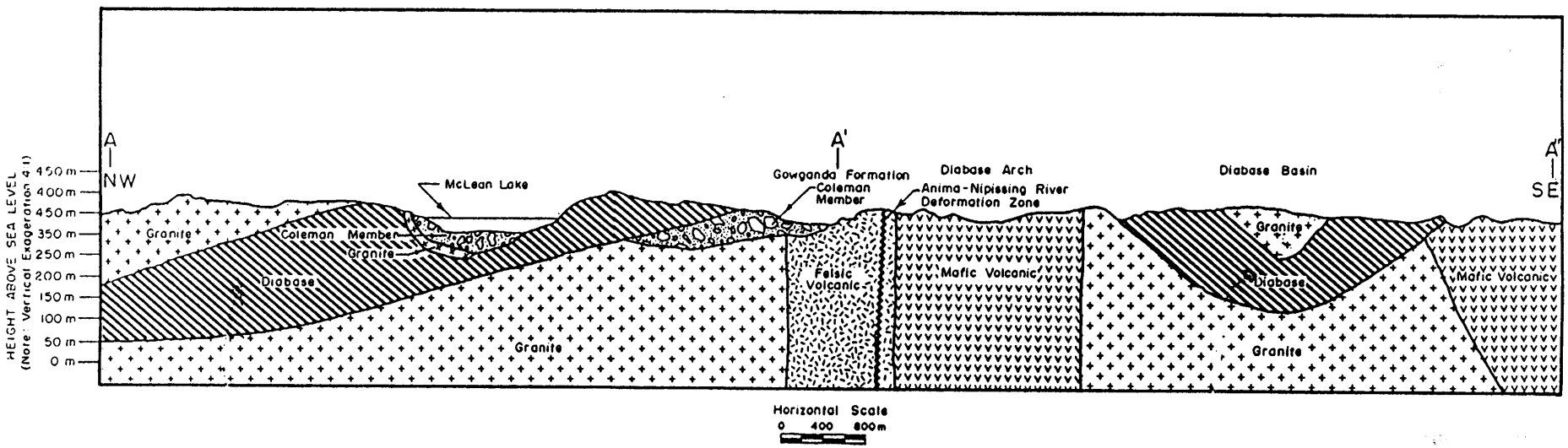

3: Geological cross-section oreinted in an Northeast-Southwest direction for the central part of Banting Township and the Western Part of Best Township.

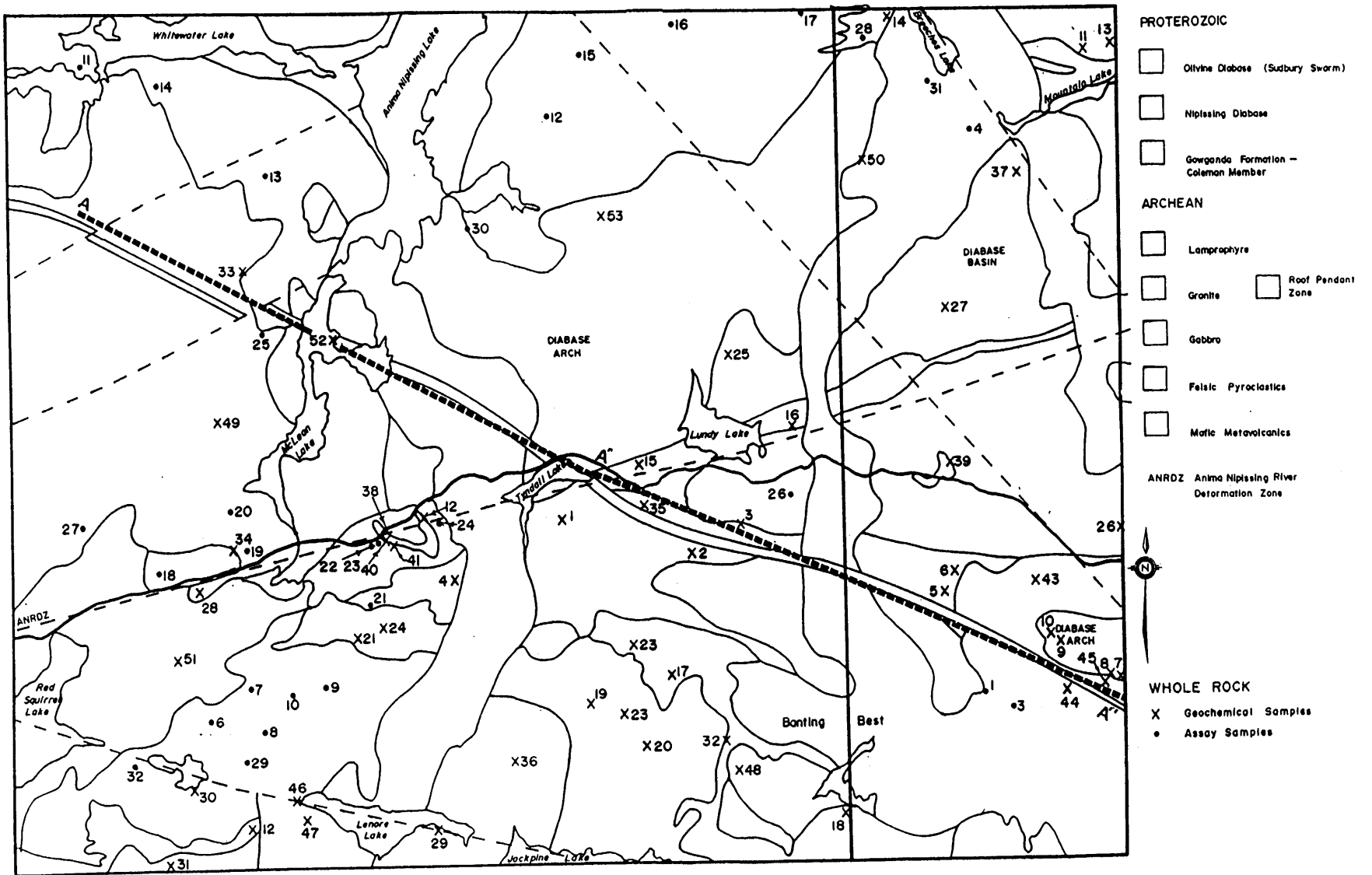

4: Location map for geological crossections and chemical analysed samples from Banting Township and the Western Part of Best Township.

BANTING METAVOLCANICS

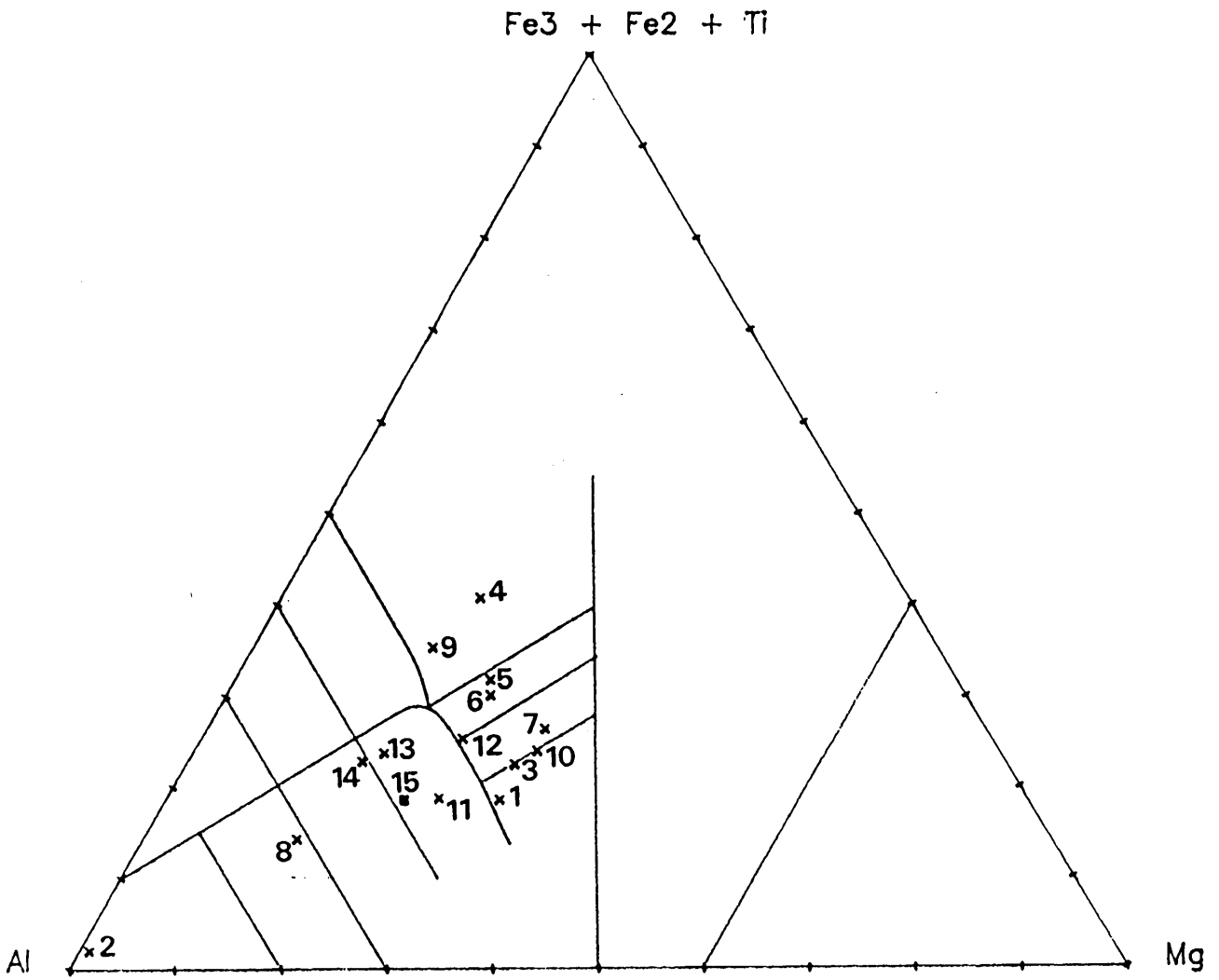

Figure 5

× **mafic volcanics** ▪ **felsic volcanics**

5: Cation plot (Jensen, 1976) - Archean metavolcanic rocks of Banting Township and the Western Part of Best Township.

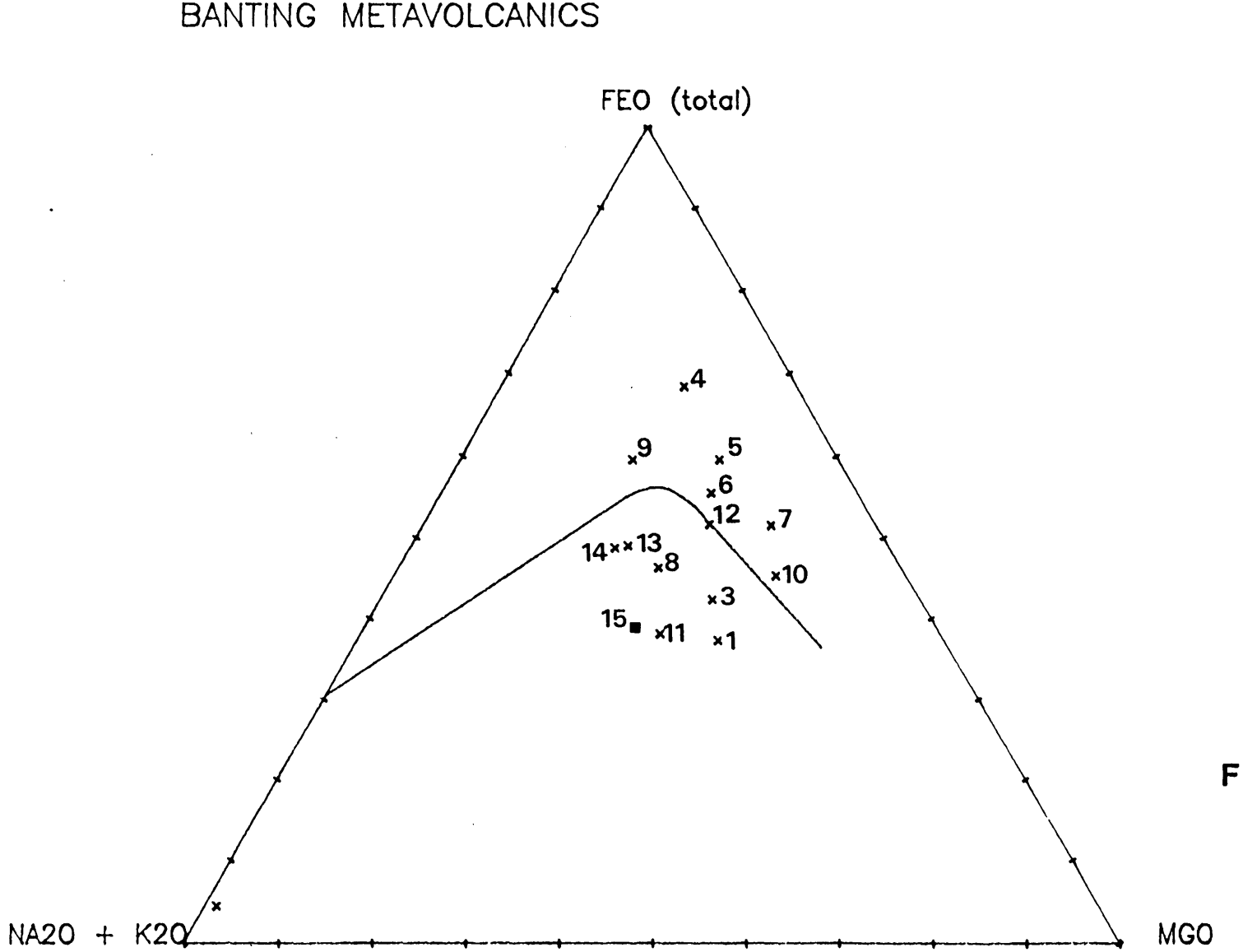

Figure 6

x mafic volcanics ▪ felsic volcanics

6: AFM (weight percent) plot - Archean metavolcanic rocks of Banting Township and the Western Part of Best Township.

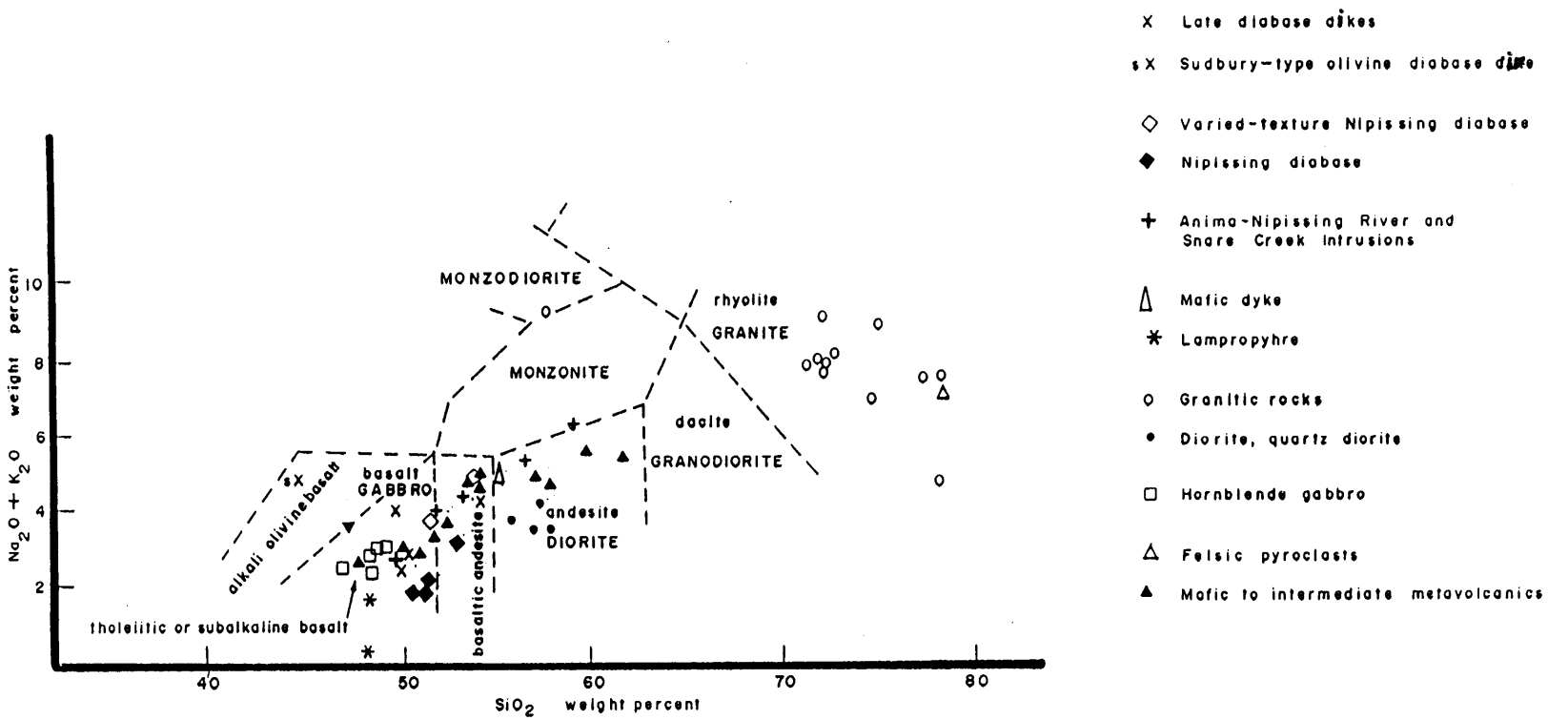

Figure 7

7: Binary weight percent plot of SiO_2 vs Na_2O+K_2O for all geochemically analyses rocks of Banting Township and the Western Part of Best Township.

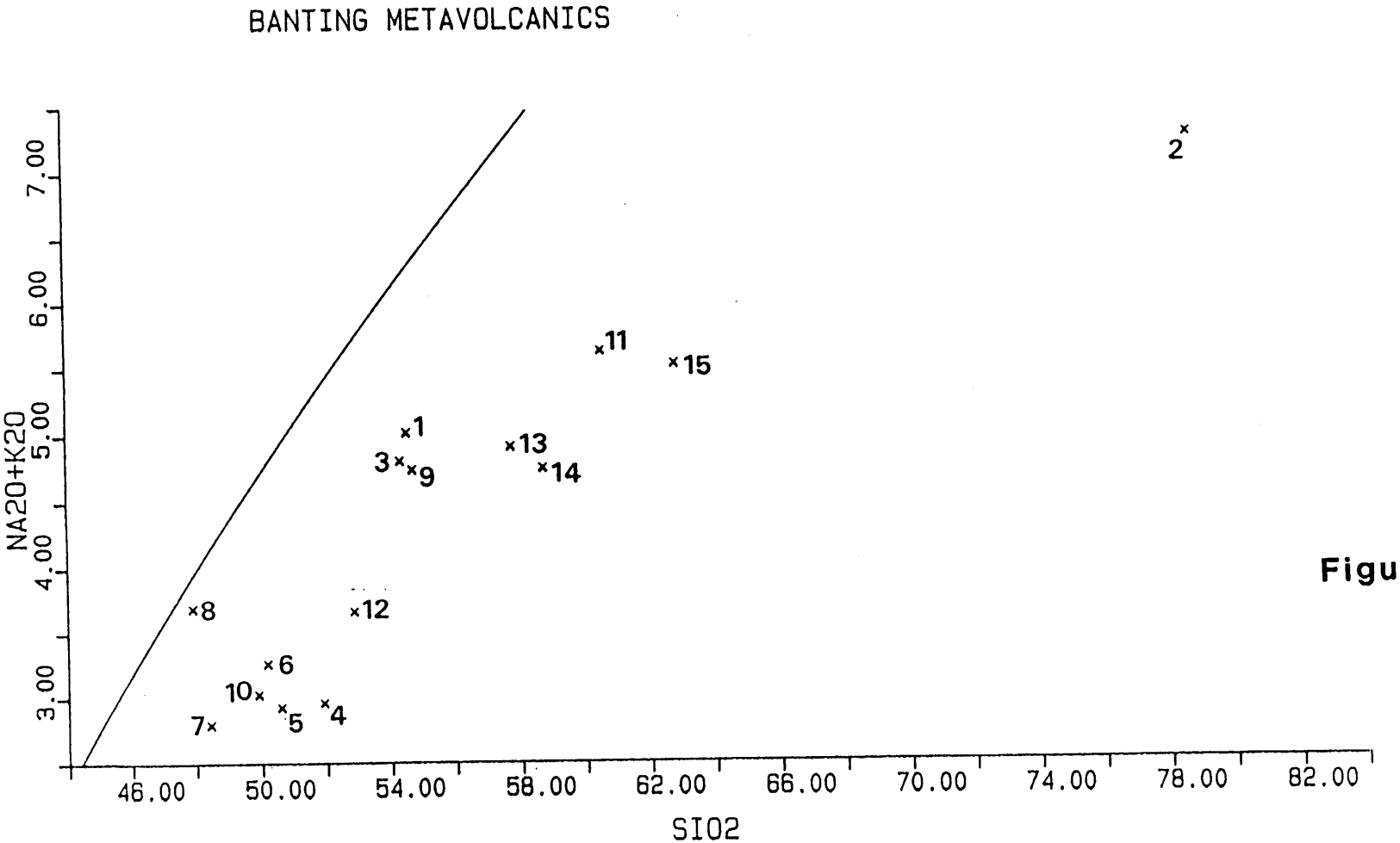

Figure 8

8: Binary weight percent plot of SiO_2 vs Na_2O+K_2O for Archean metavolcanic rocks of Banting Township and the Western Part of Best Township.

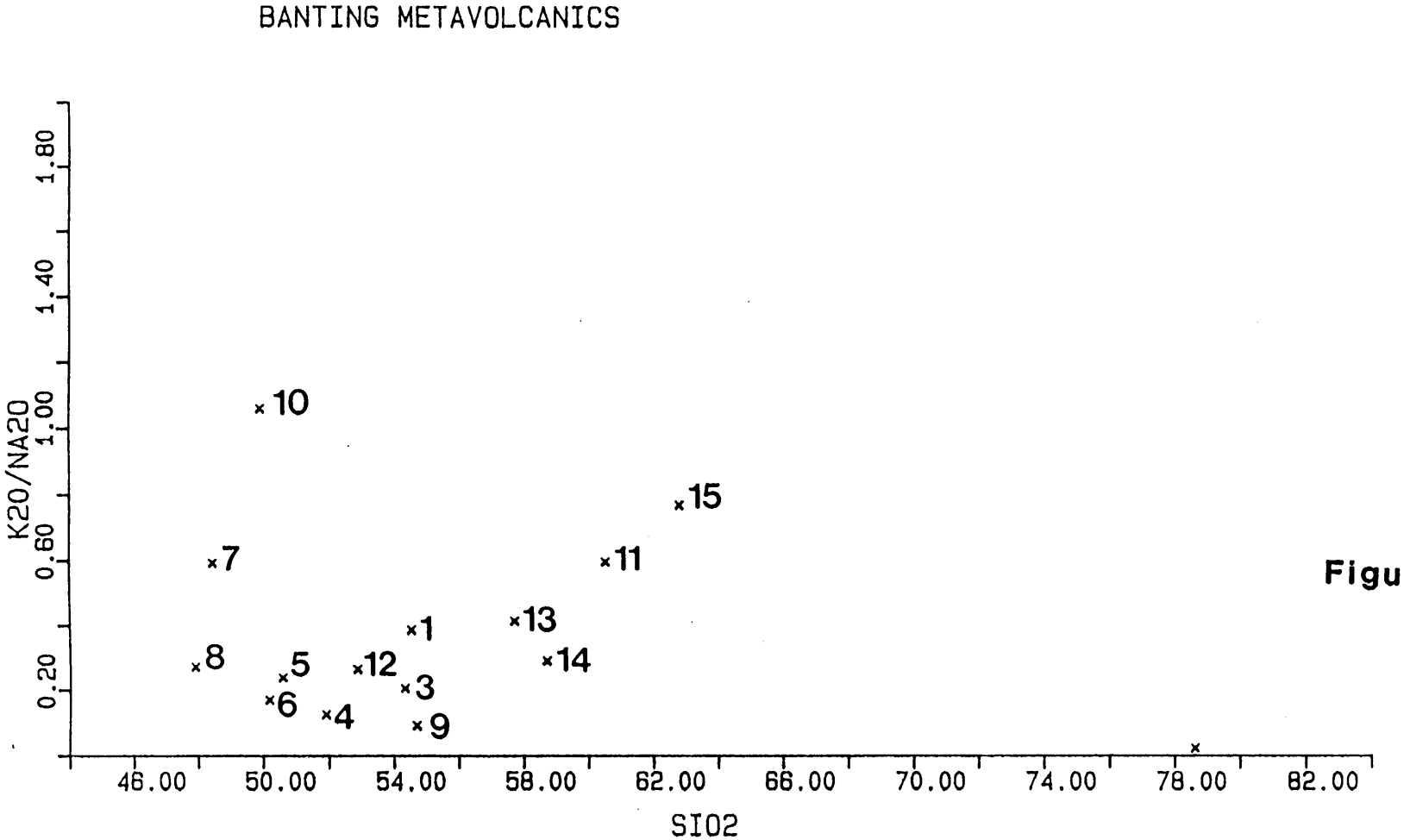

Figure 9

9: Binary weight percent plot of SiO_2 vs K_2O/Na_2O for Archean metavolcanic rocks of Banting Township and the Western Part of Best Township.

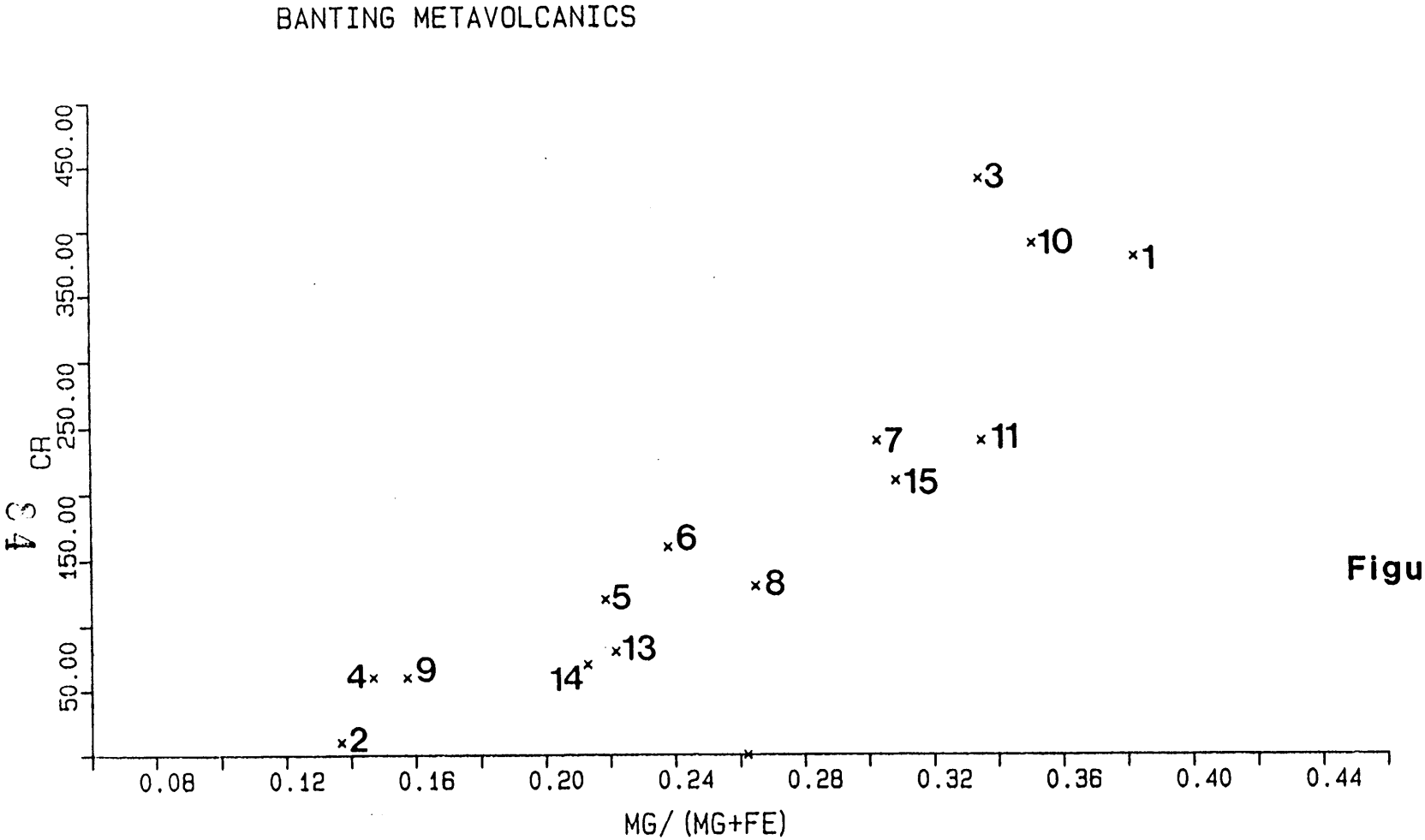

Figure 10

10: Binary weight percent plot of Mg/Mg+Fe vs Cr for Archean metavolcanic rocks of Banting Township and the Western Part of Best Township.

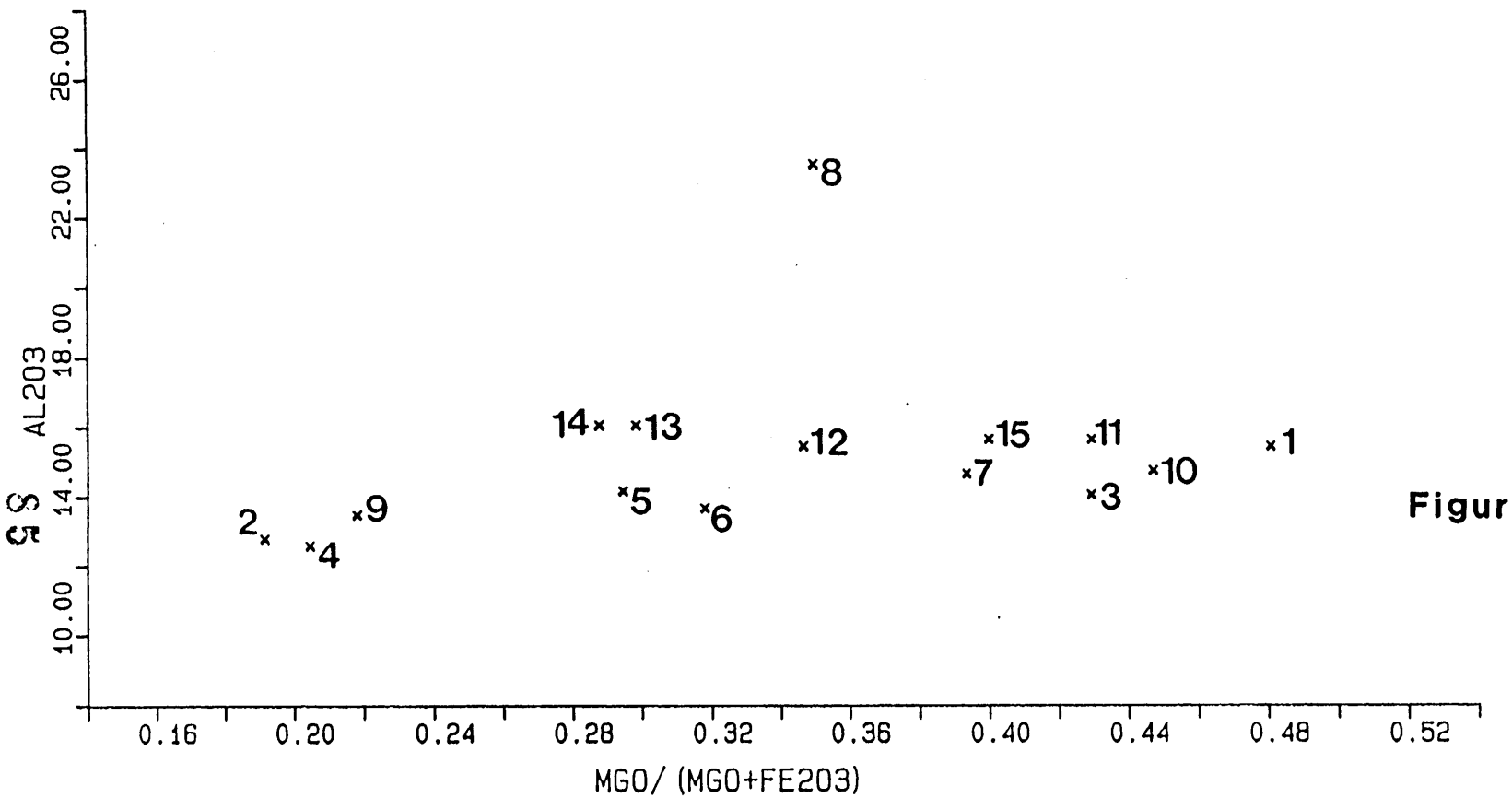

Figure 11

11: Binary weight percent plot of Al_2O_3 vs MgO/FeO+MgO for Archean metavolcanic rocks of Banting Township and the Western Part of Best Township.

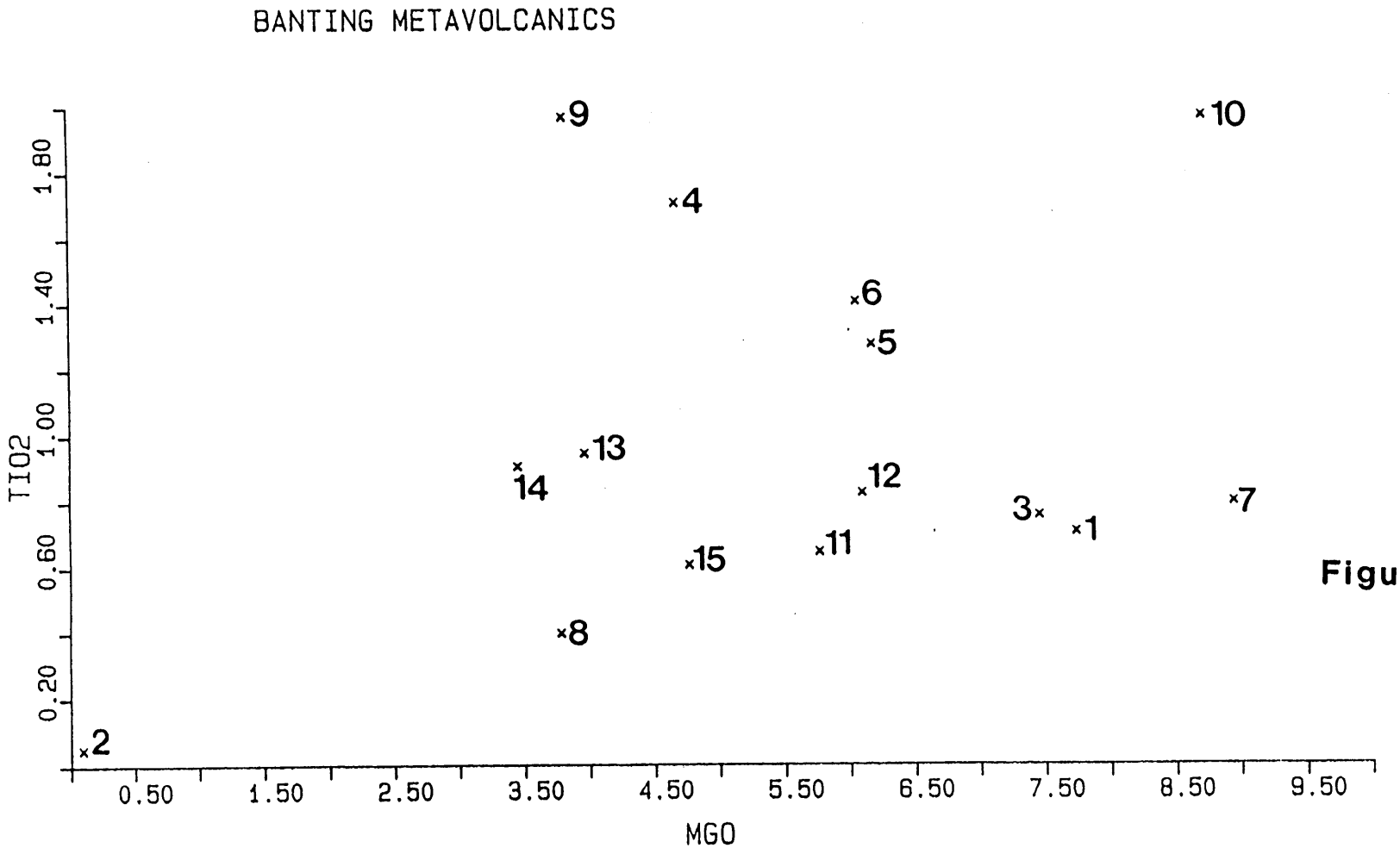

Figure 12

12: Binary weight percent plot of MgO vs TiO_2 for Archean metavolcanic rocks of Banting Township and the Western Part of Best Township.

BANTING GRANITOIDS

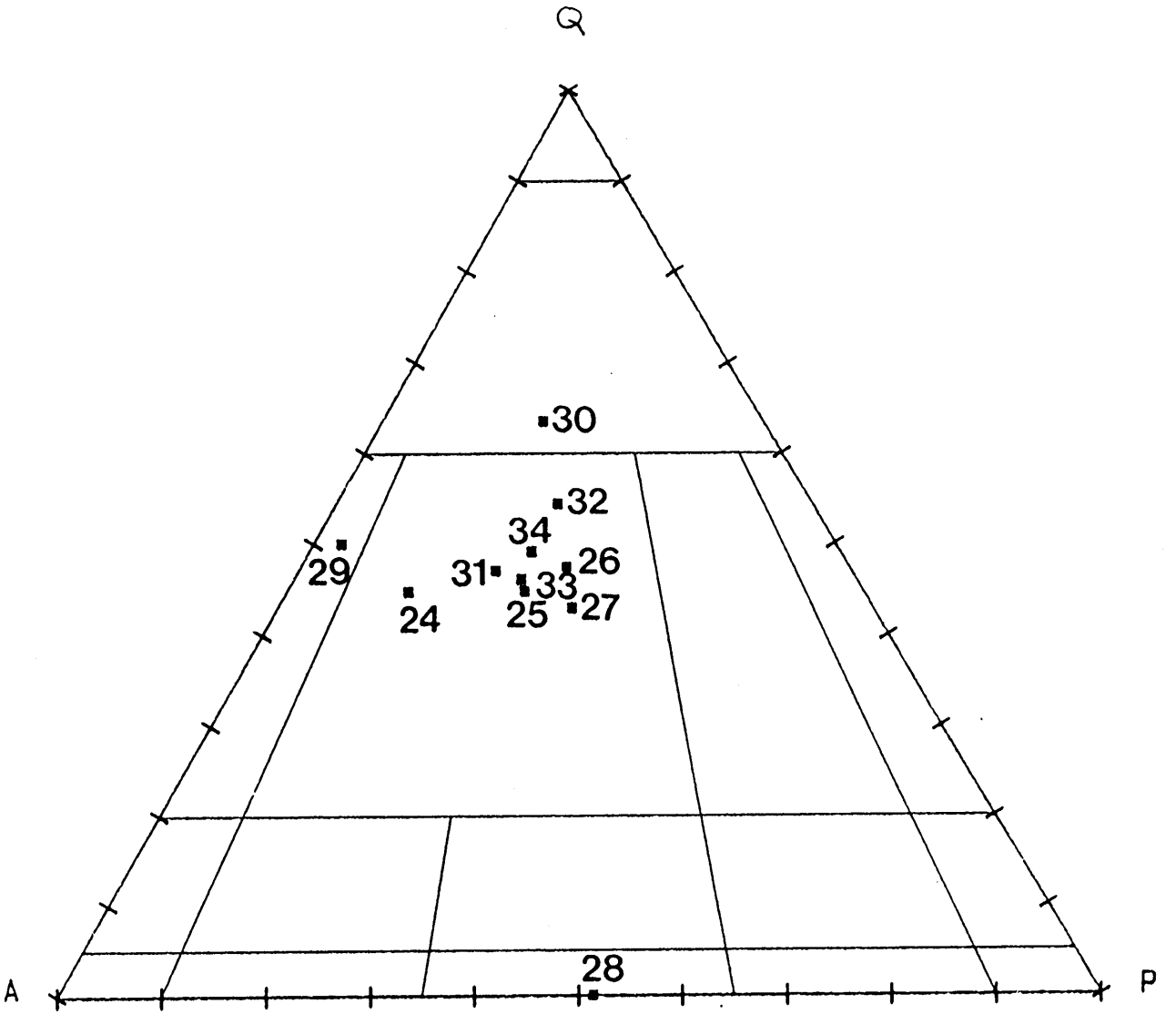

Figure 13

13: Ternary Q-A-P plot of normative minerals of some intermediate to felsic plutonic rocks of Banting Township and the Western Part of Best Township.

BANTING GRANITOIDS

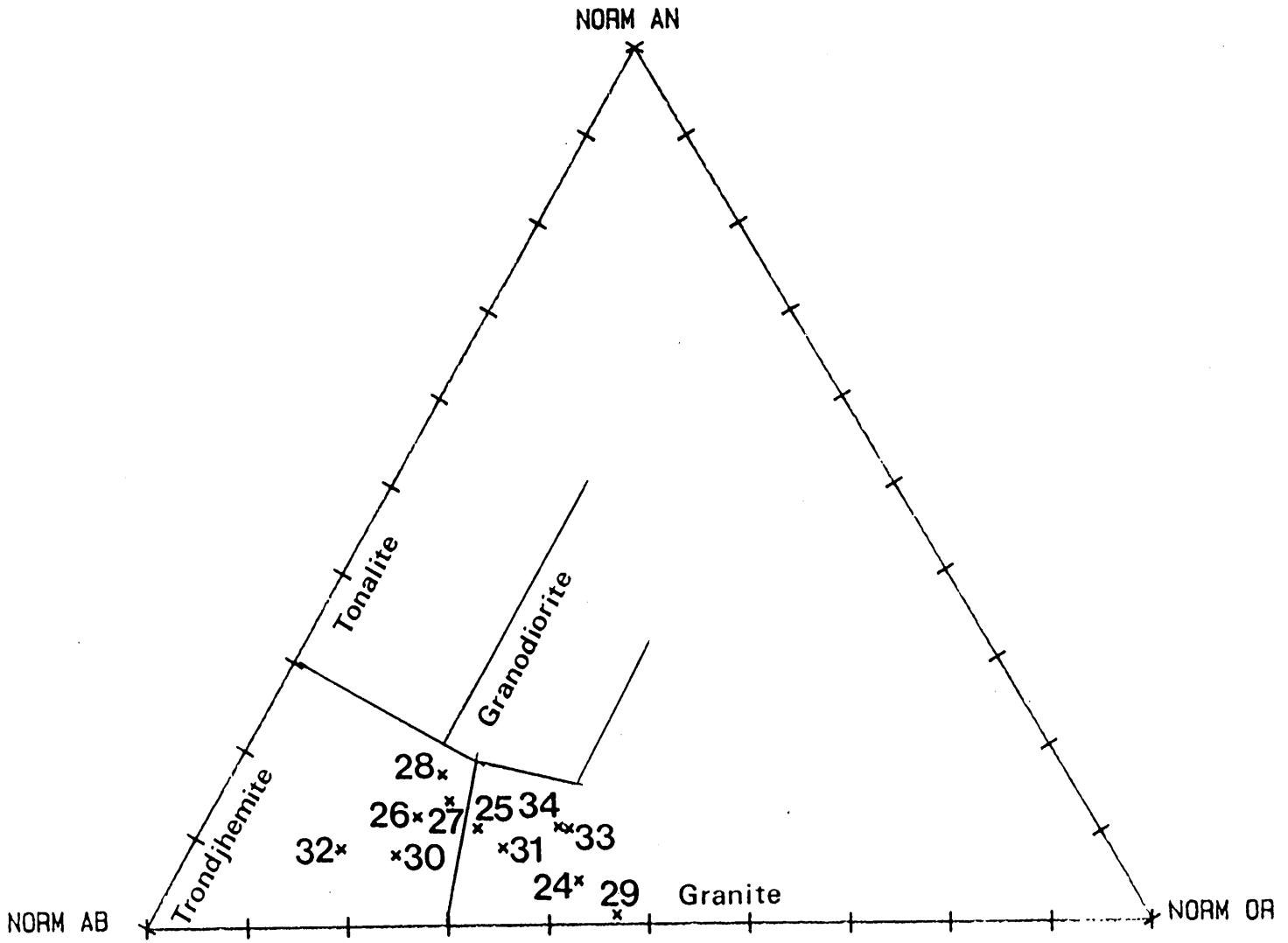

Figure 14

14: Ternary plot of normative An-Ab-Or minerals of some intermediate to felsic plutonic rocks of Banting Township and the Western Part of Best Township.

BANTING LAMPROPHYRES

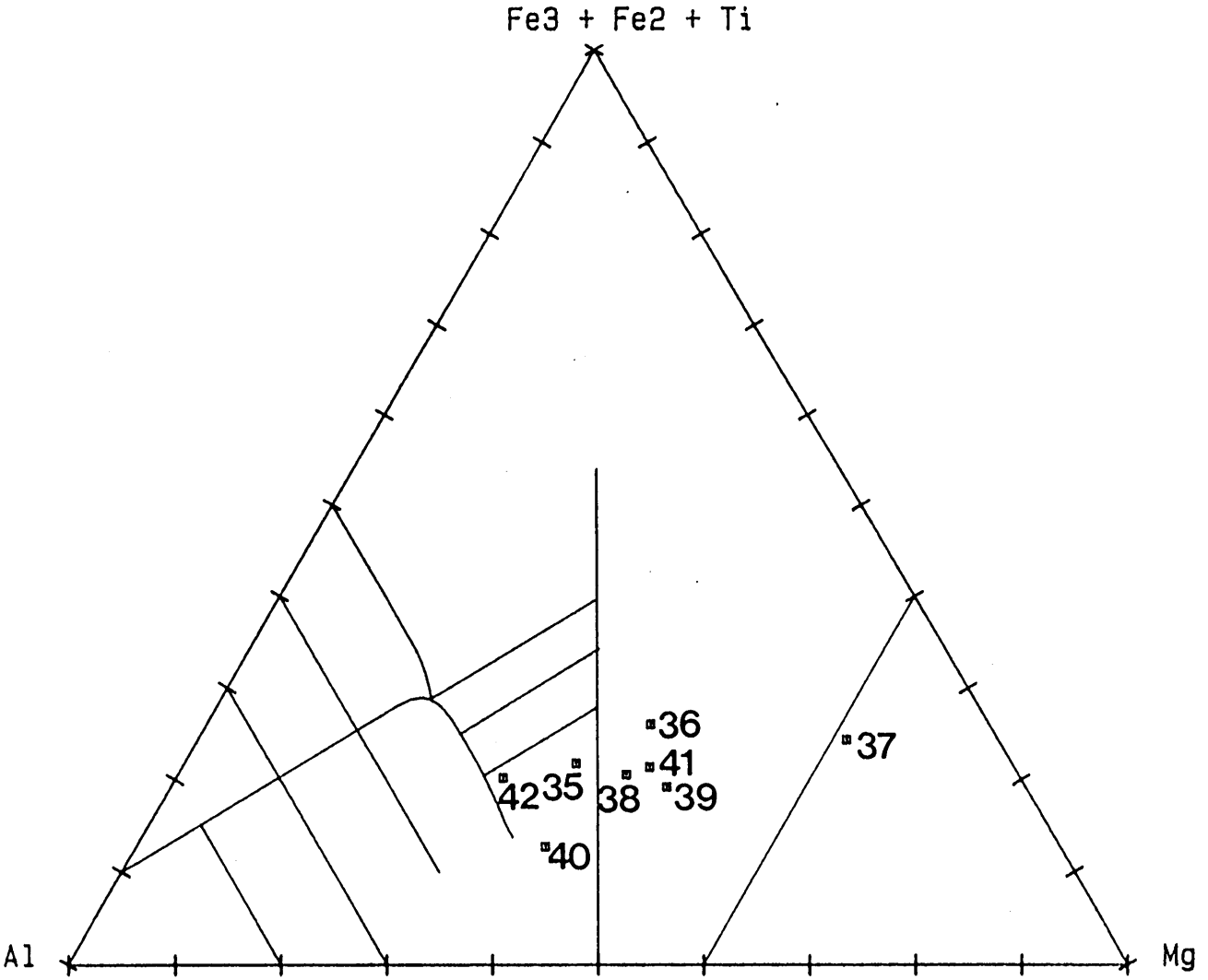

Figure 15

15: Cation plot (Jensen, 1976) of late Archean mafic to intermediate lamprophyre intrusive rocks of Banting Township and the Western Part of Best Township.

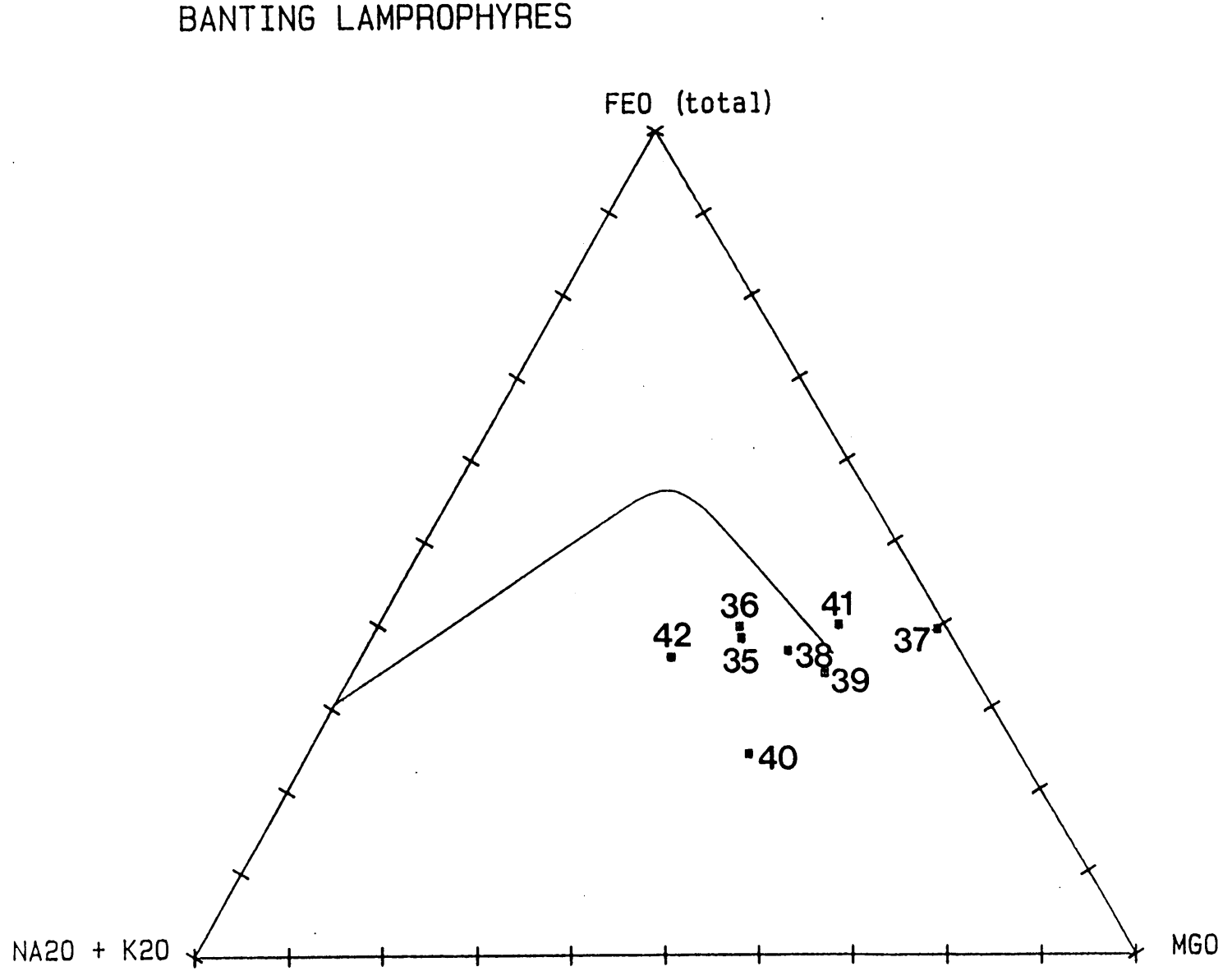

Figure 16

16: AFM (weight percent) plot of late Archean mafic to intermediate lamprophyre intrusive rocks of Banting Township and the Western Part of Best Township.

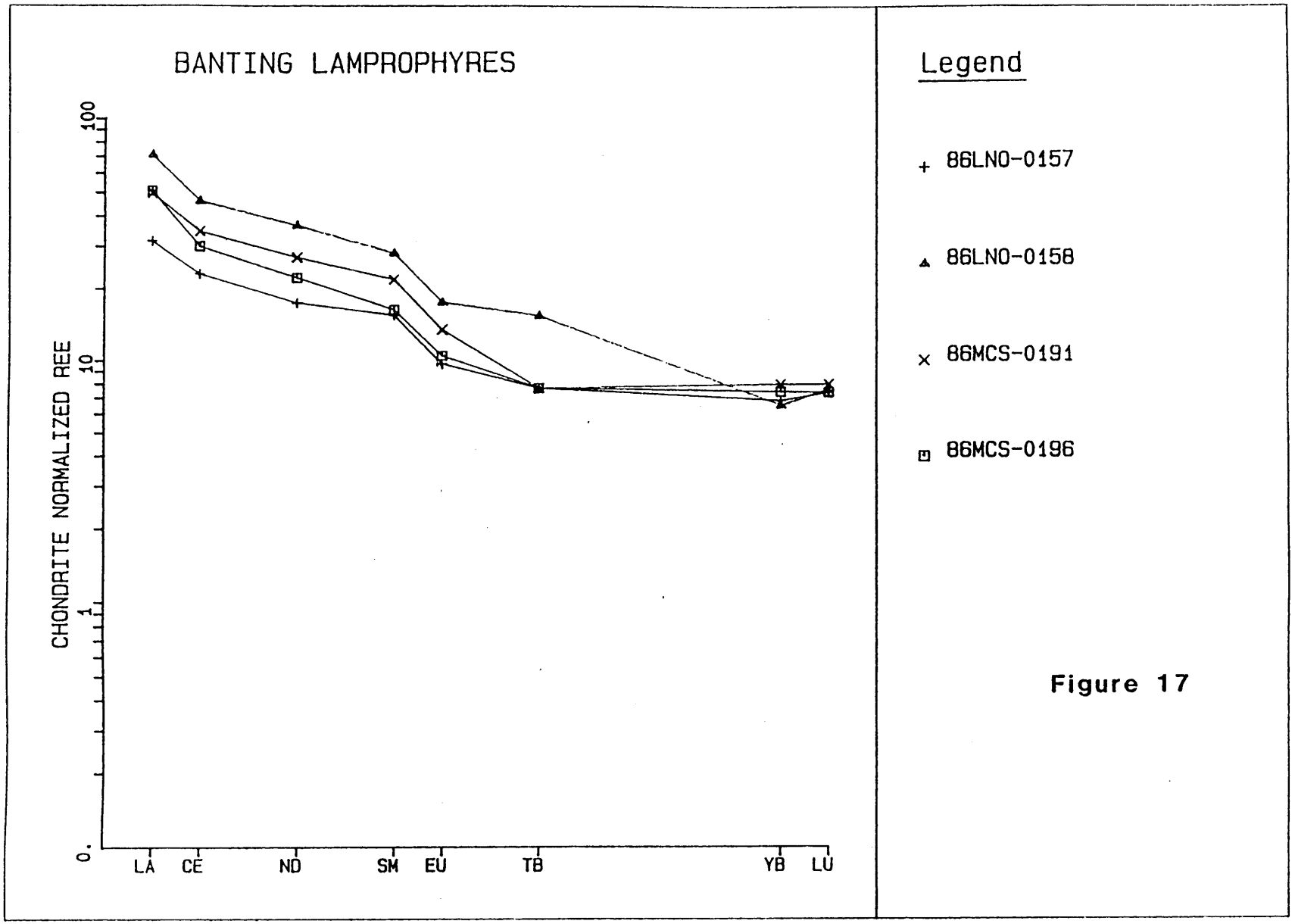

Figure 17

17: Chondrite normalized REE plot of late Archean mafic to intermediate lamprophyre intrusive rocks of Banting Township and the Western Part of Best Township.

BANTING PROTEROZOIC DIABASE

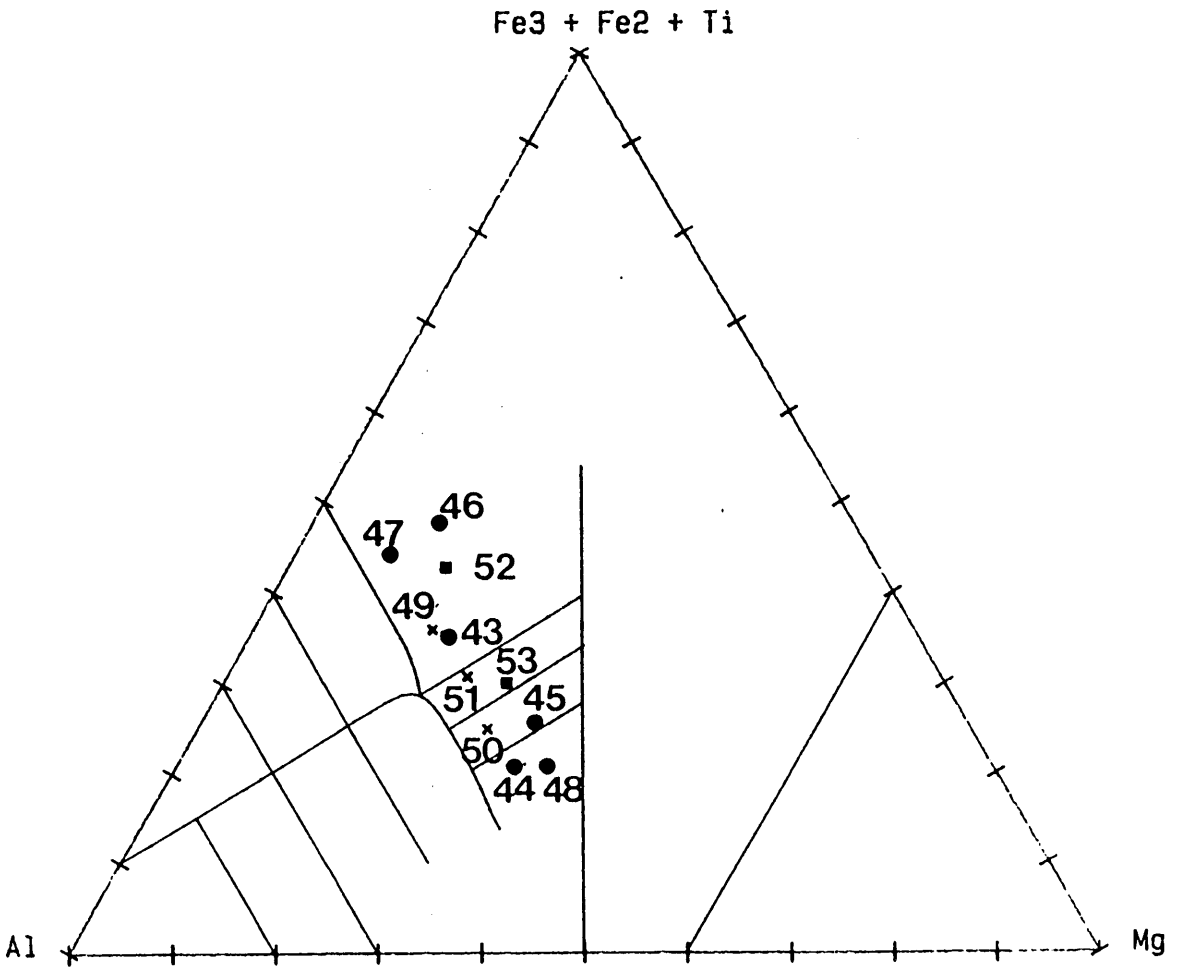

● Nipissing Diabase ▪ Sudbury Swarm × late diabase dikes

Figure 18

18: Cation plot (Jensen, 1976) -of Early Proterozoic Nipissing Diabase rocks and Middle Proterozoic olivine diabase dikes, Banting Township and the Western Part of Best Township.

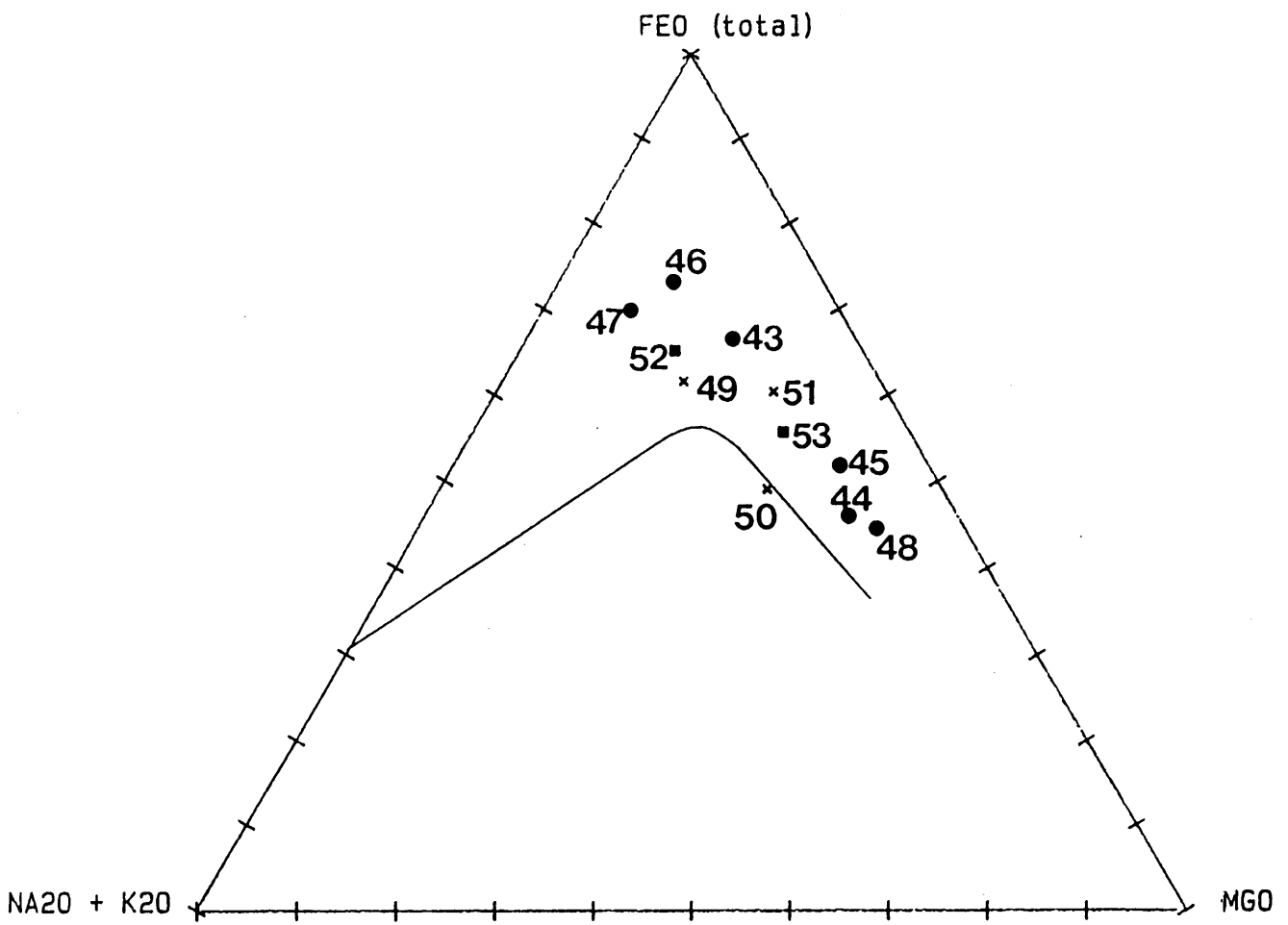

Figure 19

19: AFM (weight percent) plot of Early Proterozoic Nipissing Diabase rocks and Middle Proterozoic olivine diabase dikes, Banting Township and the Western Part of Best Township.

BANTING PROTEROZOIC DIABASE

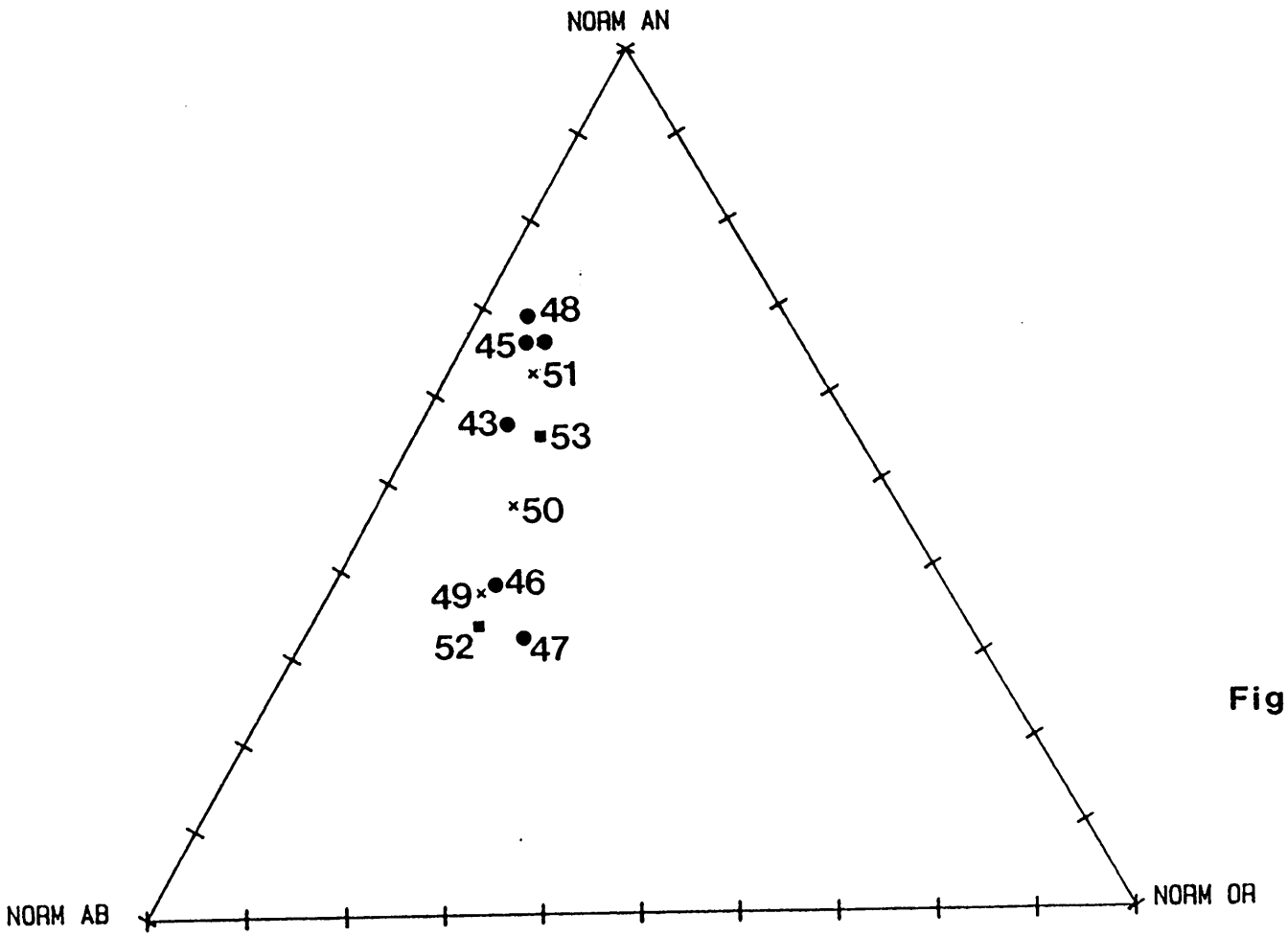

• Nipissing Diabase ▪ Sudbury Swarm × late diabase dikes

Figure 20

20: Ternary plot of normative An-Ab-Or minerals of Early Proterozoic Nipissing Diabase rocks and Middle Proterozoic olivine diabase dikes, Banting Township and the Western Part of Best Township.

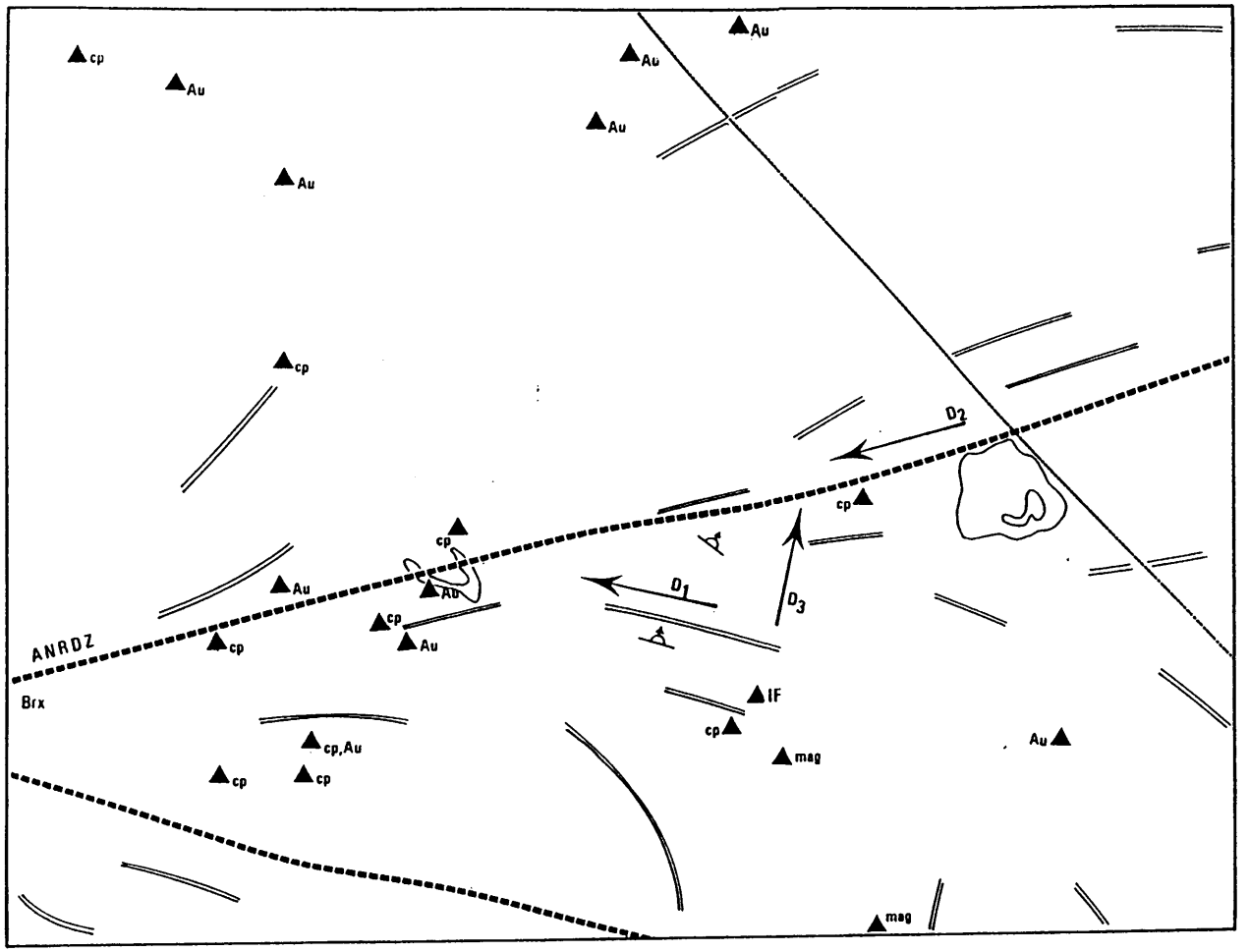

21: Simiplified geological map showing the relationship between major lithologic units, Archean-age stuctural elements and the distribution mineral occurrences. The dashed lines represent deformation zones, the arrows represent the main fold axis directions of the three deformational events (D1, D2, D3), the double curved lines represent Archean foliation trajectories, and the triangles represent mineral occurrences.

PHOTOS

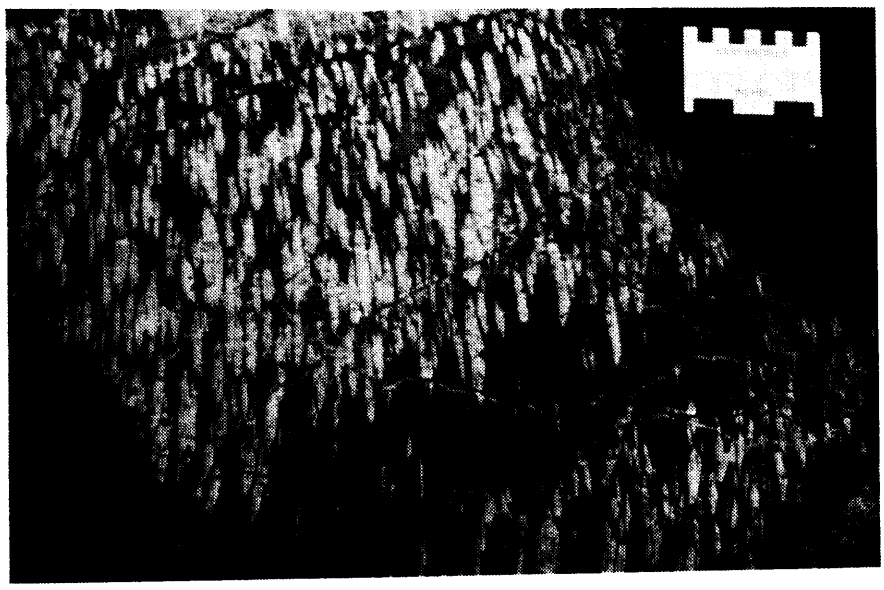

1: Archean metavolcanic rocks. Foliated, mega-feldspar phyric mafic flows. Located southeast of the southern end of McLean Lake.

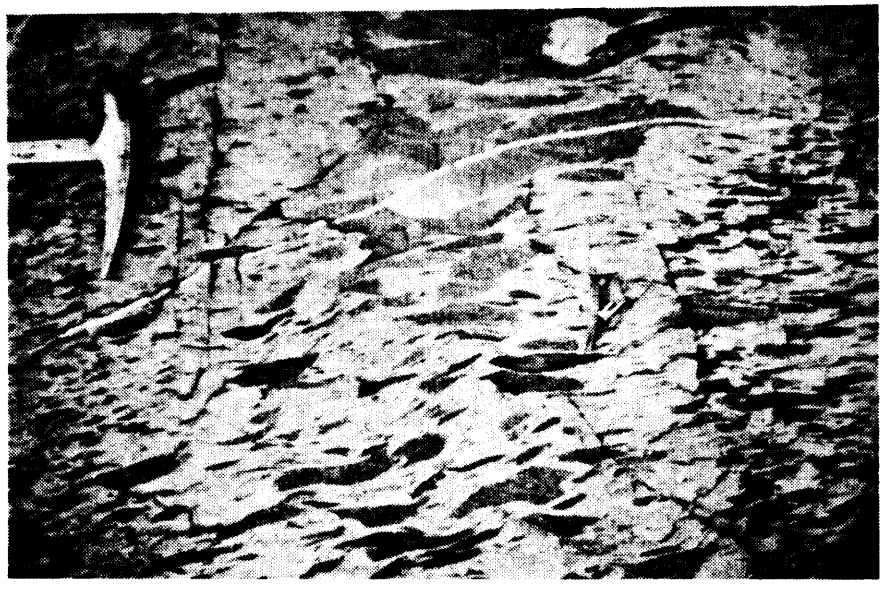

2: Archean metavolcanic rock. Foliated, heterolithic lapilli tuff. Note parallel allignment of fragments. Located south of Carrying Lake.

3: Archean intrusive rocks. Photomicrograph (crossed polarizers) of quartz diorite; note the large subhedral hornblende, altered plagioclase and anhedral quartz. Located 1 km southeast of the southern end of McLean Lake. Field of view is 12.4 mm.

4: Archean intrusive rocks. Stromatic (layered) granitic-metavolcanic migmatite. Note the abundance of dikes and late obique faults. Located southeast of the southern end of McLean Lake.

5: Archean intrusive rocks. Reticulate granite dikes in hornblende gabbro. Southeastern Banting Township.

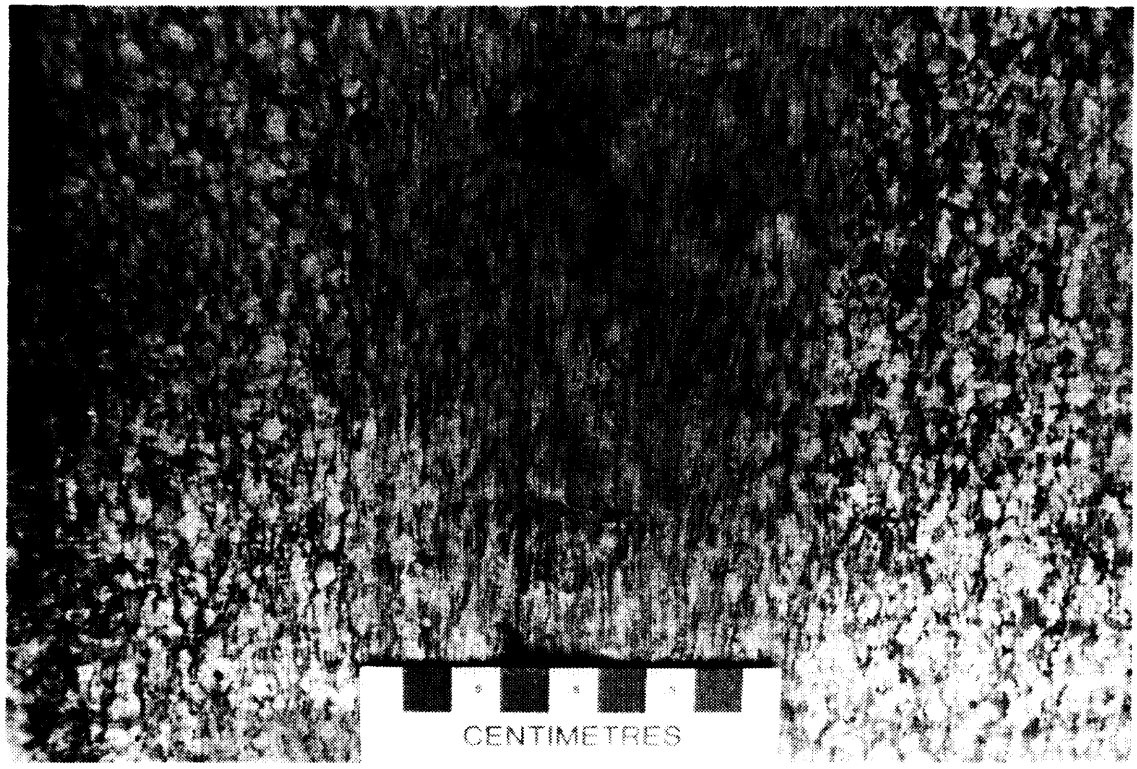

6: Archean intrusive rocks. Narrow protomylonite zone in foliated granite. North side of Red Squirrel Road, 0.5 km west of McLean Lake.

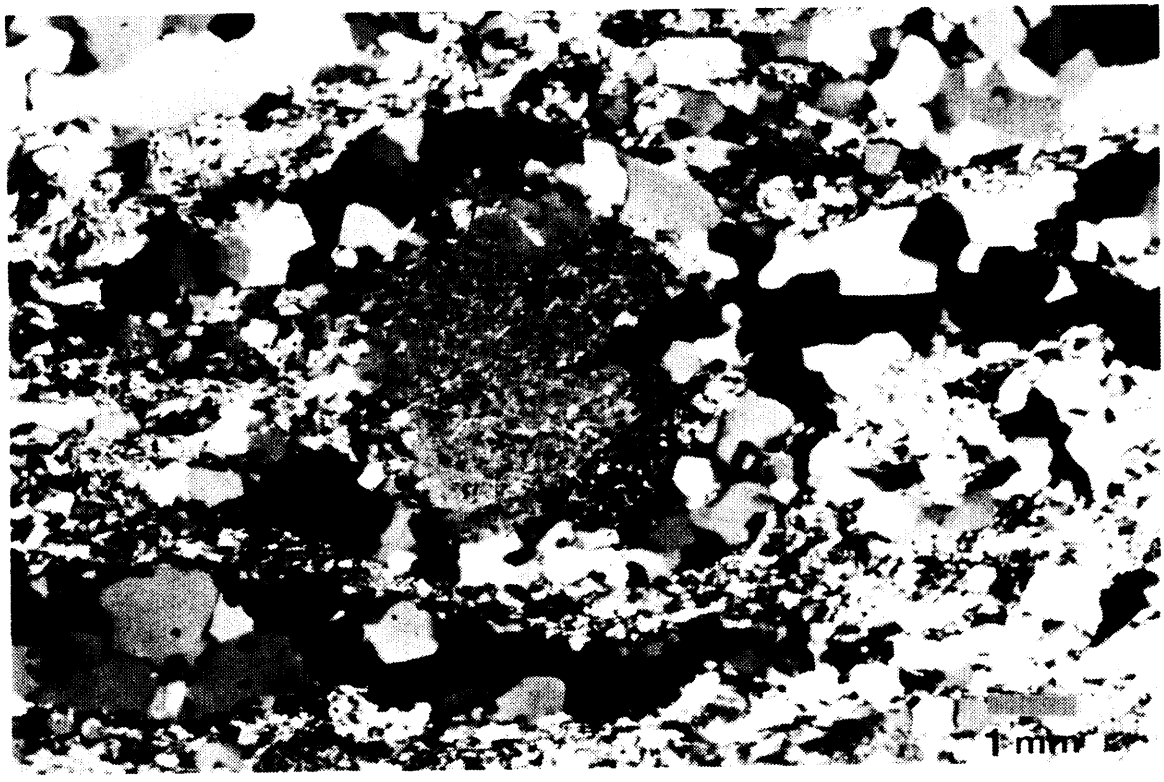

7: Archean intrusive rocks. Narrow protomylonite zone in foliated granite. Photomicrograph (crossed polarizers). Note the intense quartz sub-grain growth and quartz aggregates curving around larger feldspar grains. Field of view is 12.4 mm. South shore of Jamieson Lake.

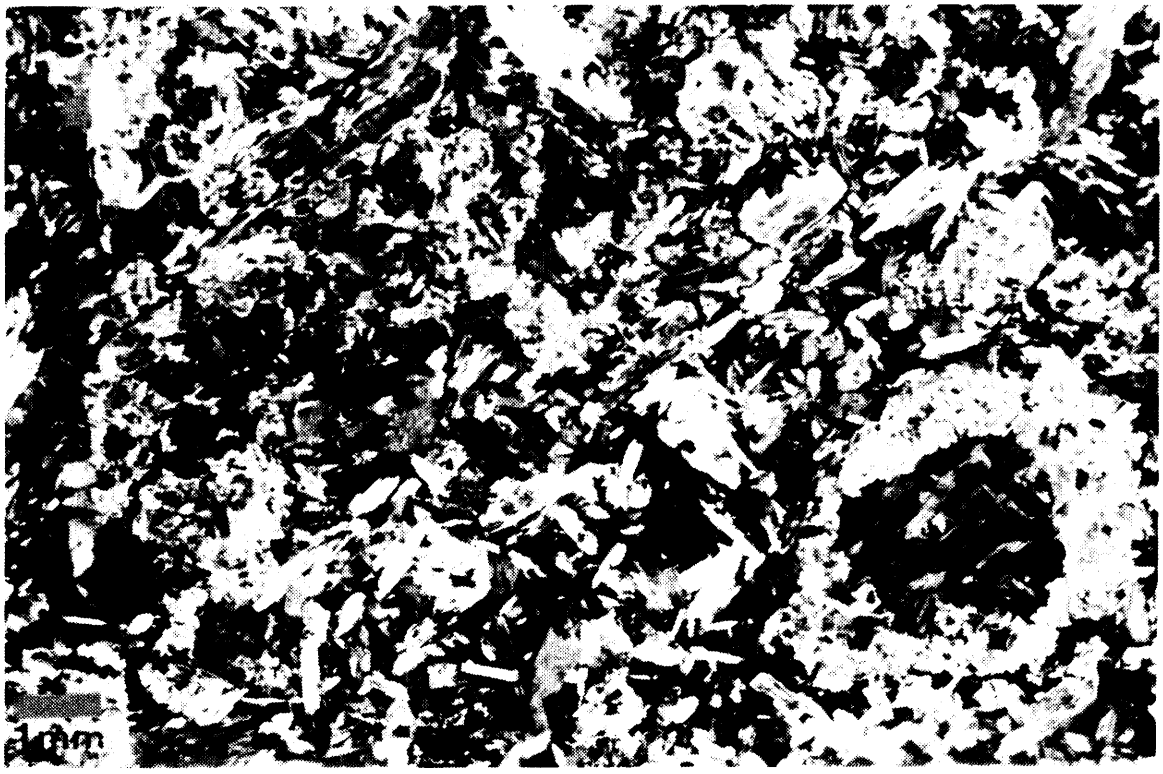

8: Archean intrusive rocks. Photomicrograph (crossed polarizers) of phlogopite-lamprophyre. Note lath-like phlogopite phenocrysts and calcite-scapolite ocellii at lower right. Field of view is 12.4 mm. Southeast of Contact Lake.

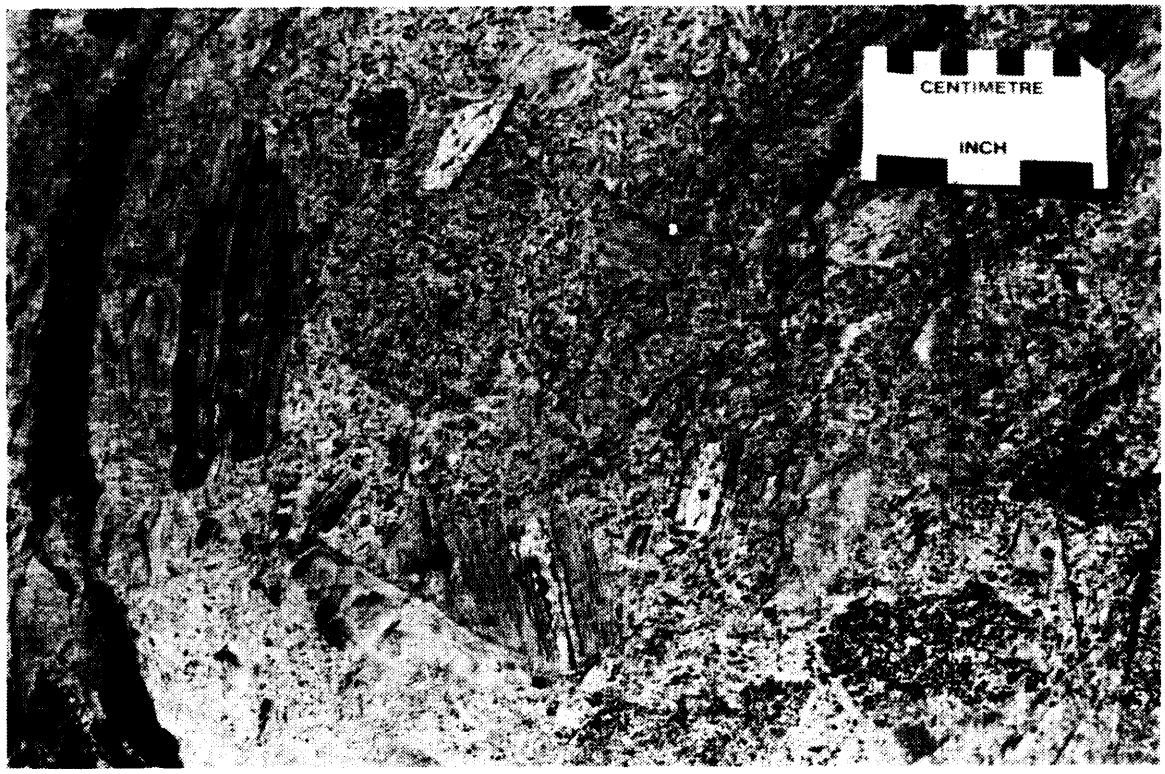

9: Archean intrusive rocks. Xenoliths of metavolcanics, granites and mafic intrusive rocks within an intrusive breccia hosted in pyroxene-phyric gabbro in the Anima-Nipissing River Intrusion. Island in a small lake 1.6 km east of McLean Lake, near Red Squirrel Road.

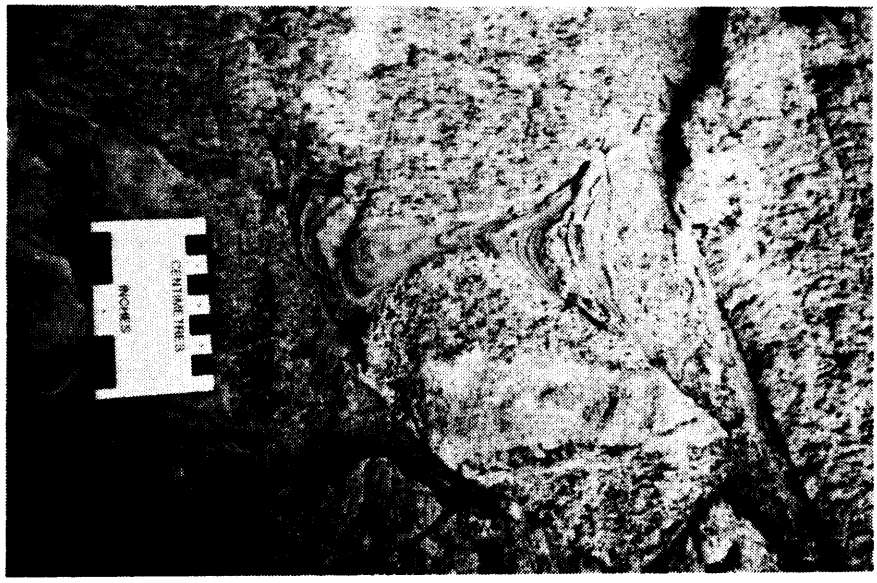

10: Early Proterozoic Gowganda Formation-Coleman Member: Mudstone drapes infilling space between granite blocks in basal breccia. East of Snare Lake.

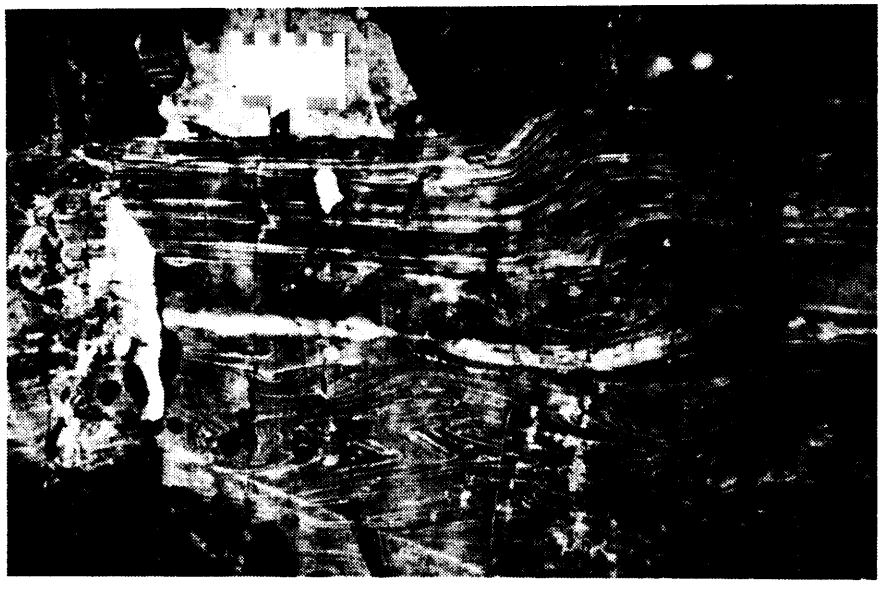

11: Early Proterozoic Gowganda Formation-Coleman Member: Thickly laminated mudstone-siltstone in a cliff exposure. Note the slump fold (syn-sedimentary deformation) and late kink band. West shore of Anima-Nipissing Lake.

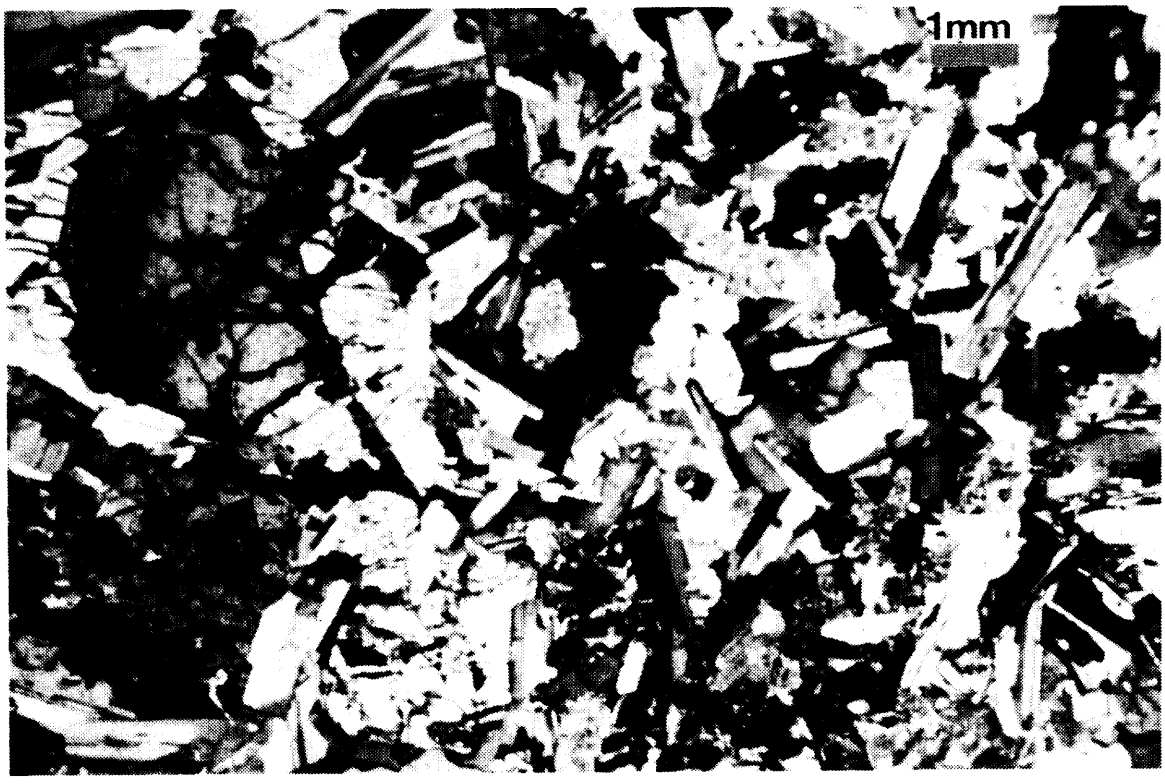

12: Early Proterozoic Nipissing Diabase. Photomicrograph (crossed polarizers) of medium-grained hypersthene diabase. Note altered anhedral olivine crystals (dark grey) in the upper left corner. Field of view is 12.4 mm. Southeast Banting Township.

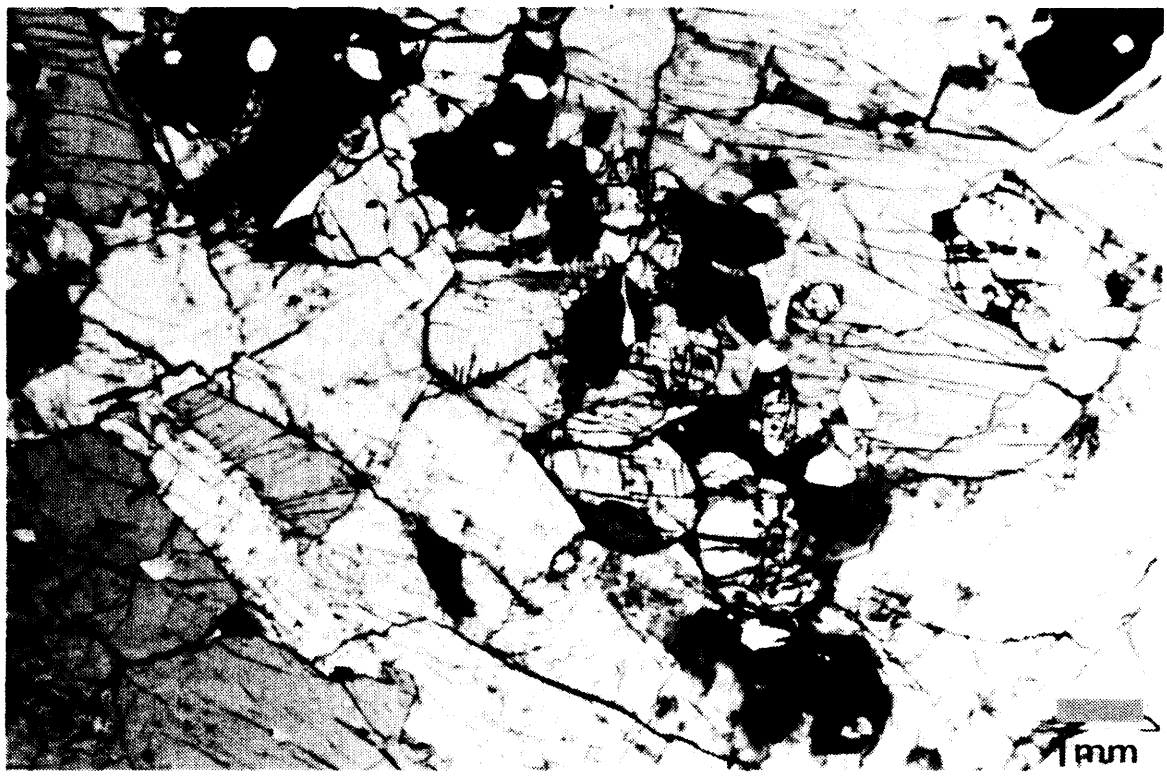

13: Middle Proterozoic Sudbury-type olivine diabase dike. Note titanaugite (dark grey), plagioclase laths, olivine (high relief, centre), small, hexagonal apatite crystals (colourless) and opaque ilmeno-magnetite. Field of view is 12.4 mm. Island in McLean Lake.

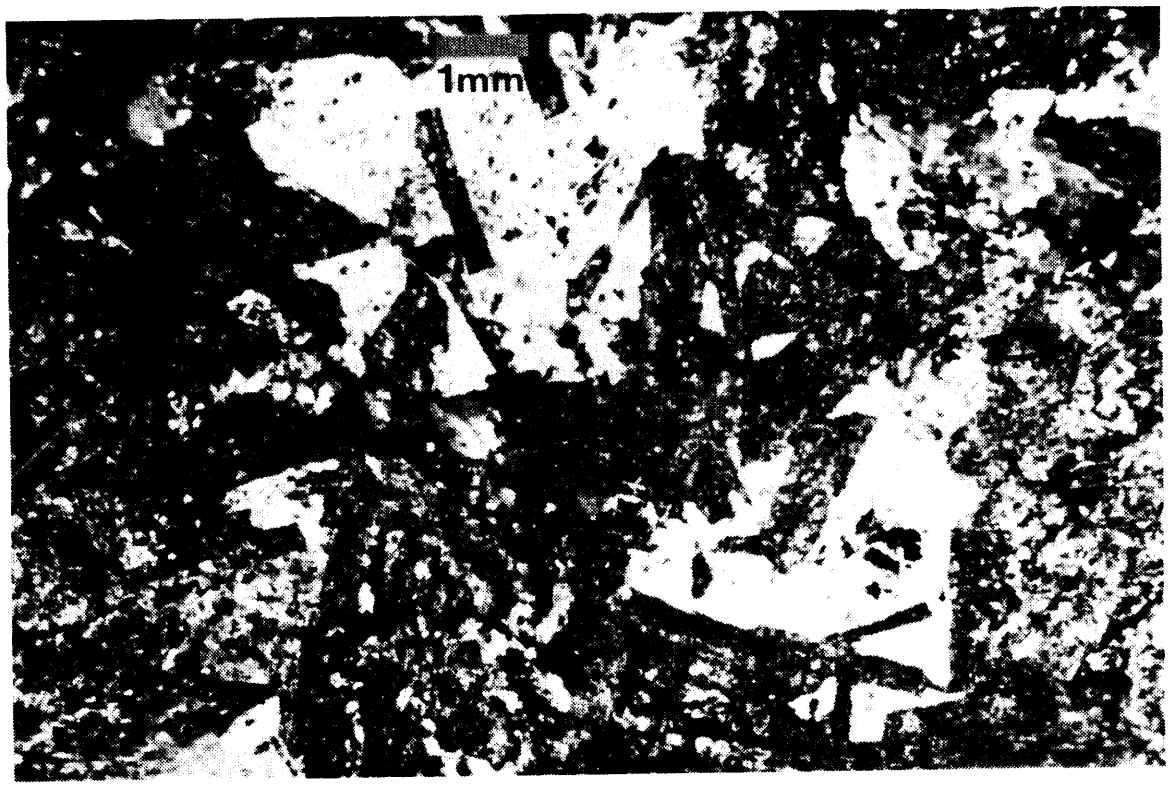

14: Middle Proterozoic late diabase dike. Photomicrograph (plane polarized light) of relict subophitic textures in late diabase dikes. Pyroxene (white) and plagioclase (darks laths) have been altered to uralite and saussurite, respectively. Field of view is 12.4 mm. Southeast of Mannajigama Lake.

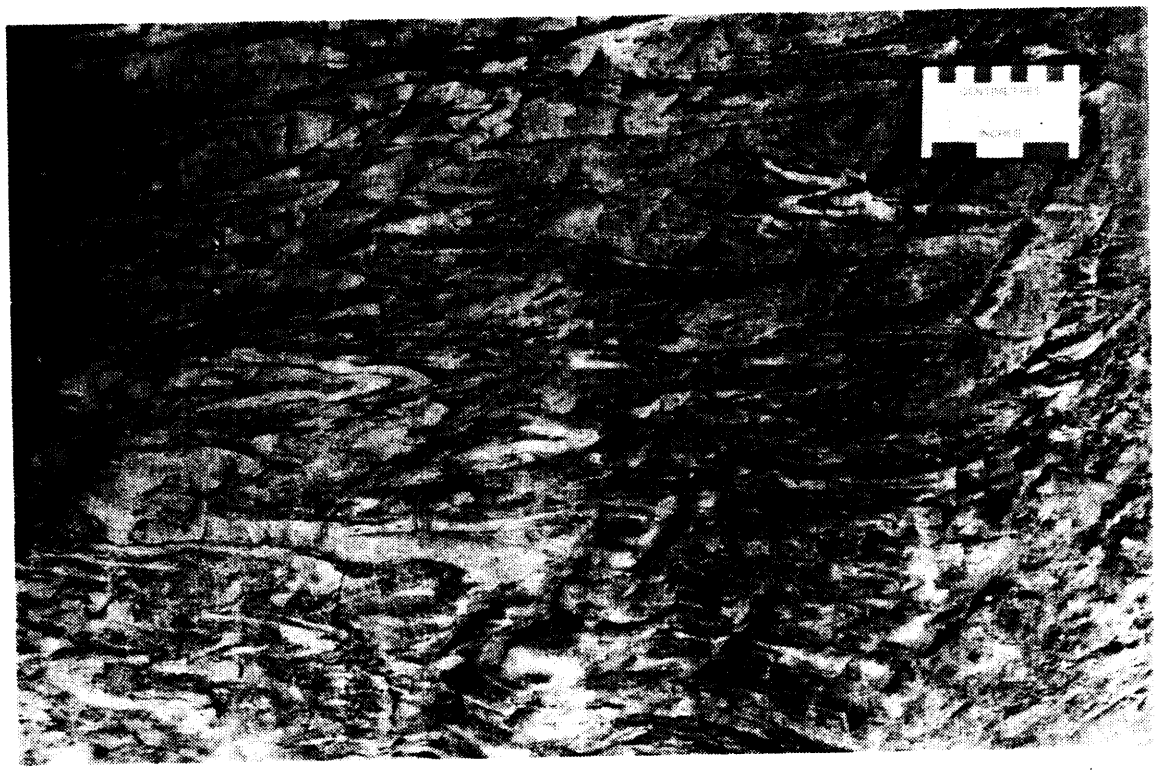

15: Minor folds in tuff-breccia. Northeast of Lundy Lake near Snare Creek.

TABLES

Table 1: Table of Lithologic Units for Banting and western Best Townships.

PHANEROZOIC

CENOZOIC

QUATERNARY

PLEISTOCENE AND RECENT

Swamp and stream deposits, till, sand and gravel

UNCONFORMITY

PRECAMBRIAN

MIDDLE PROTEROZOIC

Mafic Intrusive Rocks

Late Diabase dikes

Olivine Diabase Dikes (Sudbury Swarm)

INTRUSIVE CONTACT

EARLY PROTEROZOIC

Mafic Intrusive Rocks

Nipissing Intrusive Rocks

Varied textured diabase, felsite dikes, hypersthene diabase, quartz diabase.

Table 1 (continued)

INTRUSIVE CONTACT

HURONIAN SUPERGROUP

COBALT GROUP

Gowganda Formation

Coleman Member

Sandstone, pebbly sandstone, mudstone, pebbly mudstone, pebbly wacke, diamictite, basal diamictite, basal breccia

UNCONFORMITY

MAFIC TO INTERMEDIATE PLUTONIC ROCKS

Anima-Nipissing River and Snare Creek Intrusion

Pyroxene-phyric gabbro, diorite, intrusive and diatreme breccias, Lamprophyre and mafic dikes

INTRUSIVE CONTACT

FELSIC TO INTERMEDIATE PLUTONIC ROCKS

Granite, granitic migmatite and minor pegmatite and aplite.

INTRUSIVE CONTACT

INTERMEDIATE TO MAFIC PLUTONIC ROCKS

Diorite, quartz diorite, hornblende gabbro

Table 1 (continued)

INTRUSIVE CONTACT

HYPABYSSAL FELSIC INTRUSIVE ROCKS

Feldspar porphyry

METAVOLCANICS

INTERMEDIATE TO FELSIC METAVOLCANICS

Heterolithic tuff-breccia, tuff

MAFIC TO INTERMEDIATE METAVOLCANICS

Amphibolite; basalt; pillowed basalt; plagioclase-phyric basalt; variolitic basalt; andesite; ; albite-epidote-hornblende hornfels and dervived schists; minor tuffs

Table 2: Chemical Analyses and normative mineralogy of Archean metavolcanic rocks, Banting Township and Western Part of Best Township. (Analysed by X-Ray Assay Laboratories Limited.)

MAJOR OXIDES
WEIGHT PERCENT

Reference Number:	1	2	3	4	5	6
	84LNO-0047	84LNO-0142	84LNO-0149	84LNO-0176	85LNO-0061	85LNO-0062
SiO2	52.90	78.50	52.90	50.70	49.30	50.90
TiO2	0.71	0.05	0.76	1.71	1.28	1.41
Al2O3	15.50	12.80	14.10	12.60	14.20	13.70
Fe2O3	8.36	0.38	9.92	18.20	14.80	13.00
FeO	00.00	00.00	00.00	00.00	00.00	00.00
MnO	0.15	0.03	0.19	0.25	0.23	0.23
MgO	7.74	0.09	7.46	4.68	6.18	6.06
CaO	7.27	0.73	8.00	8.00	9.71	13.70
Na2O	3.51	7.10	3.88	2.57	2.30	2.83
K2O	1.36	0.16	0.80	0.32	0.55	0.48
P2O5	0.11	0.02	0.12	0.15	0.10	0.13
CO2	00.00	00.00	00.00	00.00	00.00	00.00
S	00.00	00.00	00.00	00.00	00.00	00.00
H2O+	00.00	00.00	00.00	00.00	00.00	00.00
H2O-	00.00	00.00	00.00	00.00	00.00	00.00
LOI	1.80	0.30	2.00	0.70	1.20	1.70
TOTAL	99.60	100.30	100.30	100.00	99.90	99.90

TRACE ELEMENT LISTING
(PPM)

	84LNO-0047	84LNO-0142	84LNO-0149	84LNO-0176	85LNO-0061	85LNO-0062
Ba	250	90	240	130	120	170
Co	50	50	220	110	100	110
Cr	380	10	440	60	120	160
Cu	30	90	60	200	120	160
Ni	130	10	150	40	80	70
Pb	20	40	20	10	50	30
Zn	70	20	110	180	200	150
Nb	20	20	10	30	20	20
Rb	80	20	40	30	50	30
Sr	170	40	200	120	100	300
Y	20	40	20	30	20	40
Zr	70	90	90			80

Table 2: (Continued)

MAJOR OXIDES
WEIGHT PERCENT

Reference Number:	7	8	9	10	11	12
	86LNO-0133	86LNO-0135	86LNO-0137	86LNO-0138	86LNO-0154	86MCS-0084
SiO2	47.00	46.10	52.50	49.30	58.20	51.50
TiO2	0.80	0.40	1.97	1.97	0.65	0.83
Al2O3	14.70	23.60	13.50	14.80	15.70	15.50
Fe2O3	13.80	7.03	13.70	10.80	7.67	11.50
FeO	00.00	00.00	00.00	00.00	00.00	00.00
MnO	0.24	0.14	0.25	0.20	0.13	0.21
MgO	8.95	3.78	3.82	8.73	5.77	6.10
CaO	9.93	12.10	6.54	10.70	3.08	9.04
Na2O	1.70	2.79	4.17	1.45	3.39	2.82
K2O	1.01	0.76	0.38	1.54	2.03	0.75
P2O5	0.06	0.04	0.17	0.05	0.12	0.06
CO2	00.00	00.00	00.00	00.00	00.00	00.00
S	00.00	00.00	00.00	00.00	00.00	00.00
H2O+	00.00	00.00	00.00	00.00	00.00	00.00
H2O-	00.00	00.00	00.00	00.00	00.00	00.00
LOI	1.90	3.00	2.00	1.90	2.70	1.20
TOTAL	100.20	99.90	99.10	100.30	99.60	99.60

TRACE ELEMENTS
(PPM)

	86LNO-0133	86LNO-0135	86LNO-0137	86LNO-0138	86LNO-0154	86MCS-0084
Ba	350	200	160	360	640	110
Co	90	40	90	90	60	70
Cr	240	130	60	390	240	0.03%
Cu	70	50	230	110	30	110
Ni	110	60	40	110	90	110
Pb	10	20	20	80	20	10
Zn	130	60	170	250	100	90
Nb	10	10	20	10	20	10
Rb	20	30	40	100	110	20
Sr	90	410	90	140	250	70
Y	30	10	50	10	10	10
Zr	10	20	120	10	100	30
Th						10
U						10
Mo						10

Table 2: (Continued)

MAJOR OXIDES
WEIGHT PERCENT

Reference Number:	13	14	15
	86MCS-0084	86MCS-0208	84LNO-0035
SiO2	56.00	57.30	60.70
TiO2	0.95	0.91	0.61
Al2O3	16.10	16.10	15.70
Fe2O3	9.34	8.57	7.16
FeO	00.00	00.00	00.00
MnO	0.14	0.17	0.12
MgO	3.97	3.46	4.77
CaO	6.33	6.91	2.65
Na2O	3.37	3.59	3.02
K2O	1.40	1.05	2.33
P2O5	0.12	0.17	0.12
CO2	00.00	00.00	00.00
S	00.00	00.00	00.00
H2O+	00.00	00.00	00.00
H2O-	00.00	00.00	00.00
LOI	1.60	1.90	2.70
TOTAL	99.40	100.30	100.10

TRACE ELEMENTS
(PPM)

	86MCS-0084	86MCS-0208	84LNO-0035
Ba	260	260	700
Co	50	50	50
Cr	80	70	210
Cu	60	10	50
Ni	80	40	80
Pb	20	20	10
Zn	70	70	70
Nb	30	10	20
Rb	70	50	130
Sr	220	260	270
Y	20	40	10
Zr	110	180	110

Table 2: (Continued)

MAJOR OXIDE STATISTICS

TOTAL NUMBER OF SAMPLES: 15

	MEAN	STD. DEVIATION
SiO2	54.25	7.85
Al2O3	15.24	2.58
Fe2O3	10.28	4.22
FeO	0.00	0.00
MgO	5.44	2.32
CaO	7.65	3.53
Na2O	3.23	1.31
K2O	0.99	0.63
TiO2	1.00	0.56
P2O5	0.10	0.05
MnO	0.18	0.06
CO2	0.00	0.00
S	0.00	0.00
H2O+	0.00	0.00
H2O-	0.00	0.00
LOI	1.77	0.73
TOTAL	99.90	0.37

TRACE ELEMENT STATISTICS

	NO. OF SAMPLES	MEAN	STD. DEVIATION
Ba	15	269.33	182.23
Co	15	82.00	45.23
Cr	15	172.67	140.84
Cu	15	92.00	63.94
Ni	15	80.00	38.17
Pb	15	25.33	18.85
Zn	15	116.00	62.77
Nb	15	17.33	7.04
Rb	15	54.67	35.43
Sr	15	182.00	102.90
Y	15	24.00	13.52
Zr	13	78.46	49.97
Th	1	10.00	0.00
U	1	10.00	0.00
Mo	1	10.00	0.00

Table 2: (Continued)

CIPW NORMATIVE VALUES

Reference Number:	1	2	3	4	5	6
	84LNO-0047	84LNO-0142	84LNO-0149	84LNO-0176	85LNO-0061	85LNO-0062
APTT	0.2686	0.0474	0.2919	0.3637	0.2431	0.3036
PYRT	0.0000	0.0000	0.0000	0.0000	0.0000	0.0000
ILMN	1.3902	0.0643	1.4825	3.3249	2.4947	2.6402
ORTH	8.2857	0.9468	4.8555	1.9359	3.3353	2.7965
ALBT	30.6212	60.1624	33.7209	22.2636	19.9721	23.6093
ACMT	0.0000	0.0000	0.0000	0.0000	0.0000	0.0000
ANRT	23.2190	2.5867	19.2004	22.4196	27.4999	22.9331
SPHN	0.0000	0.0398	0.0000	0.0000	0.0000	0.0000
RUTL	0.0000	0.0000	0.0000	0.0000	0.0000	0.0000
MGNT	3.3036	0.0000	3.3655	4.7648	4.1364	4.1598
HEMT	0.0000	0.3805	0.0000	0.0000	0.0000	0.0000
DIOP	7.9563	0.4842	11.5003	5.8497	9.2725	20.7301
HEDN	2.6780	0.0000	5.3357	8.6444	8.3393	14.8087
WOLL	0.0000	0.0963	0.0000	0.0000	0.0000	0.0000
ENST	15.7996	0.0000	11.8165	9.2208	11.4962	2.0602
FERS	6.1000	0.0000	6.2888	15.6301	11.8597	1.6881
QRTZ	0.0000	35.1930	0.0000	5.5937	1.3591	0.0000
FORS	0.2704	0.0000	1.3557	0.0000	0.0000	2.2490
FAYA	0.1151	0.0000	0.7952	0.0000	0.0000	2.0310
PVSK	0.0000	0.0000	0.0000	0.0000	0.0000	0.0000
NEPH	0.0000	0.0000	0.0000	0.0000	0.0000	0.0000
LEUC	0.0000	0.0000	0.0000	0.0000	0.0000	0.0000
DICA	0.0000	0.0000	0.0000	0.0000	0.0000	0.0000
KALP	0.0000	0.0000	0.0000	0.0000	0.0000	0.0000
CNDM	0.0000	0.0000	0.0000	0.0000	0.0000	0.0000
CALC	0.0000	0.0000	0.0000	0.0000	0.0000	0.0000
NPLG	43.1258	4.1223	36.2811	50.1746	57.9287	49.2736
FEMG	0.2561	0.0022	0.2671	0.2722	0.2808	0.2406
RMG	0.7729	1.0000	0.7117	0.4367	0.5602	0.6159
RFE	0.2271	0.0000	0.2883	0.5633	0.4398	0.3841
C.I.	37.6133	0.9290	41.9402	47.4347	47.5988	50.3670
TOTL	100.0078	100.0014	100.0089	100.0112	100.0083	100.0095

Table 2: (Continued)

CIPW NORMATIVE VALUES

Reference Number:	7	8	9	10	11	12
	86LNO-0133	86LNO-0135	86LNO-0137	86LNO-0138	86LNO-0154	86MCS-0084
APTT	0.1465	0.0985	0.4195	0.1199	0.2955	0.1459
PYRT	0.0000	0.0000	0.0000	0.0000	0.0000	0.0000
ILMN	1.5658	0.7895	3.8984	3.7867	1.2834	1.6186
ORTH	6.1506	4.6672	2.3397	9.2103	12.4714	4.5507
ALBT	14.8241	19.8715	36.7652	12.4178	29.8224	24.5013
ACMT	0.0000	0.0000	0.0000	0.0000	0.0000	0.0000
ANRT	30.3969	51.5729	17.7082	29.6808	15.0706	28.1543
SPHN	0.0000	0.0000	0.0000	0.0000	0.0000	0.0000
RUTL	0.0000	0.0000	0.0000	0.0000	0.0000	0.0000
MGNT	3.4366	2.8629	5.2422	5.0920	3.2409	3.4688
HEMT	0.0000	0.0000	0.0000	0.0000	0.0000	0.0000
DIOP	10.0011	5.3756	6.1217	15.0961	0.0000	8.4391
HEDN	6.3471	3.2389	6.3098	3.8519	0.0000	5.9307
WOLL	0.0000	0.0000	0.0000	0.0000	0.0000	0.0000
ENST	8.5642	0.0000	7.0748	15.0066	14.9400	11.6868
FERS	6.2345	0.0000	8.3646	4.3922	6.7711	9.4209
QRTZ	0.0000	0.0000	5.7683	1.3510	13.3960	2.0890
FORS	6.8464	5.1094	0.0000	0.0000	0.0000	0.0000
FAYA	5.4927	3.8918	0.0000	0.0000	0.0000	0.0000
PVSK	0.0000	0.0000	0.0000	0.0000	0.0000	0.0000
NEPH	0.0000	2.5259	0.0000	0.0000	0.0000	0.0000
LEUC	0.0000	0.0000	0.0000	0.0000	0.0000	0.0000
DICA	0.0000	0.0000	0.0000	0.0000	0.0000	0.0000
KALP	0.0000	0.0000	0.0000	0.0000	0.0000	0.0000
CNDM	0.0000	0.0000	0.0000	0.0000	2.7170	0.0000
CALC	0.0000	0.0000	0.0000	0.0000	0.0000	0.0000
NPLG	67.2187	68.1692	32.5080	70.5031	33.5700	53.4688
FEMG	0.3555	0.1487	0.1876	0.2680	0.2001	0.2507
RMG	0.6435	0.6553	0.5264	0.8178	0.7436	0.6198
RFE	0.3565	0.3447	0.4736	0.1822	0.2564	0.3802
C.I.	48.4883	21.2681	37.0115	47.2254	26.2354	40.5648
TOTL	100.0064	100.0040	100.0125	100.0052	100.0082	100.0060

Table 2: (Continued)

CIPW NORMATIVE VALUES

Reference Number:	13	14	15
	86MCS-0084	86MCS-0208	84LNO-0035
APTT	0.2929	0.4125	0.2940
PYRT	0.0000	0.0000	0.0000
ILMN	1.8595	1.7706	1.1984
ORTH	8.5262	6.3565	14.2423
ALBT	29.3890	31.1205	26.4336
ACMT	0.0000	0.0000	0.0000
ANRT	25.4237	25.3190	12.7880
SPHN	0.0000	0.0000	0.0000
RUTL	0.0000	0.0000	0.0000
MGNT	3.6610	3.5797	3.1645
HEMT	0.0000	0.0000	0.0000
DIOP	2.9473	4.1667	0.0000
HEDN	2.0925	2.9510	0.0000
WOLL	0.0000	0.0000	0.0000
ENST	8.8237	6.8963	12.2885
FERS	7.1857	5.6026	6.0170
QRTZ	9.8067	11.8359	19.7760
FORS	0.0000	0.0000	0.0000
FAYA	0.0000	0.0000	0.0000
PVSK	0.0000	0.0000	0.0000
NEPH	0.0000	0.0000	0.0000
LEUC	0.0000	0.0000	0.0000
DICA	0.0000	0.0000	0.0000
KALP	0.0000	0.0000	0.0000
CNDM	0.0000	0.0000	3.8057
CALC	0.0000	0.0000	0.0000
NPLG	46.3829	44.8605	32.6045
FEMG	0.1644	0.1423	0.1680
RMG	0.6174	0.6180	0.7285
RFE	0.3826	0.3820	0.2715
C.I.	26.5697	24.9669	22.6684
TOTL	100.0082	100.0112	100.0080

Table 2: (Continued)

Sample No. #1 84-LNO-0047: Fine-grained, massive mafic volcanic. South of Tynall Lake.

Sample No. #2 84-LNO-0142: Feldspar Knot in mega-feldspar phyric mafic flows. South of Lundy Lake.

Sample No. #3 84-LNO-0149: Amygdaloidal pillowed basalt. South of Lundy Lake.

Sample No. #4 84-LNO-0176: Massive, schistose mafic volcanics. Southwest of Tyndall Lake.

Sample No. #5 85-LNO-0061: Fine-grained, schistose mafic volcanic. South of Snare Creek.

Sample No. #6 85-LNO-0062: Fine-grained, schistose mafic volcanic. South of Snare Creek.

Sample No. #7 86-LNO-0133: Fine-grained matrix of mega-feldspar phyric mafic flows. Near the eastern boundary of the map area.

Sample No. #8 86-LNO-0135: Mafic tuff. Near the eastern boundary of the map area.

Sample No. #9 86-LNO-0137: Mafic matrix of mega-feldspar phyric mafic flows. Southeast of Snare Creek Intrusion.

Sample No. #10 86-LNO-0138: Fine-grained mafic unit intercalated with mega-feldspar phyric mafic flows. Southeast of Snare Creek Intrusion.

Sample No. #11 86-LNO-0154: Intermediate schistose volcanics. North of Mountain Lake

Sample No. #12 86-MCS-0084: Fine-grained, schistose lapilli-tuff. Southwest of Lenore Lake.

Sample No. #13 86-MCS-0204: Intermediate, schistose volcanic. North of Mountain Lake.

Sample No. #14 86-MCS-0208: Intermediate, schistose volcanic. West of Breeches Lake.

Sample No. #15 84-LNO-0035: Intermediate tuff, 70% matrix of siliceous fragments. West of Lundy Lake.

Table 3: Chemical Analyses and normative mineralogy of Archean Mafic to Intermediate Intrusive rocks, Banting Township and Western Part of Best Township. (Analysed by X-Ray Assay Labratories Limited.)

MAJOR OXIDES
WEIGHT PERCENT

Reference Number:	16	17	18	19	20
	84LNO-0015	84LNO-0165	86LNO-0088	86LNO-0105	86LNO-0110
SiO2	47.40	47.90	47.60	46.70	48.10
TiO2	0.70	1.19	1.99	1.66	1.40
Al2O3	14.10	14.40	12.60	11.70	14.10
Fe2O3	12.70	14.00	18.70	18.20	16.50
FeO	00.00	00.00	00.00	00.00	00.00
MnO	0.21	0.23	0.27	0.26	0.30
MgO	10.40	6.44	5.91	7.42	5.67
CaO	9.68	9.48	7.61	10.40	9.74
Na2O	1.85	2.09	2.23	1.47	1.77
K2O	0.53	0.86	0.66	1.01	1.07
P2O5	0.06	0.05	0.03	0.04	0.12
CO2	00.00	00.00	00.00	00.00	00.00
S	00.00	00.00	00.00	00.00	00.00
H2O+	00.00	00.00	00.00	00.00	00.00
H2O-	00.00	00.00	00.00	00.00	00.00
LOI	2.70	2.00	1.70	1.50	1.50
TOTAL	100.40	98.70	99.40	100.40	100.40

Table 3 (continued)
TRACE ELEMENTS

(PPM)	84LNO-0015	84LNO-0165	86LNO-0088	861no-0105	86LNO-0110	83LNO-0048
Ba	140	200	220	140	310	210
Co	100	170	120	90	70	70
Cr	410	50	50	0.01%	0.01%	50
Cu	100	210	140	280	150	50
Ni	260	90	40	110	60	50
Pb	30	10	10	10	20	20
Zn	110	90	140	120	130	60
Nb	10	30	10	20	10	10
Rb	30	40	50	30	50	70
Sr	140	230	190	140	130	240
Y	10	10	10	10	30	20
Zr	30	30	10	10	60	80
Th				10	10	
U				10	20	
Mo				10	10	

Table 3 (continued)
MAJOR OXIDES
WEIGHT PERCENT

Reference Number:	21	22	23
	83LNO-0048	84LNO-0126	86LNO-0103
SiO2	56.2	55.70	55.00
TiO2	0.5	1.06	0.92
Al2O3	17.0	15.70	15.60
Fe2O3	12.0	10.30	11.00
FeO	7.7	00.00	00.00
MnO	0.1	0.12	0.16
MgO	4.4	3.19	4.42
CaO	8.6	6.60	7.41
Na2O	2.4	3.19	2.65
K2O	1.0	1.28	1.05
P2O5	0.0	0.05	0.17
CO2	00.0	00.00	00.00
S	00.0	00.00	00.00
H2O+	00.0	00.00	00.00
H2O-	00.0	00.00	00.00
LOI	1.9	1.90	1.80
TOTAL	100.2	98.80	100.30

Table 3 (continued)
TRACE ELEMENTS
(PPM)

	83LNO-0048	84LNO-0126	86LNO-0103
Ba	210	350	230
Co	70	130	50
Cr	50	30	0.02%
Cu	50	90	90
Ni	50	10	70
Pb	20	10	30
Zn	60	90	100
Nb	10	10	20
Rb	70	70	70
Sr	240	200	150
Y	20	20	50
Zr	80	60	180
Th			10
U			10
Mo			10

Table 3 (continued)

MAJOR OXIDE STATISTICS

TOTAL NUMBER OF SAMPLES: 8

	MEAN	STD. DEVIATION
SiO2	50.58	4.22
Al2O3	14.40	1.72
Fe2O3	14.18	3.25
FeO	0.97	2.75
MgO	5.98	2.22
CaO	8.69	1.35
Na2O	2.21	0.55
K2O	0.94	0.24
TiO2	1.18	0.49
P2O5	0.07	0.05
MnO	0.21	0.07
CO2	0.00	0.00
S	0.00	0.00
H2O+	0.00	0.00
H2O-	0.00	0.00
LOI	1.87	0.38
TOTAL	99.82	0.74

Table 3 (continued)

TRACE ELEMENT STATISTICS

(PPM)

	NO. OF SAMPLES	MEAN	STD. DEVIATION
Ba	8	225.00	73.87
Co	8	100.00	38.91
Cr	8	73.76	137.83
Cu	8	138.75	74.92
Ni	8	86.25	76.52
Pb	8	17.50	8.86
Zn	8	105.00	25.63
Nb	8	15.00	7.56
Rb	8	51.25	17.27
Sr	8	177.50	43.34
Y	8	20.00	14.14
Zr	8	57.50	55.48
Th	3	10.00	0.00
U	3	13.33	5.77
Mo	3	10.00	0.00

Table 3 (continued)
CIPW NORMATIVE VALUES

Reference Number:	16	17	18	19	20	21
	84LNO-0015	84LNO-0165	86LNO-0088	86LNO-0105	86LNO-0110	83LNO-0048
APTT	0.1472	0.1240	0.0740	0.0973	0.2918	0.1300
PYRT	0.0000	0.0000	0.0000	0.0000	0.0000	0.0000
ILMN	1.3766	2.3664	3.9338	3.2384	2.7297	0.9211
ORTH	3.2429	5.3211	4.0594	6.1306	6.4912	5.6236
ALBT	16.2089	18.5170	19.6403	12.7769	15.3759	19.0475
ACMT	0.0000	0.0000	0.0000	0.0000	0.0000	0.0000
ANRT	29.6171	28.6580	23.3368	22.9507	28.0964	29.5306
SPHN	0.0000	0.0000	0.0000	0.0000	0.0000	0.0000
RUTL	0.0000	0.0000	0.0000	0.0000	0.0000	0.0000
MGNT	3.3028	4.0837	5.2668	4.7063	4.3166	2.6933
HEMT	0.0000	0.0000	0.0000	0.0000	0.0000	0.0000
DIOP	10.6955	9.2241	6.1124	12.7160	8.1099	2.3992
HEDN	5.3157	7.4844	7.0466	11.9871	9.1731	5.4118
WOLL	0.0000	0.0000	0.0000	0.0000	0.0000	0.0000
ENST	12.0157	12.5172	12.4865	9.7208	10.7374	8.9834
FERS	6.8501	11.6502	16.5121	10.5113	13.9313	23.2434
QRTZ	0.0000	0.0596	1.5365	0.0000	0.7571	2.0204
FORS	6.8991	0.0000	0.0000	2.3589	0.0000	0.0000
FAYA	4.3346	0.0000	0.0000	2.8111	0.0000	0.0000
PVSK	0.0000	0.0000	0.0000	0.0000	0.0000	0.0000
NEPH	0.0000	0.0000	0.0000	0.0000	0.0000	0.0000
LEUC	0.0000	0.0000	0.0000	0.0000	0.0000	0.0000
DICA	0.0000	0.0000	0.0000	0.0000	0.0000	0.0000
KALP	0.0000	0.0000	0.0000	0.0000	0.0000	0.0000
CNDM	0.0000	0.0000	0.0000	0.0000	0.0000	0.0000
CALC	0.0000	0.0000	0.0000	0.0000	0.0000	0.0000
NPLG	64.6295	60.7482	54.3005	64.2379	64.6306	60.7900
FEMG	0.3830	0.2857	0.3062	0.3447	0.2870	0.2986
RMG	0.6974	0.5854	0.4984	0.5486	0.5032	0.3368
RFE	0.3026	0.4146	0.5016	0.4514	0.4968	0.6632
C.I.	50.7900	47.3261	51.3582	58.0500	48.9979	43.6522
TOTL	100.0060	100.0058	100.0052	100.0055	100.0103	100.0042

Table 3 (continued)
CIPW NORMATIVE VALUES

Reference Number:	22	23
	84LNO-0126	86LNO-0103
APTT	0.1228	0.4129
PYRT	0.0000	0.0000
ILMN	2.0880	1.7917
ORTH	7.8452	6.3625
ALBT	27.9967	22.9937
ACMT	0.0000	0.0000
ANRT	25.6595	28.2708
SPHN	0.0000	0.0000
RUTL	0.0000	0.0000
MGNT	3.8498	3.5980
HEMT	0.0000	0.0000
DIOP	3.3035	3.6702
HEDN	3.3156	3.1845
WOLL	0.0000	0.0000
ENST	6.7087	9.5865
FERS	7.7237	9.5410
QRTZ	11.3907	10.5992
FQRS	0.0000	0.0000
FAYA	0.0000	0.0000
PVSK	0.0000	0.0000
NEPH	0.0000	0.0000
LEUC	0.0000	0.0000
DICA	0.0000	0.0000
KALP	0.0000	0.0000
CNDM	0.0000	0.0000
CALC	0.0000	0.0000
NPLG	47.8220	55.1469
FEMG	0.1540	0.1976
RMG	0.5330	0.5690
RFE	0.4670	0.4310
C.I.	26.9894	31.3719
TOTL	100.0043	100.0111

Table 3 (continued)

Sample No. #16 84-LNO-0015: Hornblende gabbro. East of Lundy Lake.

Sample No. #17 84-LNO-0165: Hornblende gabbro. East of Contact Lake.

Sample No. #18 86-LNO-0088: Hornblende Gabbro. Near the southern body of the map area.

Sample No. #19 86-MCS-0105: Hornblende gabbro. East of Contact Lake.

Sample No. #20 86-MCS-0110: Quartz Diorite. Southeast of Contact Lake.

Sample No. #21 83-LNO-0048: Quartz Diorite. Northwest of Contact Lake.

Sample No. #22 84-LNO-0126: Quartz Diorite. East of Contact Lake.

Sample No. #23 86-MCS-0103: Quartz Diorite. Southeast of Contact Lake.

Table 4: Chemical Analyses and normative mineralogy of Archean Intermediate to Felsic Intrusive rocks, Banting Township and Western Part of Best Township. (Analysed by X-Ray Assay Laboratories Limited.)

MAJOR OXIDES
WEIGHT PERCENT

Reference Number:	24	25	26	27	28	29
	83LNO-0082	84LNO-0041	86LNO-0050	86LNO-0150	86LNO-0156	86MCS-0076
SiO2	74.40	72.50	72.00	71.40	57.10	77.00
TiO2	0.12	0.15	0.12	0.21	0.51	0.07
Al2O3	13.10	15.20	15.10	15.30	21.00	12.90
Fe2O3	1.05	1.28	1.77	1.59	4.62	0.31
FeO	00.00	00.00	00.00	00.00	00.00	00.00
MnO	0.03	0.04	0.06	0.04	0.09	0.01
MgO	0.46	0.39	0.57	0.55	2.42	0.12
CaO	0.79	1.52	1.73	1.98	3.05	0.16
Na2O	4.26	4.86	5.27	5.04	6.10	4.00
K2O	4.53	3.12	2.37	2.68	2.98	5.03
P2O5	0.03	0.04	0.06	0.04	0.13	0.02
CO2	00.00	00.00	00.00	00.00	00.00	00.00
S	00.00	00.00	00.00	00.00	00.00	00.00
H2O+	00.00	00.00	00.00	00.00	00.00	00.00
H2O-	00.00	00.00	00.00	00.00	00.00	00.00
LOI	0.70	0.80	0.70	1.30	2.20	0.50
TOTAL	99.60	100.10	100.00	100.30	100.40	100.20

Table 4(continued)
TRACE ELEMENTS
(PPM)

	83LNO-0082	84LNO-0041	86LNO-0050	86LNO-0150	86LNO-0156	86MCS-0076
Ba	600	670	580	780	740	340
Co	10	10	10	10	20	10
Cr	40	30	30	30	0.01%	0.01%
Cu	30	30	30	20	130	10
Ni	10	10	10	10	20	10
Pb	10	30	20	10	10	10
Zn	20	40	40	20	60	10
Nb	20	10	30	10	10	10
Rb	190	140	130	90	140	190
Sr	50	310	230	250	300	20
Y	30	10	10	10	20	10
Zr	70	50	110	80	250	40
Th					10	10
U					10	10
Mo					20	10

Table 4(continued)

MAJOR OXIDES
WEIGHT PERCENT

Reference Number:	30	31	32	33	34
	86MCS-0089	86MCS-0091	86MCS-0126	86MCS-0161	86MCS-0180
SiO2	76.50	71.90	71.00	71.50	74.40
TiO2	0.10	0.28	0.26	0.18	0.21
Al2O3	13.60	15.10	15.50	14.80	13.20
Fe2O3	0.71	2.07	2.51	1.43	1.95
FeO	00.00	00.00	00.00	00.00	00.00
MnO	0.02	0.05	0.04	0.03	0.05
MgO	0.26	0.74	0.84	0.61	0.61
CaO	0.93	1.17	1.26	1.31	1.31
Na2O	4.68	4.45	6.04	3.55	3.55
K2O	1.97	3.30	1.71	3.55	3.38
P2O5	0.03	0.06	0.06	0.05	0.05
CO2	00.00	00.00	00.00	00.00	00.00
S	00.00	00.00	00.00	00.00	00.00
H2O+	00.00	00.00	00.00	00.00	00.00
H2O-	00.00	00.00	00.00	00.00	00.00
LOI	1.50	1.30	1.00	0.70	1.20
TOTAL	100.40	100.60	100.40	99.50	100.10

Table 4(continued)

TRACE ELEMENTS
(PPM)

	86MCS-0089	86MCS-0091	86MCS-0126	86MCS-0161	86MCS-0180
Ba	360	680	530	600	680
Co	10	10	10	10	10
Cr	0.01%	0.01%	0.01%	0.02%	0.02%
Cu	20	10	30	20	10
Ni	10	10	10	10	10
Pb	10	20	30	60	40
Zn	10	50	30	20	20
Nb	20	20	10	10	10
Rb	120	150	70	100	140
Sr	70	290	150	180	130
Y	10	10	10	10	10
Zr	80	50	180	50	120
Th	10	10	10	10	10
U	10	10	10	10	10
Mo	10	10	30	10	10

Table 4(continued)

MAJOR OXIDE STATISTICS

TOTAL NUMBER OF SAMPLES: 11

	MEAN	STD. DEVIATION
SiO2	71.79	5.29
Al2O3	14.98	2.23
Fe2O3	1.75	1.14
FeO	0.00	0.00
MgO	0.69	0.61
CaO	1.38	0.73
Na2O	4.71	0.87
K2O	3.15	1.00
TiO2	0.20	0.12
P2O5	0.05	0.03
MnO	0.04	0.02
CO2	0.00	0.00
S	0.00	0.00
H2O+	0.00	0.00
H2O-	0.00	0.00
LOI	1.08	0.49
TOTAL	100.15	0.34

Table 4(continued)
(PPM)

TRACE ELEMENT STATISTICS

	NO. OF SAMPLES	MEAN	STD. DEVIATION
Ba	11	596.36	141.44
Co	11	10.91	3.02
Cr	11	11.83	16.62
Cu	11	30.91	33.90
Ni	11	10.91	3.02
Pb	11	22.73	16.18
Zn	11	29.09	16.40
Nb	11	14.55	6.88
Rb	11	132.73	37.44
Sr	11	180.00	104.31
Y	11	12.73	6.47
Zr	11	98.18	64.93
Th	7	10.00	0.00
U	7	10.00	0.00
Mo	7	14.29	7.87

Table 4(continued)
CIPW NORMATIVE VALUES

Reference Number:	24	25	26	27	28	29
	83LNO-0082	84LNO-0041	86LNO-0050	86LNO-0150	86LNO-0156	86MCS-0076
APTT	0.0719	0.0956	0.1435	0.0959	0.3150	0.0476
PYRT	0.0000	0.0000	0.0000	0.0000	0.0000	0.0000
ILMN	0.0650	0.0863	0.2301	0.0866	0.9910	0.0215
ORTH	27.1024	18.6044	14.1414	16.0243	18.0171	29.8370
ALBT	36.4958	41.4974	45.0278	43.1520	52.8108	33.9760
ACMT	0.0000	0.0000	0.0000	0.0000	0.0000	0.0000
ANRT	3.2843	7.3455	8.2704	9.6747	14.6122	0.6656
SPHN	0.2142	0.0000	0.0000	0.0000	0.0000	0.0000
RUTL	0.0000	0.1059	0.0000	0.1669	0.0000	0.0590
MGNT	0.0000	0.0000	0.2858	0.0000	2.9817	0.0000
HEMT	1.0631	1.2916	1.4387	1.6088	0.0000	0.3112
DIOP	0.1412	0.0000	0.0000	0.0000	0.0000	0.0000
HEDN	0.0000	0.0000	0.0000	0.0000	0.0000	0.0000
WOLL	0.0000	0.0000	0.0000	0.0000	0.0000	0.0000
ENST	1.0945	0.9801	1.4334	1.3860	4.9025	0.3000
FERS	0.0000	0.0000	0.0000	0.0000	1.6083	0.0000
QRTZ	30.4697	28.8251	28.1609	27.1965	0.0000	34.1486
FORS	0.0000	0.0000	0.0000	0.0000	0.8858	0.0000
FAYA	0.0000	0.0000	0.0000	0.0000	0.3202	0.0000
PVSK	0.0000	0.0000	0.0000	0.0000	0.0000	0.0000
NEPH	0.0000	0.0000	0.0000	0.0000	0.0000	0.0000
LEUC	0.0000	0.0000	0.0000	0.0000	0.0000	0.0000
DICA	0.0000	0.0000	0.0000	0.0000	0.0000	0.0000
KALP	0.0000	0.0000	0.0000	0.0000	0.0000	0.0000
CNDM	0.0000	1.1706	0.8719	0.6110	2.5634	0.6348
CALC	0.0000	0.0000	0.0000	0.0000	0.0000	0.0000
NPLG	8.2561	15.0390	15.5171	18.3140	21.6724	1.9215
FEMG	0.0116	0.0098	0.0143	0.0138	0.0768	0.0030
RMG	1.0000	1.0000	1.0000	1.0000	0.8002	1.0000
RFE	0.0000	0.0000	0.0000	0.0000	0.1998	0.0000
C.I.	2.3637	2.3581	3.3880	3.0814	11.6895	0.6327
TOTL	100.0020	100.0026	100.0039	100.0026	100.0080	100.0012

Table 4(continued)
CIPW NORMATIVE VALUES

Reference Number:	30	31	32	33	34
	86MCS-0089	86MCS-0091	86MCS-0126	86MCS-0161	86MCS-0180
APTT	0.0719	0.1434	0.1433	0.1221	0.1200
PYRT	0.0000	0.0000	0.0000	0.0000	0.0000
ILMN	0.0433	0.5367	0.4981	0.0662	0.4041
ORTH	11.7827	19.6795	10.1920	21.6245	20.2393
ALBT	40.0818	38.0001	51.5496	30.9650	30.4391
ACMT	0.0000	0.0000	0.0000	0.0000	0.0000
ANRT	4.4714	5.4620	5.9094	6.3625	6.2544
SPHN	0.0000	0.0000	0.0000	0.0000	0.0000
RUTL	0.0784	0.0000	0.0000	0.1507	0.0000
MGNT	0.0000	0.1945	1.5653	0.0000	0.2539
HEMT	0.7186	1.6622	0.6956	1.4741	1.5576
DIOP	0.0000	0.0000	0.0000	0.0000	0.0000
HEDN	0.0000	0.0000	0.0000	0.0000	0.0000
WOLL	0.0000	0.0000	0.0000	0.0000	0.0000
ENST	0.6554	1.8599	2.1101	1.5660	1.5394
FERS	0.0000	0.0000	0.0000	0.0000	0.0000
QRTZ	39.9225	30.2211	25.7611	34.7285	37.7366
FORS	0.0000	0.0000	0.0000	0.0000	0.0000
FAYA	0.0000	0.0000	0.0000	0.0000	0.0000
PVSK	0.0000	0.0000	0.0000	0.0000	0.0000
NEPH	0.0000	0.0000	0.0000	0.0000	0.0000
LEUC	0.0000	0.0000	0.0000	0.0000	0.0000
DICA	0.0000	0.0000	0.0000	0.0000	0.0000
KALP	0.0000	0.0000	0.0000	0.0000	0.0000
CNDM	2.1758	2.2444	1.5791	2.9435	1.4587
CALC	0.0000	0.0000	0.0000	0.0000	0.0000
NPLG	10.0361	12.5673	10.2846	17.0451	17.0451
FEMG	0.0065	0.0185	0.0210	0.0156	0.0153
RMG	1.0000	1.0000	1.0000	1.0000	1.0000
RFE	0.0000	0.0000	0.0000	0.0000	0.0000
C.I.	1.4173	4.2532	4.8690	3.1063	3.7552
TOTL	100.0018	100.0038	100.0036	100.0031	100.0033

Table 4(continued)

Sample No. #24 83-LNO-0082: Red mylonitic granite. Northwest of Contact Lake.

Sample No. #25 84-LNO-0041: Coarse-grained pink granite. North of Lundy Lake

Sample No. #26 86-LNO-0050: Medium-grained, pink, foliated granite. Near the eastern boundary of the map area.

Sample No. #27 86-LNO-0150: Medium-grained, foliated granite. East of Gilbert Lake.

Sample No. #28 86-LNO-0156: Red mylonitic granite, Anima-Nipissing River

Sample No. #29 86-MCS-0076: Brick red granite. Southeast shore of Lenore Lake

Sample No. #30 86-MCS-0089: Mylonitic granite, South shore of Jamieson Lake.

Sample No. #31 86-LNO-0091: Porphyritic granite. North shore of Guppy Lake.

Sample No. #32 86-LNO-0126: Medium-grained granite. South of Lundy Lake.

Sample No. #33 86-LNO-0161: Medium-grained grey granite. Northwest of McLean Lake.

Sample No. #34 86-MCS-0180: Mylonitic granite. South of Carrying Lake.

Table 5: Chemical Analyses and normative mineralogy of Archean Mafic dike rocks, Banting Township and Western Part of Best Township. (Analysed by X-Ray Assay Laboratories Limited.)

MAJOR OXIDES
WEIGHT PERCENT

Reference Number:	35	36	37	38	39	40
	86LNO-0158	86MCS-0158	86MCS-0173	83LNO-0074	85LNO-0027	86LNO-0157
SiO2	54.00	45.80	46.60	52.20	50.40	55.10
TiO2	0.70	0.70	1.08	0.56	0.73	0.66
Al2O3	12.20	8.35	5.76	11.90	11.40	13.50
Fe2O3	9.45	10.00	14.40	9.85	9.46	4.91
FeO	00.00	00.00	00.00	00.00	00.00	00.00
MnO	0.19	0.19	0.23	0.24	0.18	0.17
MgO	8.68	8.68	19.60	10.80	12.50	8.48
CaO	6.70	6.70	7.99	7.14	7.58	4.91
Na2O	3.78	3.78	0.22	2.61	2.06	2.80
K2O	1.15	1.15	0.09	1.73	1.81	2.37
P2O5	0.51	0.51	0.11	0.28	0.26	0.27
CO2	00.00	00.00	00.00	00.00	00.00	00.00
S	00.00	00.00	00.00	00.00	00.00	00.00
H2O+	00.00	00.00	00.00	00.00	00.00	00.00
H2O-	00.00	00.00	00.00	00.00	00.00	00.00
LOI	2.70	2.70	3.50	2.50	3.00	3.20
TOTAL	100.20	100.20	99.80	100.10	99.70	100.40

Table 5: (continued)
TRACE ELEMENTS
(PPM)

	86LNO-0158	86MCS-0158	86MCS-0173	83LNO-0074	85LNO-0027	86LNO-0157
Ba	600	140	80	460	600	580
Co	50	70	110	50	130	40
Cr	0.04%	0.24%	1310	910	990	0.08%
Cu	10	50	260	80	100	60
Ni	90	850	980	180	280	130
Pb	10	160	20	40	10	10
Zn	70	350	120	210	110	100
Nb	10	20	20	10	20	10
Rb	30	150	10	60	80	100
Sr	260	50	20	270	680	220
Y	10	10	10	30	10	10
Zr	130	60	80	70	40	90
Th	10	10				10
U	10	10				10
Mo	10	10				10

Table 5: (continued)
MAJOR OXIDES
WEIGHT PERCENT

Reference Number:	41	42
	86MCS-0191	86MCS-0196
SiO2	48.20	58.50
TiO2	0.64	0.49
Al2O3	12.00	13.20
Fe2O3	11.10	8.08
FeO	00.00	00.00
MnO	0.24	0.14
MgO	12.20	6.60
CaO	8.60	4.99
Na2O	1.30	4.12
K2O	1.47	2.09
P2O5	0.33	0.24
CO2	00.00	00.00
S	00.00	00.00
H2O+	00.00	00.00
H2O-	00.00	00.00
LOI	3.80	1.70
TOTAL	100.10	100.40

Table 5:(continued)

TRACE ELEMENTS (PPM)	86MCS-0191	86MCS-0196
Ba	430	540
Co	10	40
Cr	0.14%	0.08%
Cu	40	20
Ni	200	110
Pb	30	10
Zn	190	60
Nb	20	10
Rb	50	70
Sr	100	410
Y	10	10
Zr	60	70
Th	10	10
U	10	10
Mo	10	10

Table 5:(continued)

MAJOR OXIDE STATISTICS

TOTAL NUMBER OF SAMPLES: 8

	MEAN	STD. DEVIATION
SiO2	51.35	4.43
Al2O3	11.04	2.64
Fe2O3	9.66	2.67
FeO	0.00	0.00
MgO	10.94	4.04
CaO	6.83	1.32
Na2O	2.58	1.35
K2O	1.48	0.71
TiO2	0.69	0.17
P2O5	0.31	0.14
MnO	0.20	0.04
CO2	0.00	0.00
S	0.00	0.00
H2O+	0.00	0.00
H2O-	0.00	0.00
LOI	2.89	0.65
TOTAL	100.11	0.25

Table 5:(continued)

TRACE ELEMENT STATISTICS

(PPM)

	NO. OF SAMPLES	MEAN	STD. DEVIATION
Ba	8	428.75	206.98
Co	8	62.50	39.55
Cr	8	401.32	565.16
Cu	8	77.50	79.42
Ni	8	352.50	353.91
Pb	8	36.25	51.25
Zn	8	151.25	96.13
Nb	8	15.00	5.35
Rb	8	68.75	43.24
Sr	8	251.25	216.23
Y	8	12.50	7.07
Zr	8	75.00	26.73
Th	5	10.00	0.00
U	5	10.00	0.00
Mo	5	10.00	0.00

Table 5:(continued)
CIPW NORMATIVE VALUES

Reference Number:	35	36	37	38	39	40
	86LNO-0158	86MCS-0158	86MCS-0173	83LNO-0074	85LNO-0027	86LNO-0157
APTT	1.2501	1.4198	0.2746	0.6870	0.6438	0.6884
PYRT	0.0000	0.0000	0.0000	0.0000	0.0000	0.0000
ILMN	1.3758	1.5626	2.1615	1.1018	1.4494	1.3494
ORTH	7.0324	7.9875	0.5604	10.5906	11.1816	15.0762
ALBT	33.0996	37.5951	1.9617	22.8791	18.2228	25.5051
ACMT	0.0000	0.0000	0.0000	0.0000	0.0000	0.0000
ANRT	13.3752	2.8442	15.2413	16.2078	17.2636	18.5889
SPHN	0.0000	0.0000	0.0000	0.0000	0.0000	0.0000
RUTL	0.0000	0.0000	0.0000	0.0000	0.0000	0.0000
MGNT	3.3009	3.7492	3.9420	3.0942	3.3801	3.3713
HEMT	0.0000	0.0000	0.0000	0.0000	0.0000	0.0000
DIOP	10.2894	18.4719	16.0475	11.1114	12.8748	4.1653
HEDN	3.8835	7.6488	4.5979	3.8503	3.3289	0.3414
WOLL	0.0000	0.0000	0.0000	0.0000	0.0000	0.0000
ENST	17.6007	1.8912	35.3414	19.5175	18.9767	20.8040
FERS	7.6200	0.8983	11.6152	7.7578	5.6282	1.9560
QRTZ	1.2023	0.0000	0.0000	0.0000	0.0000	8.1713
FORS	0.0000	10.4795	6.0678	2.2396	5.3258	0.0000
FAYA	0.0000	5.4855	2.1978	0.9810	1.7408	0.0000
PVSK	0.0000	0.0000	0.0000	0.0000	0.0000	0.0000
NEPH	0.0000	0.0000	0.0000	0.0000	0.0000	0.0000
LEUC	0.0000	0.0000	0.0000	0.0000	0.0000	0.0000
DICA	0.0000	0.0000	0.0000	0.0000	0.0000	0.0000
KALP	0.0000	0.0000	0.0000	0.0000	0.0000	0.0000
CNDM	0.0000	0.0000	0.0000	0.0000	0.0000	0.0000
CALC	0.0000	0.0000	0.0000	0.0000	0.0000	0.0000
NPLG	28.7794	7.0334	88.5967	41.4660	48.6484	42.1574
FEMG	0.2962	0.3446	0.6405	0.3615	0.3973	0.2427
RMG	0.7522	0.7345	0.7999	0.7678	0.8159	0.9332
RFE	0.2478	0.2655	0.2001	0.2322	0.1841	0.0668
C.I.	44.0703	50.1871	81.9711	49.6536	52.7047	31.9874
TOTL	100.0298	100.0338	100.0091	100.0182	100.0165	100.0173

Table 5:(continued)
CIPW NORMATIVE VALUES

Reference Number:	41	42
	86MCS-0191	86MCS-0196
APTT	0.8212	0.5810
PYRT	0.0000	0.0000
ILMN	1.2770	0.9512
ORTH	9.1263	12.6231
ALBT	11.5570	35.6320
ACMT	0.0000	0.0000
ANRT	23.7085	11.6018
SPHN	0.0000	0.0000
RUTL	0.0000	0.0000
MGNT	3.2598	2.9490
HEMT	0.0000	0.0000
DIOP	11.1907	6.9021
HEDN	3.9898	2.8808
WOLL	0.0000	0.0000
ENST	20.1662	13.6005
FERS	8.2473	6.5115
QRTZ	0.0000	5.7814
FORS	4.6027	0.0000
FAYA	2.0745	0.0000
PVSK	0.0000	0.0000
NEPH	0.0000	0.0000
LEUC	0.0000	0.0000
DICA	0.0000	0.0000
KALP	0.0000	0.0000
CNDM	0.0000	0.0000
CALC	0.0000	0.0000
NPLG	67.2286	24.5625
FEMG	0.4169	0.2283
RMG	0.7627	0.7330
RFE	0.2373	0.2670
C.I.	54.8081	33.7952
TOTL	100.0211	100.0145

Table 5:(continued)

Sample No. #35 86-LNO-0158: Mafic dike in volcanics. Southeast of Tyndall Lake.

Sample No. #36 86-MCS-0158: Phlogopite-augite lamprophyre dike. Southeast of Contact Lake.

Sample No. #37 86-MCS-0173: Hornblende lamprophyre dike. Southwest of Mountain Lake.

Sample No. #38 83-LNO-0074: Pyroxene-phyric gabbro, Anima Nipissing River intrusion.

Sample No. #39 85-LNO-0027: Pyroxene-phyric gabbro, Snare Creek intrusion.

Sample No. #40 86-LNO-0157: Pyroxene-phyric diorite, Anima-Nipissing River intrusion.

Sample No. #41 86-MCS-0191: Pyroxene-phyric gabbro dike, Anima-Nipissing River intrusion.

Sample No. #42 86-MCS-0196: Intrusive breccia, Anima-Nipissing River intrusion.

Table 6: Rare earth element geochemical analyses of Late Archean mafic to intermediate intrusive rocks, Banting Township and Western Part of Best Township. Analyses by X-Ray Assay Laboratories Limited

Reference Number	40	35	41	42
Sample No.	86-LNO-157	86-LNO-158	86-MCS-191	86-MCS-196
REE (ppm)				
La	10.4	23.4	16.4	16.7
Ce	20	40	30	26
Nd	11	23	17	14
Sm	3.15	5.69	4.43	3.31
Eu	0.75	1.35	1.04	0.81
Tb	0.4	0.8	0.4	0.4
Yb	1.50	1.43	1.75	1.63
Lu	0.25	0.26	0.27	0.25
$(La/Lu)_{cn}$	4.29	9.29	6.20	6.88
(Eu/Sm)	0.238	0.237	0.235	0.245

Table 6 (continued)
Notes:

Sample No. #35 86-LNO-157 pyroxene-phyric diorite, Anima-Nipissing River Intrusion

Sample No. #40 86-LNO-158 mafic dike, near Tyndall Lake

Sample No. #41 86-MCS-191 pyroxene-phyric gabbro dike in explosion breccia, Anima-Nipissing River Intrusion

Sample No. #42 86-MCS-196 late intrusive breccia, Anima-Nipissing River Intrusion

Representative REE distribution patterns for selected igneous rocks

	$(La/Lu)_{cn}$	Eu/Sm
Tholeiitic intrusive complexes[1]	0.31 - 19.3	0.23 - 1.55
Quartz diorite, tonalite, granodiorite and trondhjemite with negative Eu anomalies[2]	8.9 - 66	0.041 - 0.26
Monzogranites and syenogranites with small to moderate negative Eu anomalies[2]	2.5 - 50	0.09 - 0.23

$(La/Lu)_{cn}$	4.29	9.29	6.20	6.88
(Eu/Sm)	0.238	0.237	0.235	0.245

[1]Cullers and Graf 1984a

[2]Cullers and Graf 1984b

Table 7: Chemical Analyses and normative mineralogy of Early Proterozoic Nipissing Intrusive rocks, and Middle Proterozoic Olivine diabase dikes of the Sudbury Swarm. Banting Township and Western Part of Best Township. (Analysed by X-Ray Assay Laboratories Limited.)

MAJOR OXIDEs WEIGHT PERCENT Reference Number	43	44	45	46	47	48
	86LNO-0046	86LNO-0057	86LNO-0136	86MCS-0073	86MCS-0086	86MCS-0125
SiO2	51.80	51.20	50.50	51.30	53.20	50.80
TiO2	0.97	0.59	0.79	2.44	1.82	0.97
Al2O3	14.10	14.80	13.50	11.80	12.90	14.60
Fe2O3	16.20	9.83	12.20	19.70	17.40	10.10
FeO	00.00	00.00	00.00	00.00	00.00	00.00
MnO	0.25	0.16	0.22	0.28	0.36	0.17
MgO	4.65	8.33	8.30	2.84	2.02	9.54
CaO	6.71	12.10	10.70	6.56	5.67	12.30
Na2O	1.96	1.49	1.43	2.44	2.80	1.43
K2O	0.75	0.64	0.49	1.28	1.98	0.38
P2O5	0.10	0.05	0.07	0.16	0.17	0.05
CO2	00.00	00.00	00.00	00.00	00.00	00.00
S	00.00	00.00	00.00	00.00	00.00	00.00
H2O+	00.00	00.00	00.00	00.00	00.00	00.00
H2O-	00.00	00.00	00.00	00.00	00.00	00.00
LOI	2.60	0.90	1.90	0.80	1.30	0.50
TOTAL	100.20	100.20	100.20	99.70	99.70	100.50

Table 7:(continued)
TRACE ELEMENTS
(PPM)

Reference Number	43	44	45	46	47	48
	86LNO-0046	86LNO-0057	86LNO-0136	86MCS-0073	86MCS-0086	86MCS-0125
Ba	230	120	110	320	440	120
Co	110	90	100	70	70	60
Cr	30	240	140	0.01	30	0.04
Cu	130	110	130	70	60	90
Ni	40	110	150	10	10	180
Pb	10	10	10	20	20	10
Zn	100	60	90	100	180	60
Nb	10	20	10	20	20	30
Rb	50	30	40	100	140	40
Sr	170	180	140	120	140	140
Y	30	10	10	20	20	10
Zr	70	10	30	140	150	20
Th				10		10
U				10		10
Mo				10		10

Table 7:(continued)
MAJOR OXIDES
WEIGHT PERCENT

Reference Number	49	50	51	52	53	48
	83LNO-0117	86LNO-0149	86MCS-0064	86MCS-0151	86MCS-0170	
SiO2	53.80	48.30	49.10	44.60	48.90	
TiO2	1.52	0.89	1.42	3.91	1.51	
Al2O3	13.20	15.60	14.50	14.10	13.70	
Fe2O3	14.50	12.20	13.90	18.70	13.80	
FeO	00.00	00.00	00.00	00.00	00.00	
MnO	0.17	0.20	0.21	0.24	0.24	
MgO	3.91	7.42	5.84	4.09	7.05	
CaO	7.15	7.93	10.10	7.65	8.38	
Na2O	2.86	2.60	1.64	3.28	1.78	
K2O	1.36	1.36	0.72	1.64	1.05	
P2O5	0.23	0.09	0.13	1.21	0.13	
CO2	00.00	00.00	00.00	00.00	00.00	
S	00.00	00.00	00.00	00.00	00.00	
H2O+	00.00	00.00	00.00	00.00	00.00	
H2O-	00.00	00.00	00.00	00.00	00.00	
LOI	1.50	2.60	2.50	00.00	2.60	
TOTAL	100.40	99.40	100.20	99.60	99.30	

Table 7:(continued)
TRACE ELEMENTS
(PPM)

	83LNO-0117	86LNO-0149	86MCS-0064	86MCS-0151	86MCS-0170
Ba	470	660	130	850	210
Co	190	80	60	60	70
Cr	40	290	0.02%	0.01%	180
Cu	190	120	120	60	50
Ni	60	130	70	40	100
Pb	10	20	10	100	30
Zn	110	180	90	160	100
Nb	10	10	20	50	20
Rb	80	80	60	50	80
Sr	390	250	200	410	220
Y	10	20	40	40	30
Zr	150	70	70	340	90
Th			10	10	
U			10	10	
Mo			10	10	

Table 7:(continued)
MAJOR OXIDE STATISTICS

TOTAL NUMBER OF SAMPLES: 11

	MEAN	STD. DEVIATION
SiO2	50.32	2.55
Al2O3	13.89	1.04
Fe2O3	14.41	3.29
FeO	0.00	0.00
MgO	5.82	2.48
CaO	8.66	2.29
Na2O	2.16	0.66
K2O	1.06	0.51
TiO2	1.53	0.95
P2O5	0.22	0.33
MnO	0.23	0.06
CO2	0.00	0.00
S	0.00	0.00
H2O+	0.00	0.00
H2O-	0.00	0.00
LOI	1.56	0.94
TOTAL	99.95	0.41

Table 7:(continued)
TRACE ELEMENT STATISTICS
(PPM)

	NO. OF SAMPLES	MEAN	STD. DEVIATION
Ba	11	332.73	247.39
Co	11	87.27	37.97
Cr	11	86.37	107.26
Cu	11	102.73	41.74
Ni	11	81.82	56.71
Pb	11	22.73	26.49
Zn	11	111.82	42.85
Nb	11	20.00	11.83
Rb	11	68.18	32.19
Sr	11	214.55	99.64
Y	11	21.82	11.68
Zr	11	103.64	92.87
Th	4	10.00	0.00
U	4	10.00	0.00
Mo	4	10.00	0.00

Table 7:(continued)
CIPW NORMATIVE VALUES

Reference Number	43	44	45	46	47	48
	86LNO-0046	86LNO-0057	86LNO-0136	86MCS-0073	86MCS-0086	86MCS-0125
APTT	0.2464	0.1203	0.1706	0.3898	0.4155	0.1189
PYRT	0.0000	0.0000	0.0000	0.0000	0.0000	0.0000
ILMN	1.9167	1.1386	1.5435	4.7666	3.5668	1.8501
ORTH	4.6111	3.8429	2.9787	7.7801	12.0735	2.2551
ALBT	17.2555	12.8111	12.4479	21.2368	24.4485	12.1518
ACMT	0.0000	0.0000	0.0000	0.0000	0.0000	0.0000
ANRT	28.5703	32.3171	29.8022	17.9637	17.3180	32.4339
SPHN	0.0000	0.0000	0.0000	0.0000	0.0000	0.0000
RUTL	0.0000	0.0000	0.0000	0.0000	0.0000	0.0000
MGNT	3.7260	3.0791	3.4157	5.8759	4.9672	3.5965
HEMT	0.0000	0.0000	0.0000	0.0000	0.0000	0.0000
DIOP	1.8366	15.9781	12.6269	3.6555	2.1919	17.1124
HEDN	2.6972	6.9731	7.2354	8.6852	6.9076	5.8274
WOLL	0.0000	0.0000	0.0000	0.0000	0.0000	0.0000
ENST	11.1977	13.6729	15.4114	5.5806	4.1751	15.9276
FERS	18.8631	6.8447	10.1298	15.2094	15.0925	6.2216
QRTZ	9.0880	3.2268	4.2443	8.8686	8.8571	2.5094
FORS	0.0000	0.0000	0.0000	0.0000	0.0000	0.0000
FAYA	0.0000	0.0000	0.0000	0.0000	0.0000	0.0000
PVSK	0.0000	0.0000	0.0000	0.0000	0.0000	0.0000
NEPH	0.0000	0.0000	0.0000	0.0000	0.0000	0.0000
LEUC	0.0000	0.0000	0.0000	0.0000	0.0000	0.0000
DICA	0.0000	0.0000	0.0000	0.0000	0.0000	0.0000
KALP	0.0000	0.0000	0.0000	0.0000	0.0000	0.0000
CNDM	0.0000	0.0000	0.0000	0.0000	0.0000	0.0000
CALC	0.0000	0.0000	0.0000	0.0000	0.0000	0.0000
NPLG	62.3455	71.6118	70.5376	45.8252	41.4638	72.7450
FEMG	0.2739	0.2900	0.3178	0.2228	0.1939	0.3083
RMG	0.4382	0.7241	0.6666	0.3253	0.2666	0.7709
RFE	0.5618	0.2759	0.3334	0.6747	0.7334	0.2291
C.I.	40.2374	47.6864	50.3628	43.7731	36.9012	50.5356
TOTL	100.0087	100.0047	100.0066	100.0122	100.0138	100.0048

Table 7:(continued)

CIPW NORMATIVE VALUES

Reference Number	49	50	51	52	53	48
	83LNO-0117	86LNO-0149	86MCS-0064	86MCS-0151	86MCS-0170	
APTT	0.5585	0.2230	0.3192	2.9218	0.3226	
PYRT	0.0000	0.0000	0.0000	0.0000	0.0000	
ILMN	2.9593	1.7680	2.7959	7.5707	3.0042	
ORTH	8.2385	8.4059	4.4108	9.8801	6.4999	
ALBT	24.8084	23.0113	14.3865	28.2954	15.7784	
ACMT	0.0000	0.0000	0.0000	0.0000	0.0000	
ANRT	19.6443	28.1137	31.1804	19.2750	27.5414	
SPHN	0.0000	0.0000	0.0000	0.0000	0.0000	
RUTL	0.0000	0.0000	0.0000	0.0000	0.0000	
MGNT	4.4887	3.6245	4.3891	7.9969	4.5718	
HEMT	0.0000	0.0000	0.0000	0.0000	0.0000	
DIOP	5.5836	6.2737	8.9949	4.7590	7.4670	
HEDN	7.1379	3.8881	7.4271	4.6756	4.9289	
WOLL	0.0000	0.0000	0.0000	0.0000	0.0000	
ENST	7.3940	9.0603	10.9084	3.3158	14.9318	
FERS	10.8426	6.4408	10.3317	3.7368	11.3059	
QRTZ	8.3586	0.0000	4.8656	0.0000	3.6584	
FORS	0.0000	5.1576	0.0000	3.4076	0.0000	
FAYA	0.0000	4.0407	0.0000	4.2322	0.0000	
PVSK	0.0000	0.0000	0.0000	0.0000	0.0000	
NEPH	0.0000	0.0000	0.0000	0.0000	0.0000	
LEUC	0.0000	0.0000	0.0000	0.0000	0.0000	
DICA	0.0000	0.0000	0.0000	0.0000	0.0000	
KALP	0.0000	0.0000	0.0000	0.0000	0.0000	
CNDM	0.0000	0.0000	0.0000	0.0000	0.0000	
CALC	0.0000	0.0000	0.0000	0.0000	0.0000	
NPLG	44.1915	54.9901	68.4277	40.5189	63.5769	
FEMG	0.2104	0.2967	0.2584	0.1921	0.2888	
RMG	0.4726	0.6489	0.5811	0.5383	0.6344	
RFE	0.5274	0.3511	0.4189	0.4617	0.3656	
C.I.	38.4061	40.2536	44.8471	39.6946	46.2096	
TOTL	100.0144	100.0075	100.0098	100.0668	100.0103	

Table 7:(continued)

Sample No. #43 86-LNO-0046: Varied textured diabase from the upper part of the Nipissing Diabase sill. Southeast of Snare Creek Intrusion.

Sample No. #44 86-LNO-0057: Medium-grained hypersthene diabase from the upper part of the Nipissing Diabase sill. Near the eastern boundary of the map area.

Sample No. #45 86-LNO-0136: Quartz diabase from the lower contact of the Nipissing Diabase sill. Near the eastern boundary of the map area.

Sample No. #46 86-MCS-0073: Pegmatitic diabase from the upper contact of the Nipissing Diabase sill. Island in Lenore Lake.

Sample No. #47 86-MCS-0086: Varied textured diabase from the upper part of the Nipissing Diabase sill. Southwest of Lenore Lake.

Sample No. #48 86-MCS-0125: Medium-grained hypersthene diabase from the upper part of the Nipissing Diabase sill. South of Lundy Lake.

Sample No. #49 83-LNO-0117: NNW-trending diabase dike-Middle Proterozoic age. West of McLean Lake.

Sample No. #50 86-LNO-0149: North-trending porphyritic diabase dike-Middle Proterozoic age. Southwest of Breeches Lake.

Sample No. #51 86-MCS-0064: Northeast-trending porphyritic diabase dike-Middle Proterozoic age. East of Red Squirrel Lake.

Sample No. #52 86-MCS-0151: Northwest-trending olivine diabase dike (Sudbury Swarm)-Middle Proterozoic age. Island in McLean Lake.

Sample No. #53 86-MCS-0170: Northeast-trending diabase dike-Middle Proterozoic age. South of Snare Lake.

Table 8: Grab sample assay values for mineralized rock specimens collected from Banting and Best Townships, 1983-1989. Sample numbers correspond to location numbers in Figure 4. Values in % or oz./ton. (Temiskaming Testing Laboratory)

Reference No.	Sample No.	Host Rock	Au (oz/ton)	Ag (oz/ton)	Cu(%)	Pb(%)	Zn(%)
01	86-LNO-068	QV in granite	0.049	na	na	na	na
02	86-LNO-074	QCV in diabase	nil	tr	tr	na	na
03	86-LNO-131	CV in diabase	nil	0.028	na	na	0.013% Co
04	86-LNO-148	CV in diabase	tr	nil	0.010	na	na
05	86-MCS-019	QV in granite	tr	na	nil	nil	0.01
06	86-MCS-024	QV in granite	tr	0.05	0.01	0.03	nil
07	86-MCS-029	QV in granite	nil	na	0.01	0.01	nil
08	86-MCS-041	QV in granite	tr	na	nil	0.01	nil
09	86-MCS-043	QV in granite	0.003	na	nil	nil	nil
10	86-MCS-045	QV in granite	0.020	na	nil	nil	nil
11	86-MCS-139	QCV in diabase	tr	tr	0.48	na	na
12	86-MCS-143	QV in granite	0.004	na	na	na	na
13	86-MCS-152	QCV in diabase	0.012	na	na	na	na
14	86-MCS-156	QCV in diabase	0.006	tr	na	na	na
15	86-MCS-162	QV in granite	0.009	na	na	na	na
16	86-MCS-163	QV in granite	0.010	na	na	na	na

Table 8(continued)

Reference	Sample No.	Host Rock	Au (oz/ton)	Ag (oz/ton)	Cu(%)	Pb(%)	Zn(%)
17	86-MCS-165	QV in granite	Q.002	na	na	na	na
18	86-MCS-174	QV in mafic volc	0.002	na	na	na	na
19	86-MCS-182	QV in granite	0.029	na	na	na	na
20	86-MCS-185	QV in granite	0.004	na	na	na	na
21	86-MCS-190	QV in mafic volc	0.001	na	na	na	na
22	86-MCS-191	SU in pyroxenite	0.002	na	na	na	na
23	86-MCS-192	QV in mafic volc	0.012	na	na	na	na
24	86-MCS-194	QV in diabase	0.001	na	na	na	na
25	87-LNO-001	CP in diabase	nil	tr	0.012	na	na
26	87-LNO-007	QV in granite	0.004	na	na	na	na
27	88-LNO-004	float	tr	nil	27.04%Fe	na	na
28	88-LNO-012	float	nil	nil	0.068	na	na
29	86-MCS-032	QV in granite	nil	tr	nil	0.01	nil
30	87-MCS-010	QV in granite	nil	na	0.019	na	na
31	87-MCS-100	QV in granite	0.005	nil	na	na	na
32	86-EMD-003	QV in granite	0.002	na	na	na	na

Abbreviations:QV-quartz vein;QCV-quartz-carbonate vein; CV-carbonate vein; SU-sulphides; CP-chalcopyrite; na-not analysed

Table 9: Sample Location list of UTM coordinates for Geochemical data for Banting Township and the Western Part of Best Township. Compare with location map (Figure 4).

Locations of Samples for Whole Rock Geochemical Data

Reference No	Sample No	UTM coordinates Zone	Easting	Northing
01	84LNO-0047	17	580720	5225620
02	84LNO-0142	17	582170	5225200
03	84LNO-0149	17	582800	5225520
04	84LNO-0176	17	579480	5224980
05	85LNO-0061	17	585050	5224820
06	85LNO-0062	17	585180	5225060
07	86LNO-0133	17	587100	5223800
08	86LNO-0135	17	587000	5223800
09	86LNO-0137	17	586520	5224370
10	86LNO-0138	17	586300	5224330
11	86LNO-0154	17	586720	5231100
12	86MCS-0084	17	577580	5222100
13	86MCS-0204	17	587050	5231100
14	86MCS-0208	17	584420	5231480
15	84LNO-0035	17	582580	5227500
16	84LNO-0015	17	583350	5226650
17	84LNO-0165	17	581950	5223930
18	86LNO-0088	17	583880	5222320
19	86MCS-0105	17	581050	5223570
20	86MCS-0110	17	581720	5223020
21	83LNO-0048	17	578360	5224380
22	84LNO-0126	17	581580	5224330
23	86MCS-0103	17	581440	5223420
24	83LNO-0082	17	578640	5224460
25	84LNO-0041	17	582600	5227500
26	86LNO-0050	17	587120	5225560
27	86LNO-0150	17	585160	5228040
28	86LNO-0156	17	576480	5224860
29	86MCS-0076	17	579280	5222060
30	86MCS-0089	17	576380	5222530
31	86MCS-0091	17	576120	5221680
32	86MCS-0126	17	582520	5223050
33	86MCS-0161	17	577040	5228460
34	86MCS-0180	17	576880	5225320
35	86LNO-0158	17	581650	5225750
36	86MCS-0158	17	580120	5222900
37	86MCS-0173	17	585920	5229600
38	83LNO-0074	17	578600	5225460
39	85LNO-0027	17	585210	5226280
40	86LNO-0157	17	578600	5225380
41	86MCS-0191	17	578660	5225330
42	86MCS-0196	17	579080	5225680

43	86LNO-0046	17	586100	5224930

Table 9 (continued)

44	86LNO-0057	17	586460	5223680
45	86LNO-0136	17	586980	5223780
46	86MCS-0073	17	577580	5222400
47	86MCS-0086	17	577680	5222220
48	86MCS-0125	17	582710	5222780
49	83LNO-0117	17	576760	5226730
50	86LNO-0149	17	584120	5222980
51	86MCS-0064	17	576270	5224040
52	86MCS-0151	17	578020	5227680
53	86MCS-0170	17	584140	5239800

Locations of Assay Samples Data

01	86LNO-0068	17	585530	5223680
02	86LNO-0072	17	584480	5223420
03	86LNO-0131	17	585840	5223500
04	86LNO-0148	17	585340	5230130
05	86MCS-0019	17	576260	5223190
06	86MCS-0024	17	576650	5223390
07	86MCS-0029	17	577120	5223710
08	86MCS-0041	17	577270	5223260
09	86MCS-0043	17	577970	5223760
10	86MCS-0045	17	577560	5223610
11	86MCS-0139	17	575200	5230820
12	86MCS-0143	17	580480	5230250
13	86MCS-0152	17	577320	5229620
14	86MCS-0156	17	576080	5230390
15	86MCS-0162	17	580860	5230930
16	86MCS-0163	17	581950	5231030
17	86MCS-0165	17	583470	5231450
18	86MCS-0174	17	576000	5225000
19	86MCS-0182	17	577060	5225290
20	86MCS-0185	17	576850	5225700
21	86MCS-0190	17	578480	5224380
22	86MCS-0191	17	578630	5225300
23	86MCS-0192	17	578630	5225330
24	86MCS-0194	17	579290	5225590
25	87LNO-0001	17	577280	5227770
26	87LNO-0007	17	583330	5225880
27	88LNO-0004	17	575140	5225520
28	88LNO-0012	17	584150	5231170
29	86MCS-0032	17	577000	5222900
30	87MCS-0010	17	579650	5229000
31	87MCS-0100	17	584920	5230720
32	86EMD-0003	17	575730	5222840

CONVERSION FACTORS FOR MEASUREMENTS IN ONTARIO GEOLOGICAL SURVEY PUBLICATIONS

Conversion from SI to Imperial			Conversion from Imperial to SI		
SI Unit	*Multiplied by*	*Gives*	*Imperial Unit*	*Multiplied by*	*Gives*
		LENGTH			
1 mm	0.039 37	inches	1 inch	**25.4**	mm
1 cm	0.393 70	inches	1 inch	**2.54**	cm
1 m	3.280 84	feet	1 foot	**0.304 8**	m
1 m	0.049 709 7	chains	1 chain	20.116 8	m
1 km	0.621 371	miles (statute)	1 mile (statute)	**1.609 344**	km
		AREA			
1 cm^2	0.155 0	square inches	1 square inch	**6.451 6**	cm^2
1 m^2	10.763 9	square feet	1 square foot	**0.092 903 04**	m^2
1 km^2	0.386 10	square miles	1 square mile	2.589 988	km^2
1 ha	2.471 054	acres	1 acre	0.404 685 6	ha
		VOLUME			
1 cm^3	0.061 02	cubic inches	1 cubic inch	**16.387 064**	cm^3
1 m^3	35.314 7	cubic feet	1 cubic foot	0.028 316 85	m^3
1 m^3	1.308 0	cubic yards	1 cubic yard	0.764 555	m^3
		CAPACITY			
1 L	1.759 755	pints	1 pint	0.568 261	L
1 L	0.879 877	quarts	1 quart	1.136 522	L
1 L	0.219 969	gallons	1 gallon	**4.546 090**	L
		MASS			
1 g	0.035 273 96	ounces (avdp)	1 ounce (avdp)	28.349 523	g
1 g	0.032 150 75	ounces (troy)	1 ounce (troy)	**31.103 476 8**	g
1 kg	2.204 62	pounds (avdp)	1 pound (avdp)	**0.453 592 37**	kg
1 kg	0.001 102 3	tons (short)	1 ton (short)	**907.184 74**	kg
1 t	1.102 311	tons (short)	1 ton (short)	**0.907 184 74**	t
1 kg	0.000 984 21	tons (long)	1 ton (long)	**1016.046 908 8**	kg
1 t	0.984 206 5	tons (long)	1 ton (long)	**1.016 046 908 8**	t
		CONCENTRATION			
1 g/t	0.029 166 6	ounce (troy)/ ton (short)	1 ounce (troy)/ ton (short)	34.285 714 2	g/t
1 g/t	0.583 333 33	pennyweights/ ton (short)	1 pennyweight/ ton (short)	1.714 285 7	g/t

OTHER USEFUL CONVERSION FACTORS

	Multiplied by	
1 ounce (troy) per ton (short)	20.0	pennyweights per ton (short)
1 pennyweight per ton (short)	0.05	ounces (troy) per ton (short)

Note: Conversion factors which are in bold type are exact. The conversion factors have been taken from or have been derived from factors given in the Metric Practice Guide for the Canadian Mining and Metallurgical Industries, published by the Mining Association of Canada in co-operation with the Coal Association of Canada.


5
5
5
CENTIMETRES

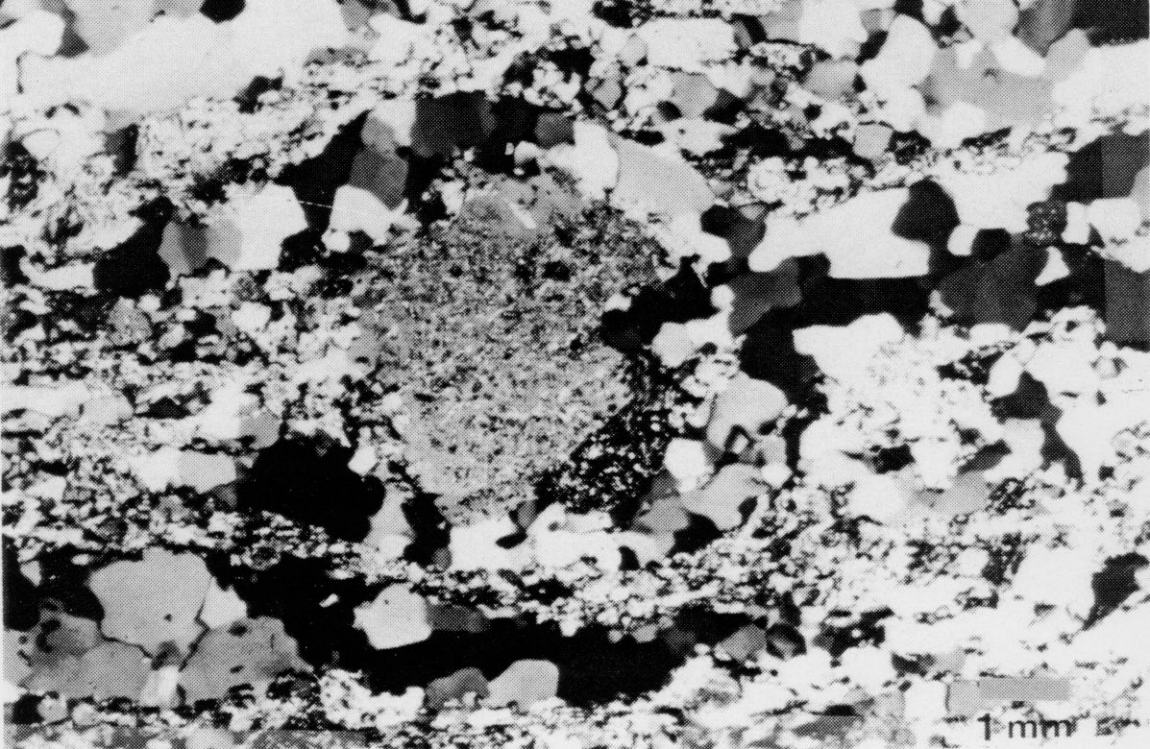
1 mm


1mm


CENTIMETRE
INCH

GENUINE TIRES
INCHES

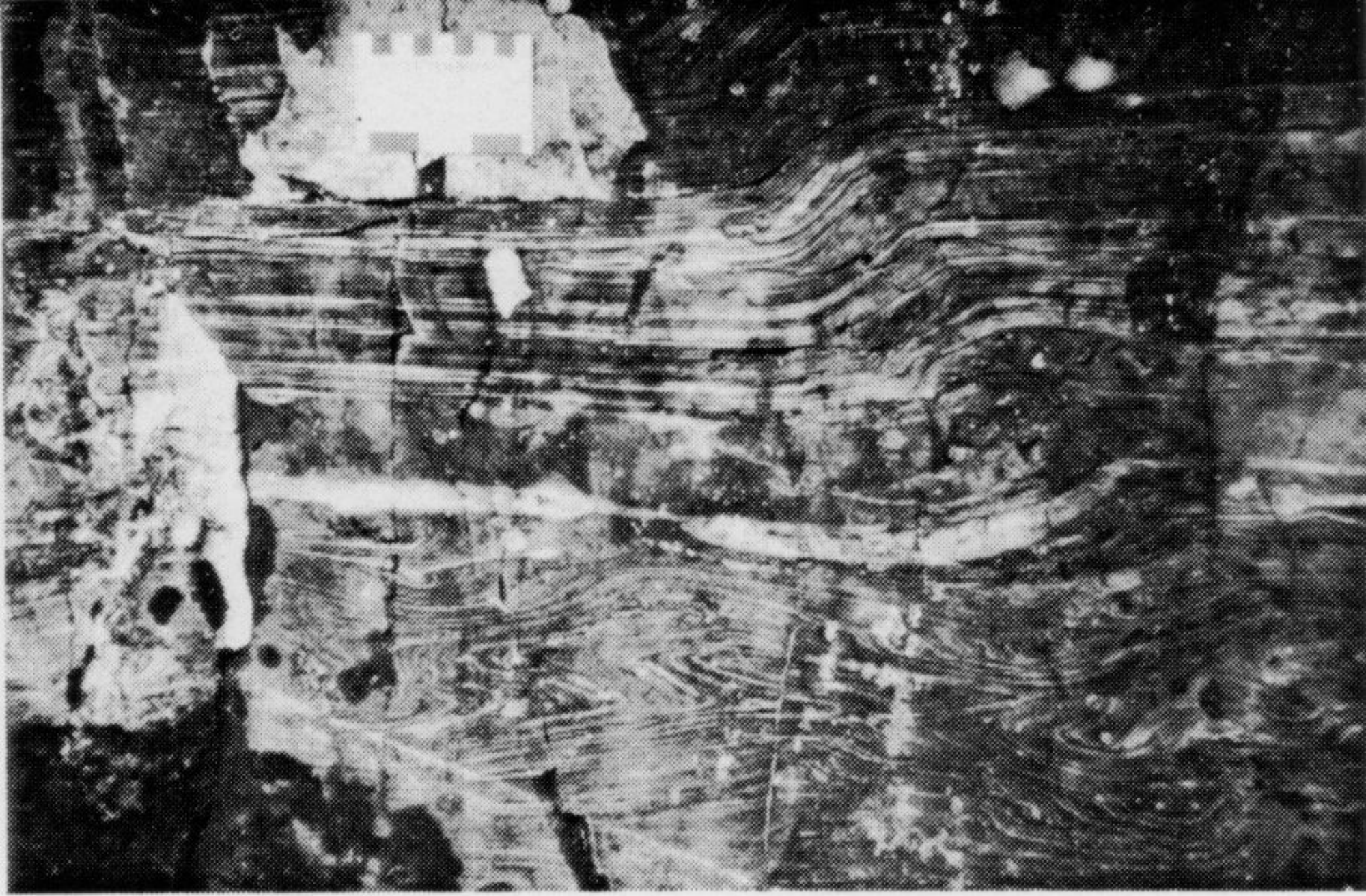


1mm

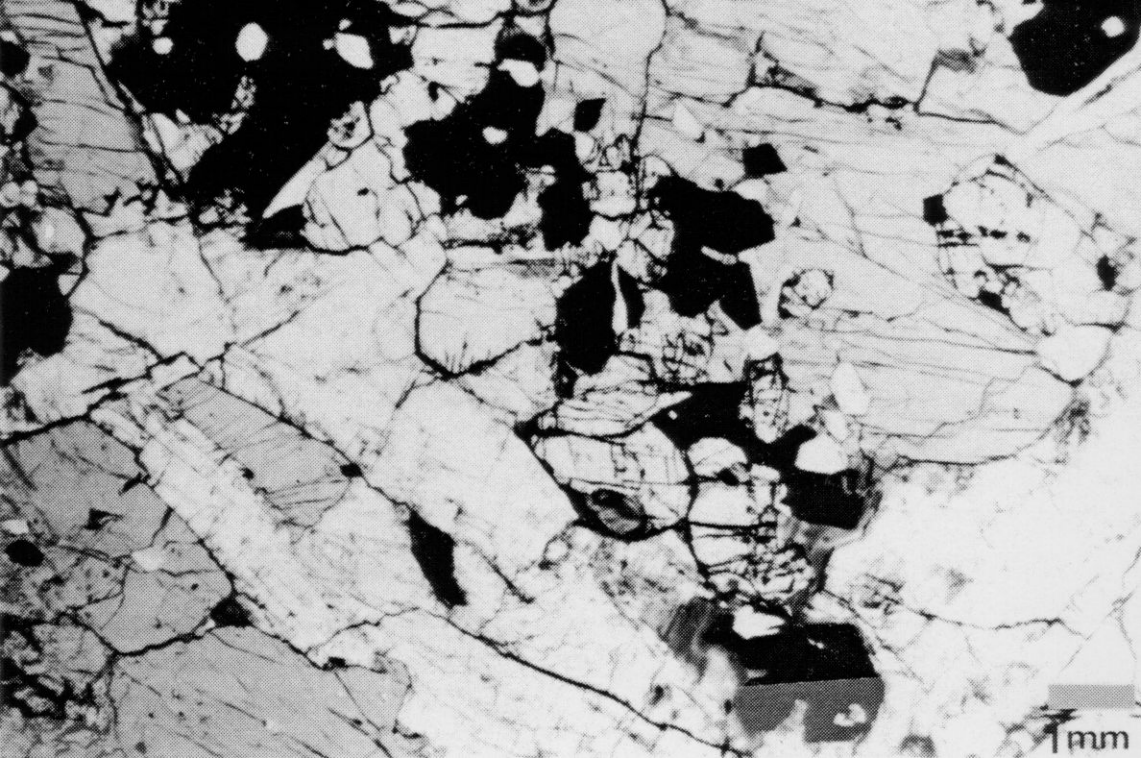
1mm

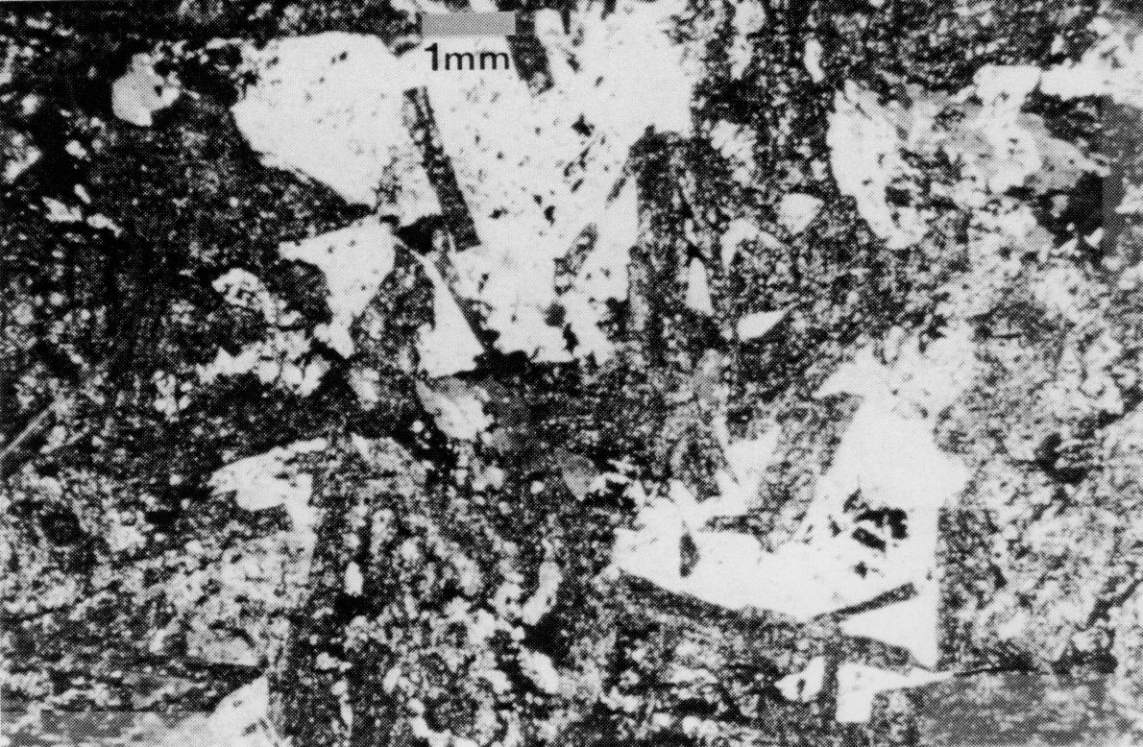
1mm


CENTIMETRES
INCHES

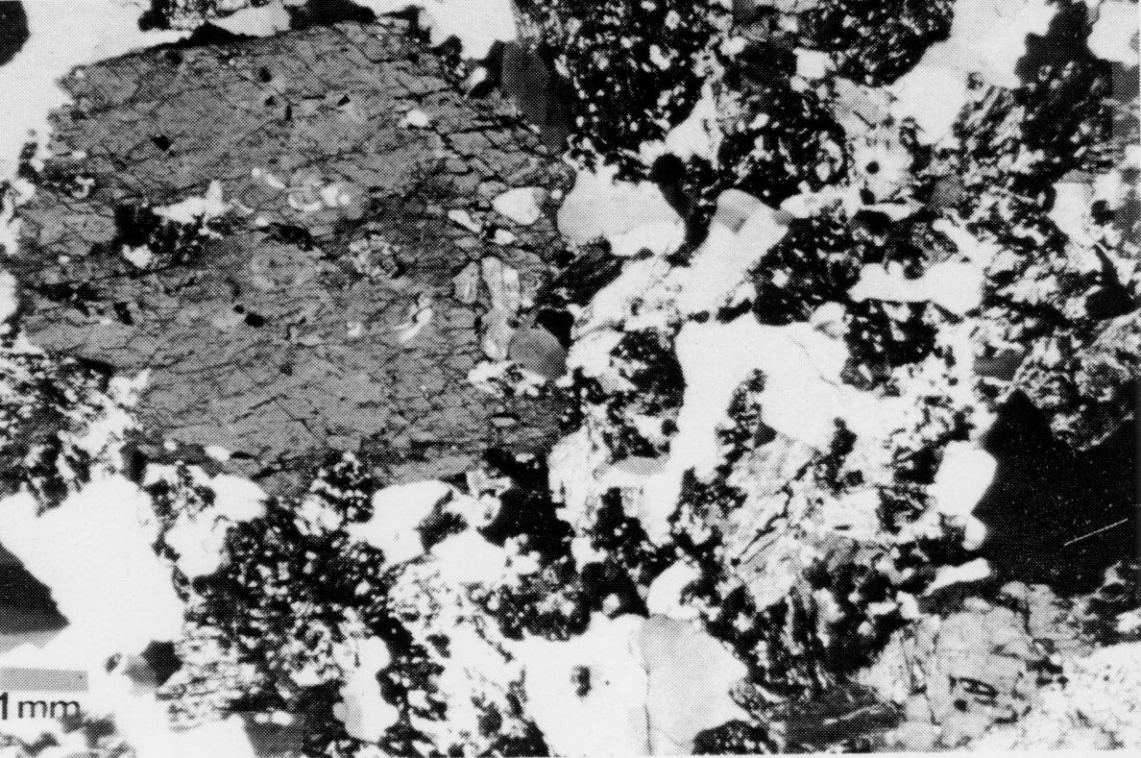
1 mm